Grant agreement no.:
101060634

Project acronym:
PURPEST

Project full title:

Plant pest prevention through technology-guided monitoring and site-specific control

Collaborative Project (RIA Research and Innovation action)

HORIZON EUROPE CALL – HORIZON-CL6-2021-FARM2FORK-01

Start date of project: 2023-01-01
Duration: 4 years

D 2.2
Report on performance of individual sensor system components

Due delivery date: 30-06-2024
Actual delivery date: 05-07-2024

Organization name of lead contractor for this deliverable:
SINTEF

Project co-funded by the European Commission within HORIZON 2020 (2016-2020)		
Dissemination Level		
PU	Public, fully open, e.g. web	X
CO	Confidential, restricted under conditions set out in Model Grant Agreement	
Cl	Classified, information as referred to in Commission Decision 2001/844/EC.	

Deliverable number:	D2.2 / D9
Deliverable name:	Report on performance of individual sensor system components
Work package:	WP2
Lead contractor:	SIN

Author(s)		
Name	**Organisation**	**E-mail**
Daniel Nilsen Wright	SINTEF	daniel.nilsen.wright@sintef.no
Lucas Lopez	VOL	lucas@volatile.ai
Adomas Malaiska	VOL	adomas@volatile.ai
Damien Bazin	AIRMO	damien.bazin@chromatotec.com
Ali Ghaddar	AIRMO	ali.ghaddar@chromatotec.com
Marina Cole	UWAR	marina.cole@warwick.ac.uk
Julian Gardner	UWAR	j.w.gardner@warwick.ac.uk
Usman Yaqoob	UWAR	usman.yaqoob@warwick.ac.uk
Siavash Esfahani	UWAR	siavash.esfahani@warwick.ac.uk
Firehun Dullo	SINTEF	firehun.t.dullo@sintef.no
Jesil Jose	SINTEF	jesil.jose@sintef.no
Karolina Milenko	SINTEF	karolina.milenko@sintef.no
Stanislav Roučka	Saftra Photonics	Stanislav.roucka@saftra-photonics.org

Abstract

This deliverable is a report on the performance of the individual components that will make up the Sensor System Prototype (SSP). The report is a combination of tests done at the partners and at the intercomparison campaign at AIRMOTEC in April 2024. Performance is defined by the components' ability to detect and identify different VOCs from D1.6 "List of VOCs released from relevant pest described in the literature". These VOCs include ethanol, 2-methyl-1-butanol, d-limonene and (E)-2-hexenal.

In total, two gas chromatography systems, AIRMO (microVOC) and VOL (Scout3), and different sensor technologies, SINTEF (SERS), Saftra (SERS) and UWAR (SMR), as well as, compound separation technology from UWAR (µ-GC) were tested. The two systems from AIRMO (microVOC) and VOL (Scout3) showed full or partial ability to detect the VOCs of interest. The components from SINTEF (SERS), Saftra (SERS) and UWAR (µ-GC and e-nose) need further development to be able to detect the target VOCs.

Public introduction[1]

This deliverable is a report on the performance of the individual components, systems and sensors that will make up the Sensor System Prototype (SSP). The SSP is a solution being developed as part of the PurPest project, with a goal of an on-site and field screening of plants for early detection of pest infections. One of the eventual applications of the SSP would be better customs controls for plant imports and safeguarding EU and EEA's plant ecosystems. The report is a combination of tests done at the partners and at the intercomparison campaign at AIRMOTEC in April

---

[1] According to Deliverables list in Annex I, all restricted (RE) deliverables will contain an introduction that will be made public through the project WEBSITE

2024. In the previous work during the project, tests were conducted with target plants and pests and have identified the initial list of volatile organic compounds (VOCs), which are released by either plants or pests at the early phases of a pest infection. This report outlines the available technologies from the Project partners and outlines the Performance of the components' ability to detect and identify different VOCs from D1.6 "List of VOCs released from relevant pest described in the literature". The VOCs of interest at this Project stage include ethanol, 2-methyl-1-butanol, d-limonene and (E)-2-hexenal.

The two systems from AIRMO (microVOC) and VOL (Scout3) showed full or partial ability to detect the VOCs of interest. The components from SINTEF (SERS), Saftra (SERS) and UWAR (μ-GC and e-nose) need further development to be able to detect the VOCs of interest.

TABLE OF CONTENTS

1   INTRODUCTION

This deliverable reports the performance of the individual components that will make up the Sensor System Prototype (SSP). The report is a combination of tests done at the individual partner institutions and at the intercomparison campaign at Airmo's facilities in Bordeaux, April 2024.

This deliverable will also be used as a basis for D2.3 "first compatible sensor system components to be integrated in WP3" (DEM).

A conceptual illustration of the SSP is given in Figure 1-1. It will be portable on the back of the operator with a sensing probe connected to the unit via a tube (not illustrated).
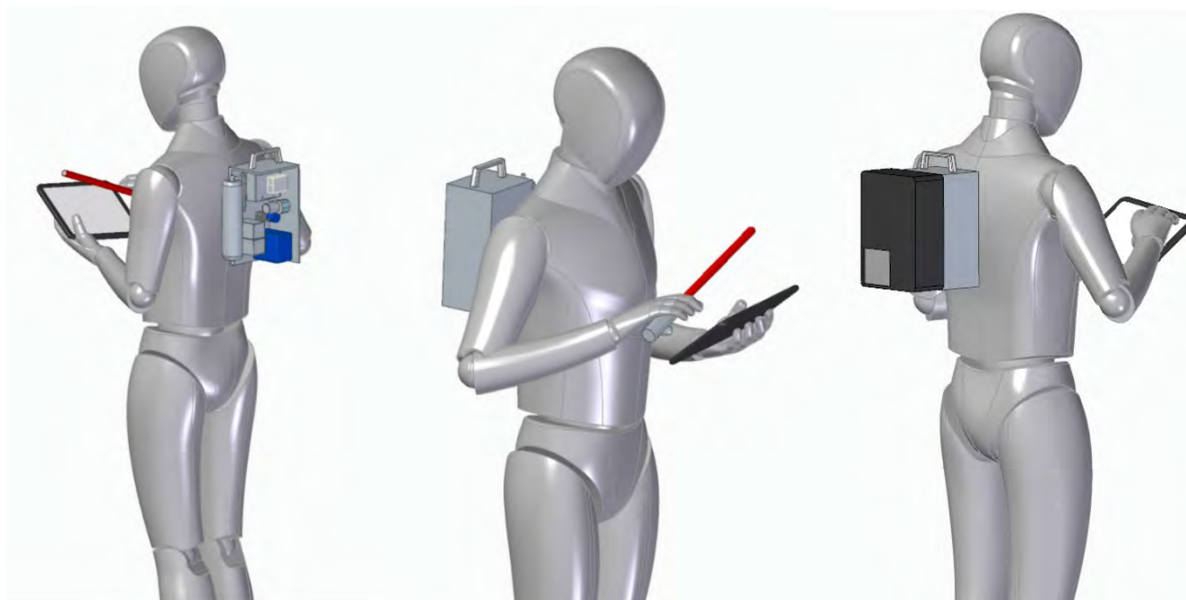
Figure 1-1: 3D representation of user carrying the analytical system. The two to the left are without SAFTRA's Ramascope, while the one to the right is with it.

1.1   VOCs from infected plants

As preparation for the list of VOCs identified in the ongoing plant experiments, WP1 prepared a literature review of VOCs emanating from plants infected with the pests and/or VOCs emanating from the pests themselves. This was reported in D1.6 which was submitted June 30th 2023. Selected VOCs from these lists have been used to pre-test the SSP components while waiting for the VOCs from PurPest's own plant experiments. These VOCs are listed in **Table 1-1**.

Table 1-1: list of most relevant VOCs from D1.6.

Pest	VOC name	Cas Nr	Chemical formula
BMSB	(E)-2-Hexenal	6728-26-3	$C_6H_{10}O$
BMSB	(E)-2-Octenal	2548-87-0	$C_8H_{14}O$
FAW	Indole	120-72-9	C_8H_7N
FAW	Linalool	78-70-6	$C_{10}H_{18}O$
CBW	β-Pinene	18172-67-3	$C_{10}H_{16}$
CBW	d-limonene	5989-27-5	$C_{10}H_{16}$
PHY	Ethanol	64-17-5	C_2H_5OH
PHY	2-Methyl-1- butanol	78-92-2	$C_5H_{12}O$

2 COMPONENTS OF THE SSP

In this chapter the different components of the SSP are briefly described (taken mostly from D2.1). Their performance is summarised in the next chapter.
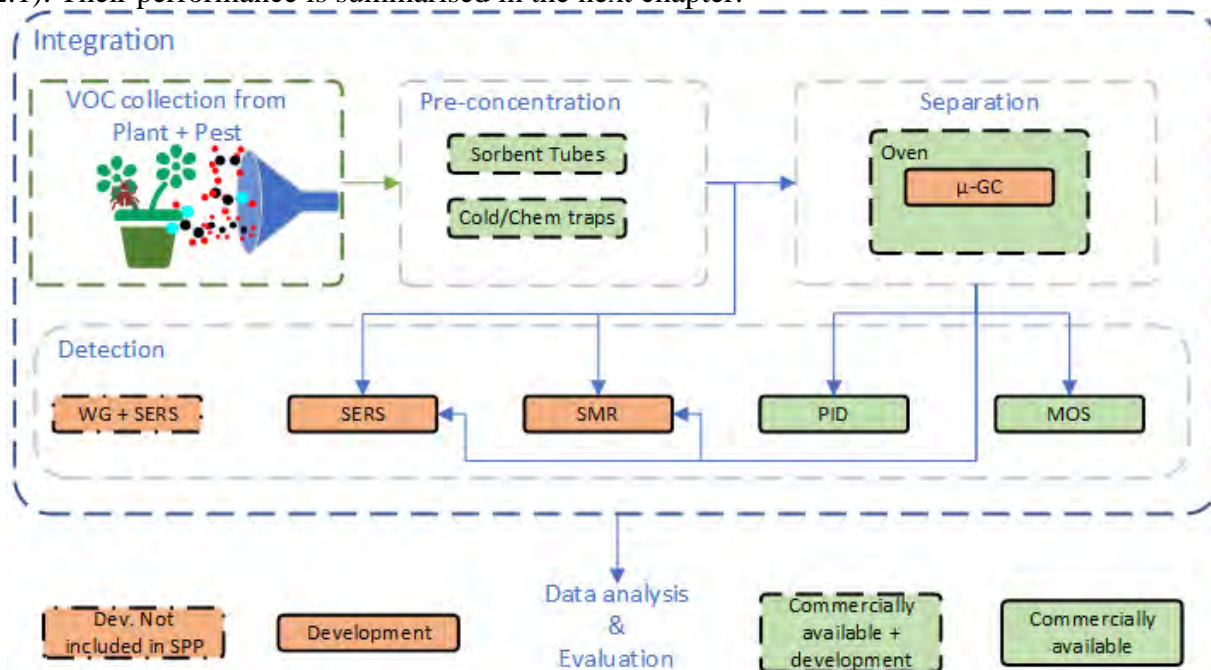
Figure 2-1: Conceptual illustration of the PurPest SSP. The system will only use one or two of the detection systems illustrated. The µGC bypass can be applied to SERS and SMR detection principles since these might be sufficiently selective.

2.1 Pre-concentrators

A pre-concentration unit is a component of the gas chromatograph that is designed to enhance the sensitivity and detection limits of the analysis by concentrating the analytes of interest. This unit is particularly useful when the target analytes are present in low concentrations or when the sample matrix is complex and can interfere with the detection. The pre-concentration unit typically consists of an adsorption device and a desorption mechanism. The adsorbent material will be optimised to target the molecules of interest. For desorption, heating the adsorbent material is usually used to release the molecule because it does not require human intervention and can be easily automatised.

2.1.1 AIRMOTEC pre-concentration unit

The pre-concentration unit (**Figure 2-2**) is made of a glass tube filled with adsorbent material which can be heated up to 380 °C in less than 60 s. The control of temperature and duration of thermodesorption is controlled by the embedded electronic board.
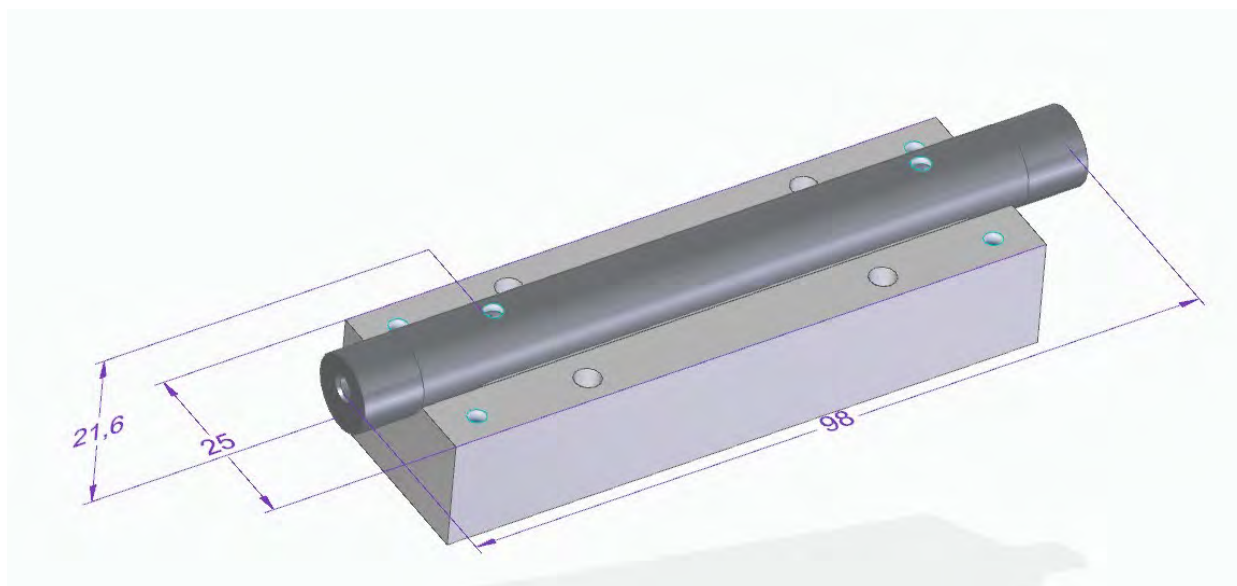
Figure 2-2: Dimensions of the AIRMO pre-concentration unit (mm)

2.1.2 UWAR pre-concentration unit

During previous work at UWAR, two chambers were fabricated, one as a pre-concentrator chamber and one as inlet temperature/humidity chamber [Harun 2009]. The inlet temperature/humidity chamber houses a Sensirion SHT15 temperature sensor, to monitor the VOC temperature at the inlet of the system. This is followed by the pre-concentrator chamber as shown in **Figure 2-3**.
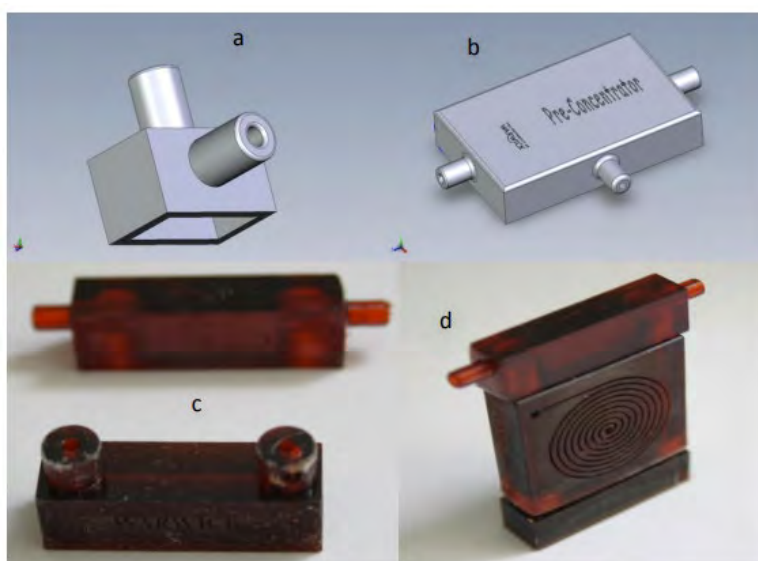
Figure 2-3:a) CAD Design of Temperature/Humidity Sensor chamber b) CAD Design of pre-concentrator chamber c) 3D printed Connection Converter & column bridge d) Assembled 3D printed Retentive column with connection adapter.

The sampling and VOC delivery system can be divided into 4 period steps: pre-concentrator period, reference period, test period and flush period. **Figure 2-4** shows the block diagram of VOC delivery system.
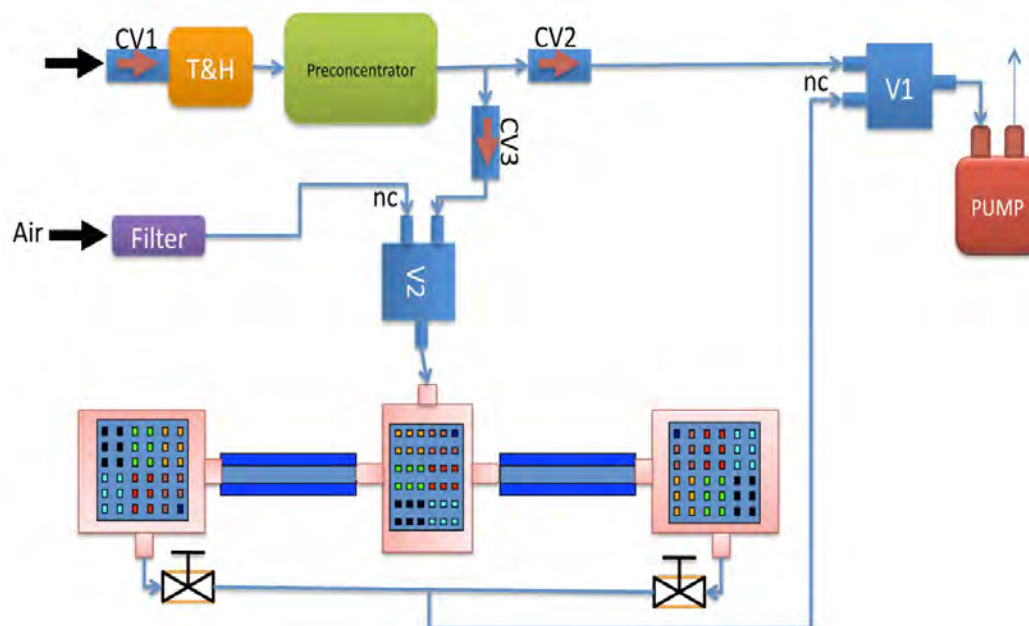
Figure 2-4: Block diagram of odour flow in the system [Harun et al. 2009].

2.2   Separation

The separation unit plays a crucial role in separating the components of a mixture based on their physical and chemical properties. The separation unit is often a column which can be heated at different temperatures. The column is a long, narrow tube packed with a stationary phase or coated with a stationary phase film. The stationary phase is responsible for the separation of analytes in the sample and is optimised to achieve the separation of the molecules of interest. Typically, an inert gas that carries the sample through a column is used to facilitate separation of analytes.

2.2.1   AIRMOTEC column oven

The column oven can be heated up to 200 °C and can integrate standard columns from ID 0.18 to 0.53 mm. The column length can be adjusted up to 30 m. The oven is illustrated in Figure 2-5. The oven can accommodate both commercially available µ-GC and the one from UWAR, described below.
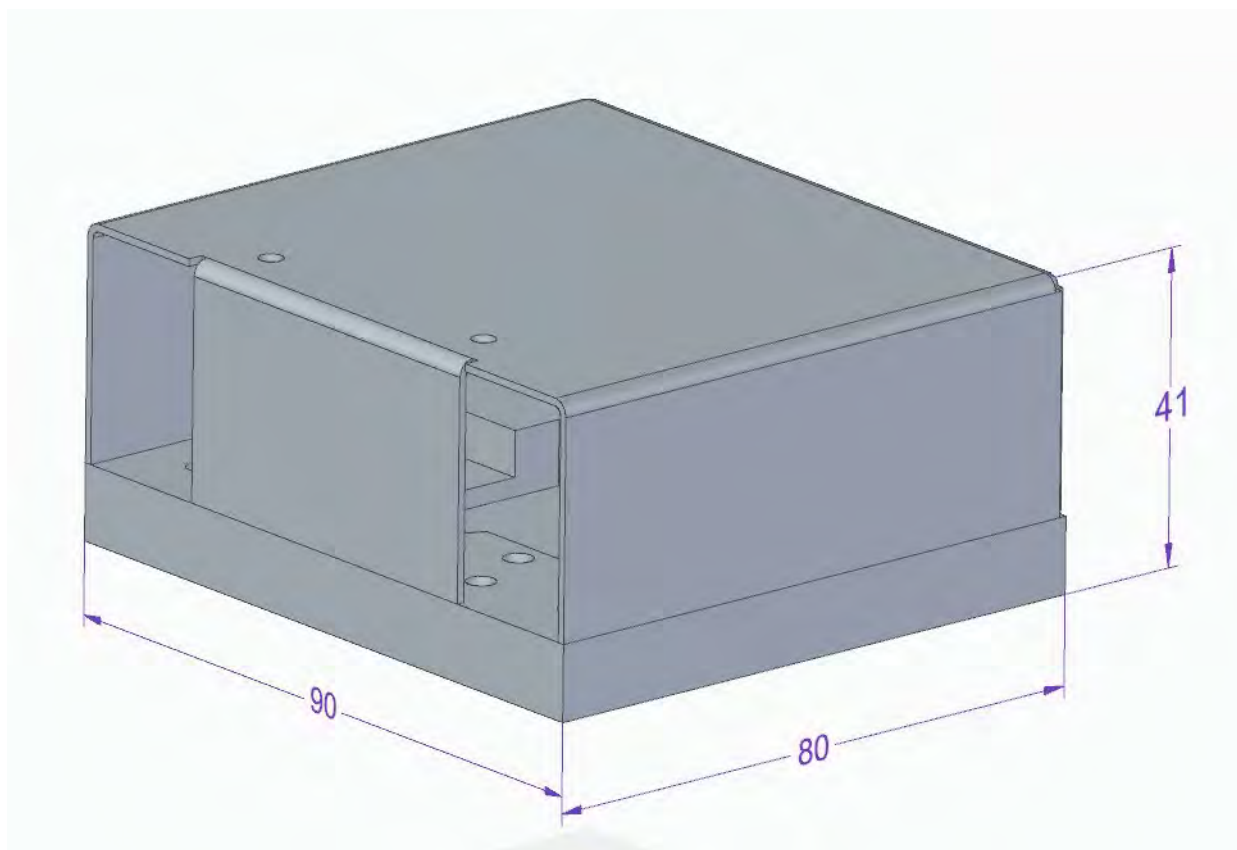
Figure 2-5: AIRMO column oven of the µ-GC system

2.2.2   Warwick's 3D printed µ-GC

2.2.2.1 UWAR µ-GC

Conventional gas chromatography (GC) is known for its high accuracy and versatility in analysing complex mixtures of chemical compounds with similar physiochemical properties. However, these systems are expensive, bulky, and require high power, making them unsuitable for field-portable applications. Therefore, there is a clear need for economical, compact, and energy-efficient alternatives that can provide comparable performance. Development of an efficient and inexpensive 3D printed µ-GC column is one of the key deliverables of the PurPest project, which aims to facilitate quick onsite analysis of compound mixtures. The goal is to integrate this µ-GC column with an electronic nose (e-nose) system comprised of an array of four highly sensitive solidly mounted resonators (SMR) devices coated with different selective sensing materials. The integration of the µ-GC column will assist in separating compound mixtures so that they reach the SMR sensor array with a variable time delay, providing enhanced compound classification using machine learning algorithms. The overall scheme of this integrated system is shown in **Figure 2-6**.
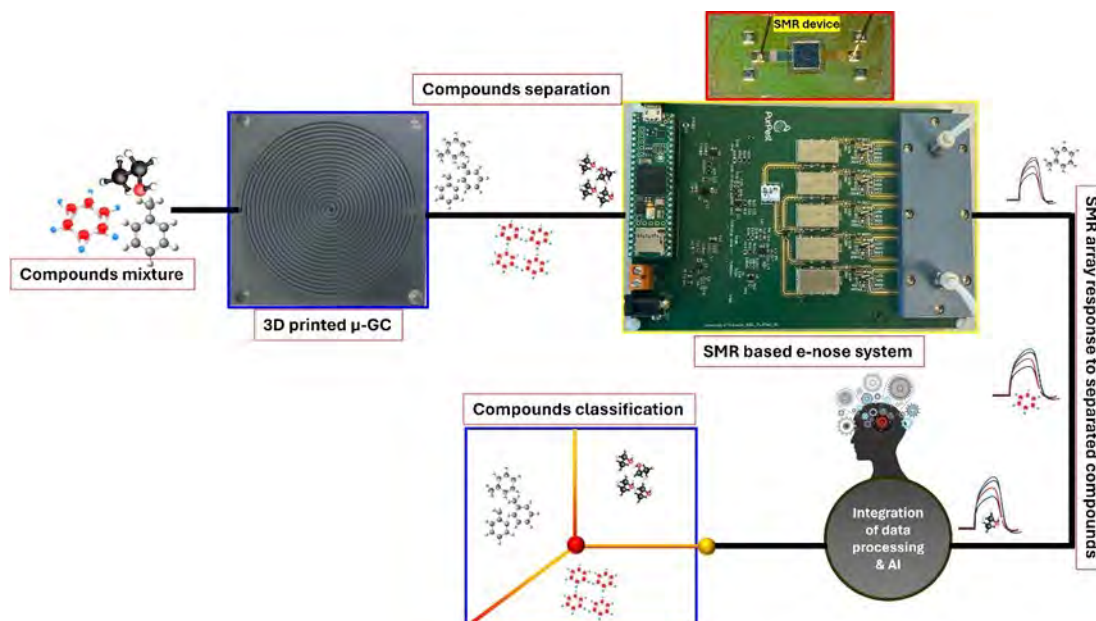
Figure 2-6: Overall scheme of UWAR sensing unit for PurPest project.

2.2.2.2 COMSOL Multiphysics simulations of UWAR µ-GC

To understand the diffusion and fluid mechanics of the target VOCs while passing through the µ-GC, a 2D model of a spiral-shaped micro-gas chromatography (µ-GC) column was developed using COMSOL Multiphysics. The column features a thin polydimethylsiloxane (PDMS) retention layer with a thickness of 10 µm. The initial designed column has a channel length of 0.4 metres and a width of 0.5 millimetres, as illustrated in **Figure 2-7**.
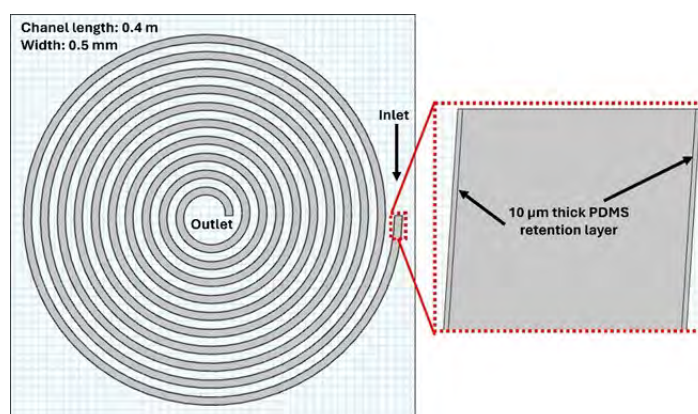
Figure 2-7: COMSOL Multiphysics 2D model of a µ-GC.

To simulate the performance of the µ-GC column, two primary physics modules were employed:

Transport of Diluted Species: This module was used to model the diffusion and convection of chemical species within the column. It simulates the move of different species through the column under the influence of concentration gradients and flow conditions.

Laminar Flow: Given the small dimensions and low Reynolds number typical of microfluidic systems, laminar flow conditions were assumed. This module helps in simulating the velocity profile of the carrier gas within the spiral column.

Visual representation of ethanol at different time interval as it passes through the channel and diffused in PDMS retention layer is shown in **Figure 2-8**.

The results of the simulation, depicted in **Figure 2-9,** demonstrate the separation performance of the µ-GC column for three different chemical species: ethanol, benzene, and toluene. The separation is achieved due to the differential interaction of each species with the PDMS retention layer, which affects their respective migration rates through the column. However, the resolution of the species separation needs to be further improved. The obvious way to achieve better resolution is by increasing the channel length from the short 0.4 m, which will lead to finding the optimal channel length for pest odour separation.

Figure 2-10 illustrates the velocity and pressure drop profiles throughout the channel length. A uniform velocity profile is observed along the entire channel, whereas the pressure significantly drops as it passes through the channel, nearly reaching zero at the outlet.

We are working on optimizing the column dimensions (length and channel) and the material for the retention layer, to further improve the separation efficiency and resolution of the designed model.

Simulation plays a crucial role in the design and optimization of micro-gas chromatography (µ-GC) columns. Here is how simulation can help:

1- Optimization of µ-GC dimensions.
2- Help to analyse the column efficiency (number of theoretical plates).
3- Help to understand the retention layer thickness effect.
4- Prediction of retention time for different species
5- Prediction of separation resolution, how well species peaks are separated.
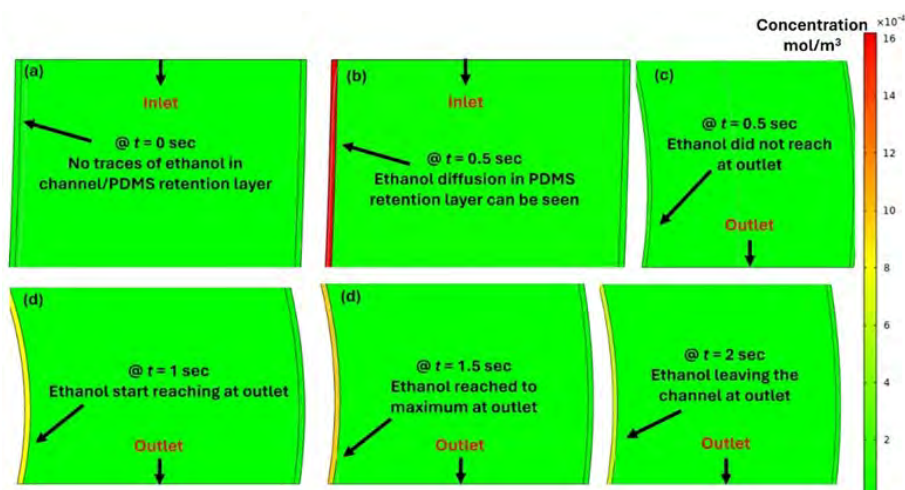
Figure 2-8: Visual representation of ethanol flowing through the channel at different time intervals.
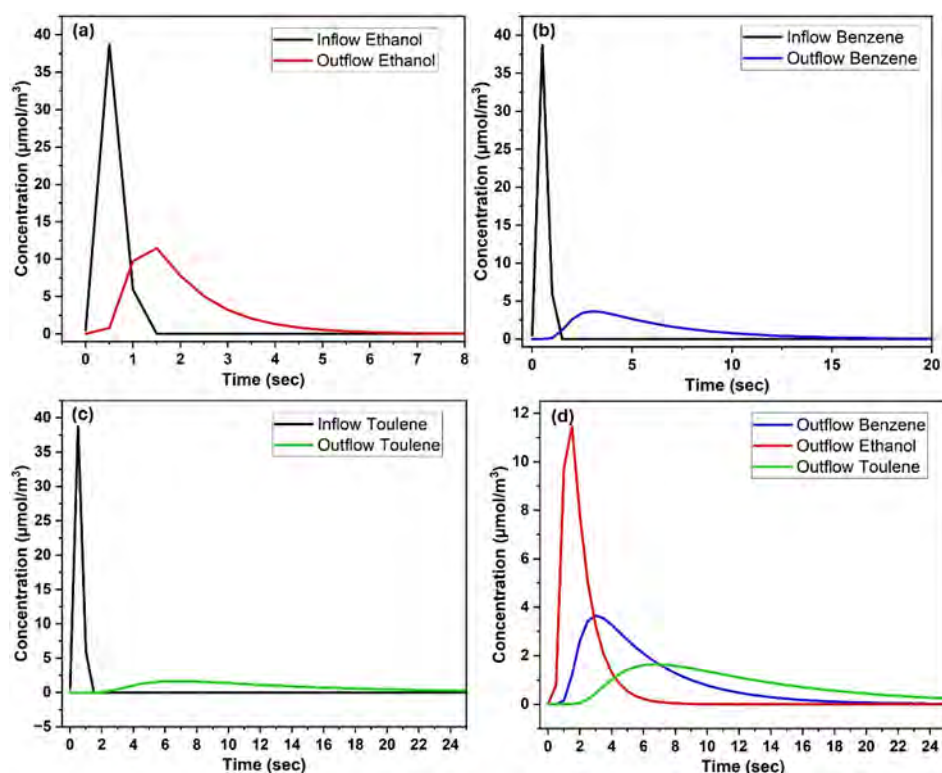
Figure 2-9: Simulated inflow/outflow profiles of three different species, (a) ethanol, (b) benzene, (c) toluene, and (d) outflow of all three species.
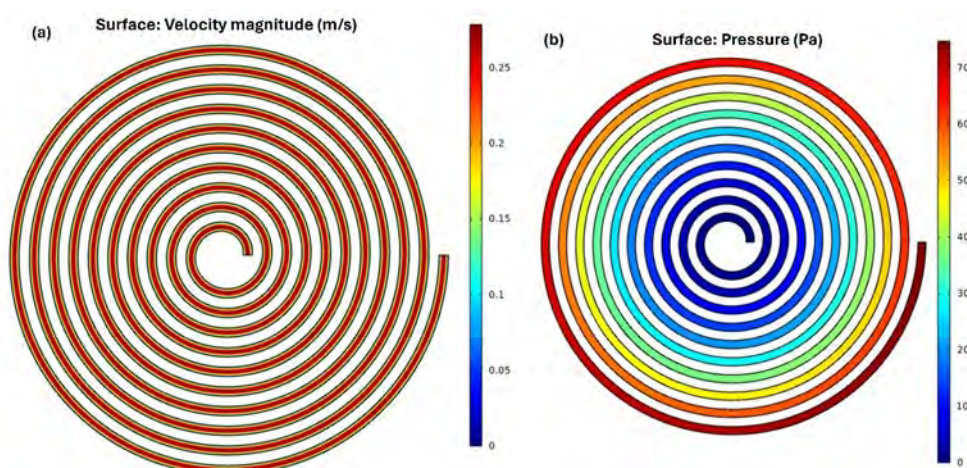
Figure 2-10: Simulation results for velocity and pressure profile throughout the channel.

2.2.2.3 Design and Fabrication of µ-GC Columns

The spiral shaped 3D model of the µ-GC Columns was designed in SolidWorks and printed using a low-cost 3D printer (Elegoo Mars 4 Ultra). For our initial studies, we have made a relatively short column length but up from 0.4 m to 1.2 m (see **Figure 2-11**). The overall dimensions of the printed µ-GC substrate are 40 mm × 40 mm × 5 mm (length, width, and height) with a channel length of approximately 1.2 m, width of 0.5 mm, and depth of 0.4 mm. After coating with appropriate material, the column was sealed with the 1mm thick resin coated PETG substrate. Polyethylene glycol (PEG) and OV-1 (PDMS) coated µ-GC columns were tested during the intercomparison campaign at AIRMO and the results are displayed in the "testing and performance of component section". **Figure 2-12** displays the fully sealed PEG and OV-1 coated µ-GC columns.
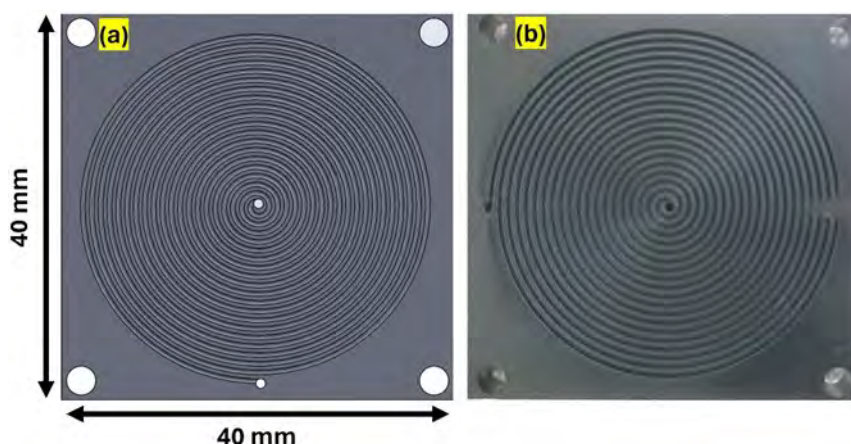
Figure 2-11: Spiral shaped µ-GC Column (I =1.2m, w =0.5mm, d =0.4mm), (a) SolidWorks design, and (b) 3D printed column.

For comparison and to identify best coating we are planning to test multiple stationary phase coatings including PEG (for polar compounds), Ethyl cellulose (non-polar), OV-1 (non-polar), and OV-5/7 (slightly polar). See **Figure 2-12**. Beside coating material there are several parameters which play pivotal role in optimizing the performance efficiency of a GC column such as operating temperature, flow rate, and injection pulse width. The µ-GC research plan, outlined in a flow chart,

involves a systematic approach to design, fabrication, initial testing, parameter optimization, and comparative analysis to refine the performance of these µ-GC columns for various compounds, and is shown in the "testing and performance of component" section.
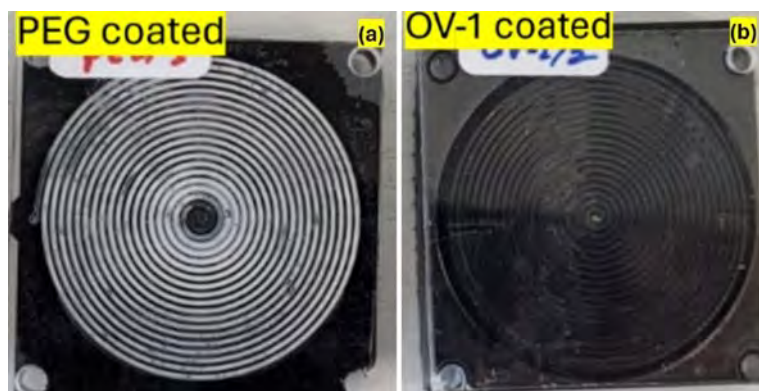
Figure 2-12: Fully sealed 1.2 m µ-GC Columns (a) PEG coated, and (b) OV-1 coated.

2.3   Detection elements

2.3.1   SERS sensing

Raman spectroscopy is a powerful technique providing "fingerprints" of specific molecules without the need of labelling elements. However, Raman signal is very low and therefore requires enhancement for practical applications. In PurPest, SINTEF and Saftra Photonics are working on developing a surface-enhanced Raman spectroscopy (SERS) system for VOCs detection. The SERS sensing comprises three parts; the Raman spectrometer, flow cell and SERS chip.

2.3.1.1   Raman spectrometer – Saftra Photonic's Ramascope

Ramascope[TM] (**Figure 2-13**)is a versatile portable Raman instrument with full control of measurement parameters (laser power, acquisition time, multiple acquisitions). The device consists of a polychromator based on transmission gratings, CCD detector, laser excitation source (785 nm) and mechanics for placing a nanostructured chip. Ramascope is equipped with data acquisition and evaluation software. The technical parameters of the Ramascope are as follows: excitation wavelength 785 nm, laser power is adjustable up to 100 mW, spectral resolution 8 cm^{-1}, spectral range 250 - 2200 cm^{-1}, SERS averaging area 0.3 x 0.3 mm, base dimensions 250 x 180 x 80 mm.

To achieve the main goal of the PurPest project – the detection of very low concentrations of VOCs, RAMASCOPE was modified/tailored in its optical part (optimizing the trajectory of the excitation light) and mechanical part (optimizing the position of the flow cell holder). Moreover, software was developed for measuring VOCs (repeated measurements).

Figure 2-13: left: RAMASCOPE detection system. Right: Installation of RAMASCOPE on the testing table

2.3.1.2   Flow cell and chip holders

VOCs measurement by RAMASCOPE detection system needed a development of a specific Flow cell assures an optimal air flow condition in the location of the detection nanostructured chip. Final solution is presented on **Figure 2-14**. This flow cell construction required only minimal change in "scanning sample holder", and thus by such flow cell construction we have expanded the possibilities of RAMASCOPE for measurements in the gas phase as well. Related laminar flow and cuvette sealing tests were carried out in the SAFTRA photonics laboratories and therefore before the intercomparison campaign described in section 3.2.1.

Figure 2-14: Flow cell and chip holder by SAFTRA Photonics.

2.3.1.3   SAFTRA PickMol SERS chip

PickMol^{TM} technology is based on plasmonic enhanced Raman scattering and is represented by a nano-optical/nanostructured chip (PickMol^{TM} Sensing Chip), detection system (PickMol^{TM} RAMASCOPE), measurement & evaluation software (PickMol^{TM} sw/application) and database of pure forms of detected molecules (PickMol^{TM} database). The technology is dedicated for high-sensitive screening (sub-nanomolar) of the organic and inorganic compounds mainly in liquid samples.

Nanostructured chip has designed surface for sensitive and selective detection of molecules based on PERS/SERS effect. The reproducibility of PERS/SERS detection is significantly increased by area-averaging of the Raman signal.

The physico-chemical principle of a detection of organic molecules by the PickMol technology is based on Plasmon/surface enhanced Raman scattering (PERS/SERS). This technique has been adopted by SAFTRA photonics and tailored in a way assured high sensitivity, selectivity,

robustness, and reproducibility of detection of the molecule of interest. To reach this objective, the basic technology must be optimized a tailored by so coaled "functionalization" on nanostructured surface. Appropriate functionalization of the nanostructured surface assures an approaching of the molecule of interest close to the nanostructured surface which consequently increases the Raman signal of the molecule of interest after an excitation of the surface by laser light. Therefore, surface functionalization plays the role of a selector of detection and for each molecule of interest the functionalization is different (in the majority of cases) and thus, must be chosen for each molecule of interest – "tailored technology".

2.3.1.4   SINTEF SERS chip

SINTEF's SERS platform has a customised die size and active SERS area to meet Saftra Photonics Raman spectrometer specifications. The SERS structures, including C-shape, Y-shape and a Star-shape nanopattern lattices, are designed and optimised to obtain surface plasmon resonance within the 700 – 900 nm range.

Two of the potential target VOCs, namely indole (consisting of phenyl ring) and terpenes (which has C=C double bonds) exhibit characteristic Raman shifted peaks within the fingerprint region (450-1700 cm^{-1}). Based on our choice excitation wavelength (785 nm), this corresponds to a detection wavelength range of 800-900 nm. The plasmon response of the SERS platform (700-900 nm) covers the planned detection wavelength range (800-900 nm), ensuring maximum SERS enhancement.

Two types of SERS substrates were fabricated, both are based on UV-NIL imprinted nanopatterns in resist on 6" Si wafer. First, were imprinted resist coated with a thin layer of gold (Figure 2-15). Second, the pattern was etched in Si and then coated with Au.
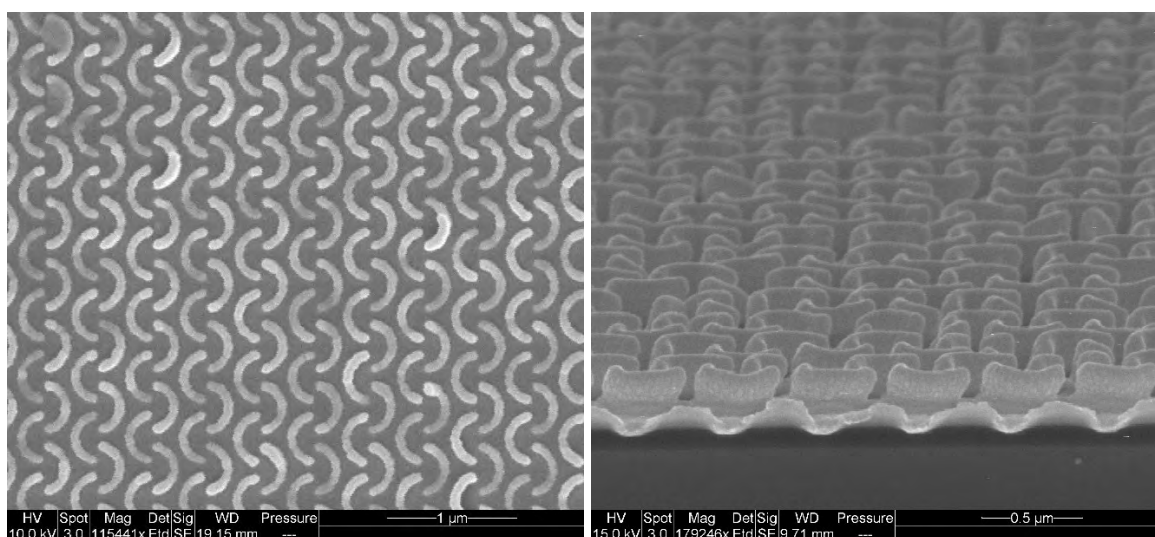
Figure 2-15 SEM picture of the C-shape SERS substrate

2.3.1.5   SINTEF MOF chips

MOFs where prepared onto Si chips covered with Au. This was to test to see if the MOFs themselves could work as SERS surfaces.

Our approach was to use spin coating to deposit a MOF layer onto the Si chips. We screened eight MOFs and seven liquids at various spin rates, spin times, and initial amounts (**Table 2-1**). Not all possible combinations were explored.

Table 2-1: Parameters that were varied when applying MOFs to Au covered dies.

MOFs	Liquids	Spin rates (rpm)	Spin time (s)	Amount (drops)
HKUST-1	H_2O	0	0	1
MOF-177	DMF	500	5	2
UTSA-16	C_8F_8	750	10	4
UiO-67	C_9F_9	1000	15	7
ZIF-9	PGMEA	1500	20	12
ZIF-12	TEGDME	2000	30	19*
NU-1000	Galden HT 170	2500		
MOF-808		3000		*drops also added during spinning
		3500		

Based on SEM studies of the observed coating, UiO-67 and NU-1000 were found to be the most promising materials. PGMEA was found to be a suitable liquid. Surprisingly, the coatings prepared at 0 rpm spin rate, i.e. drop casting, were superior to the ones prepared at 500 rpm or higher.

For further testing twelve samples were prepared with UiO-67 and NU1000. For each MOF, two samples with one, two and three coating applications were made (two of each). After each MOF dispersion was deposited the sample was dried at 80 °C for two hours.

All dies were placed in Saftra's chip holders. Each sample was marked with sample name on the back of the holder.

2.3.2 SMR sensor array

2.3.2.1 *SMR devices and coating materials*

Solidly mounted resonators (SMRs) are sensors in which a thin piezoelectric films are excited to resonate in an oscillator circuit and produce a standing acoustic wave in the device. The frequency of this standing wave is proportional to the mass loading on the resonator surface, a feature that can be exploited to detect volatile organic compounds (VOCs). However, the selection of the appropriate coating material is crucial to ensure high sensitivity and selectivity for detecting a target compound. Figure 2-16 shows a SMR device coated with ethyl cellulose (EC) and its resonance before and after EC coating measured with a low-cost commercial LiteVNA (**note: this is a basic low-cost handheld device and we use expensive accurate spectrum analysers to validate any results**). A slight change in the resonance characteristic peak can be seen after EC coating which can be attributed to the mass loading of the coating material. With our coating testing setup of LiteVNA we are expecting to see the similar change in resonance upon exposure of the target compound to the coated SMR.
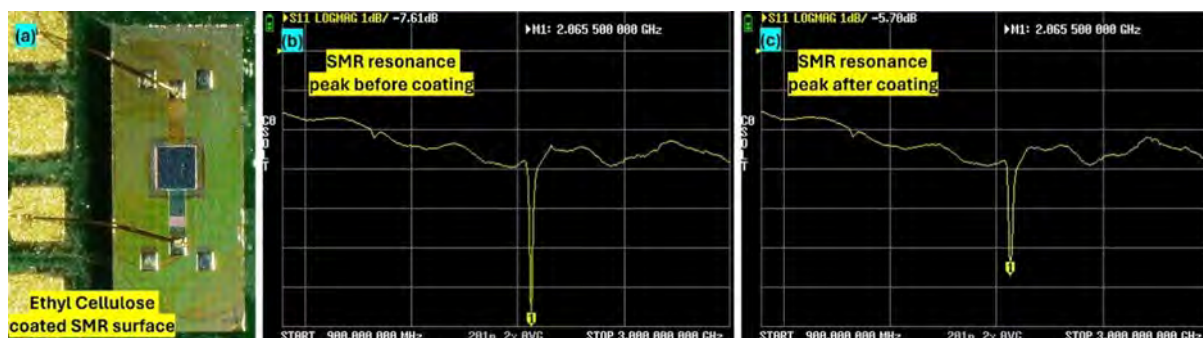
Figure 2**-16**: (a) a microscopic image of the EC coated SMR, resonance peak measured using LiteVNA (b) before, and (c) after EC coating.

During the initial investigation in Work Package 1 (WP1), PurPest partners identified four different compounds of interest: 2-methylbutanol, trans-2-hexanal, D-limonene, and linalool. By carefully selecting and applying the correct coating materials on the SMRs, the sensors can achieve optimal performance in detecting these VOCs, a literature review was conducted to identify different coating materials for the target VOCs. Following sensing materials are found to be most suitable for the target compounds.

1- Tungsten trioxide nanostructures (WO$_3$ NSs) for slightly polar/nonpolar compounds
2- Ethyl cellulose for nonpolar compounds
3- Silica OV-1 for nonpolar compounds
4- Thiol functionalized gold nanoparticles (Au NPs) for nonpolar compounds
5- Reduced graphene oxide for polar compounds
6- Polyethylene glycol for polar compounds
7- Highly porous polyaniline (PANI) for polar compounds

Furthermore, the formation of composites or hybrids of suitable materials is worth exploring due to the synergistic effects of the individual components. This synergy can enhance both the selectivity and sensitivity of the composite material, leading to superior performance compared to the individual materials alone.

2.3.2.2 SMR testing setup

The setup for a quick test of the prepared coating material involves the following components: a portable LiteVNA, a 3D printed chamber, and an SMR-mounted PCB. The prepared coating will be applied either by drop-casting or spin coating onto the SMR surface. When the coating is exposed to the target compound, it is expected to cause a shift in the resonance frequency and a change in the dip intensity. This setup allows for convenient and rapid testing of the sensitivity of the prepared coating to the target compound. **Figure 2-**17 shows the setup for coating testing.

Here we would like to acknowledge SINTEF for providing the chamber design file and PCB design to mount the SMR device.
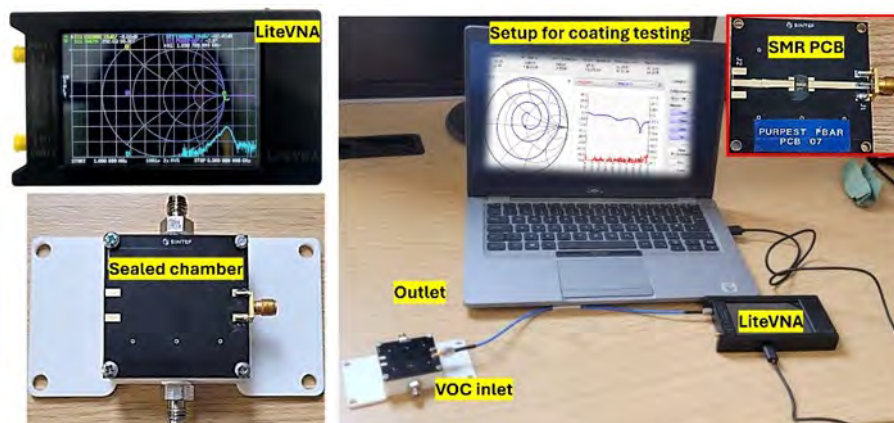
Figure 2-17: Setup for coating testing.

3 TESTING COMPONENTS AT INDIVIDUAL PARTNERS

This chapter describes the test setups used by the individual partners in the initial testing of their components.

3.1 SERS chip testing at SINTEF

3.1.1 SINTEF SERS setup

SINTEF made a setup for the SERS measurements, shown in **Figure 3-1**. The VOCs are delivered via a permeation test setup from AIRMOTEC via a valve manifold. The latter is manually operated and can guide the VOCs either to the ambient or to the gas cell. It also has a by-pass to that the gas cell can receive clean air. The Raman probe (B&W Tek iRaman Plus portable Raman spectrometer) is held by a manual XYZ translator stage (Thorlabs).
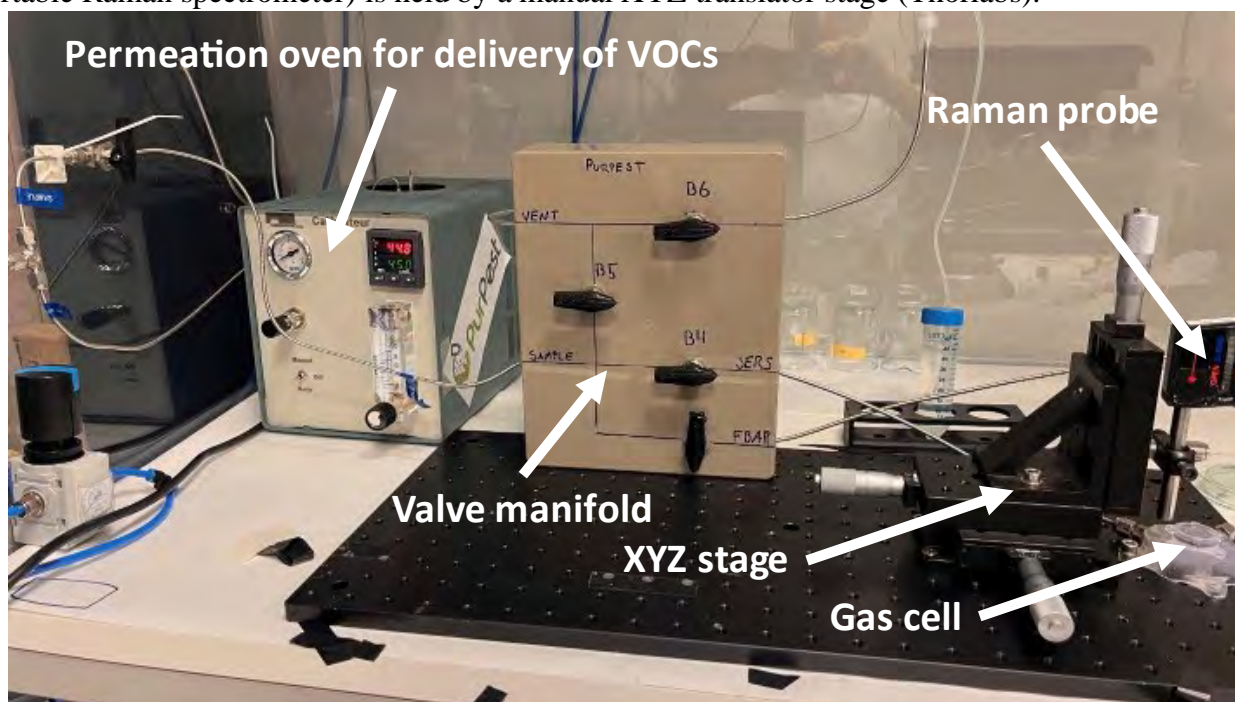
Figure 3-1: Test setup at SINTEF.

The gas cell is custom 3D printed setup for measuring Raman reflectance (**Figure 3-2**). The 3D-printed gas test cell is printed in clear resin (Formlabs 3) which is a solid construction that should not leak. A 150 µm thick glass sheet was attached using cyanoacrylate adhesive (super glue).

One disadvantage of this gas cell is that the Raman probe must be moved when changing the sample. Therefore, a new gas cell has been designed and 3D printed in which only the sample is exchanged (**Figure 3-3**). For this setup the sample is situated in a chip holder that is compatible with Saftra's flow cell.
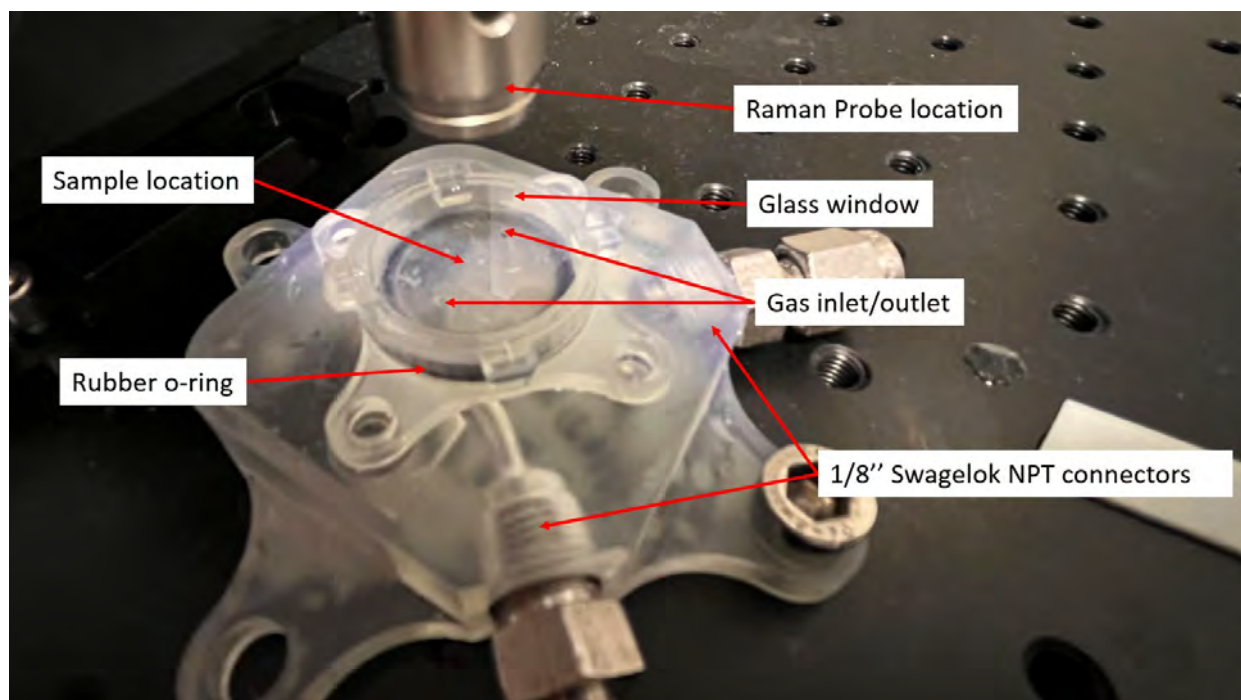
Figure 3-2: The original SERS gas cell at SINTEF

A permeation unit from AIRMO was used to deliver VOCs in gas in a controlled manner. The system is based on a flow oven with high precision temperature control through which a constant gas flow runs through. The gas flow is controlled by the inlet pressure into the system.
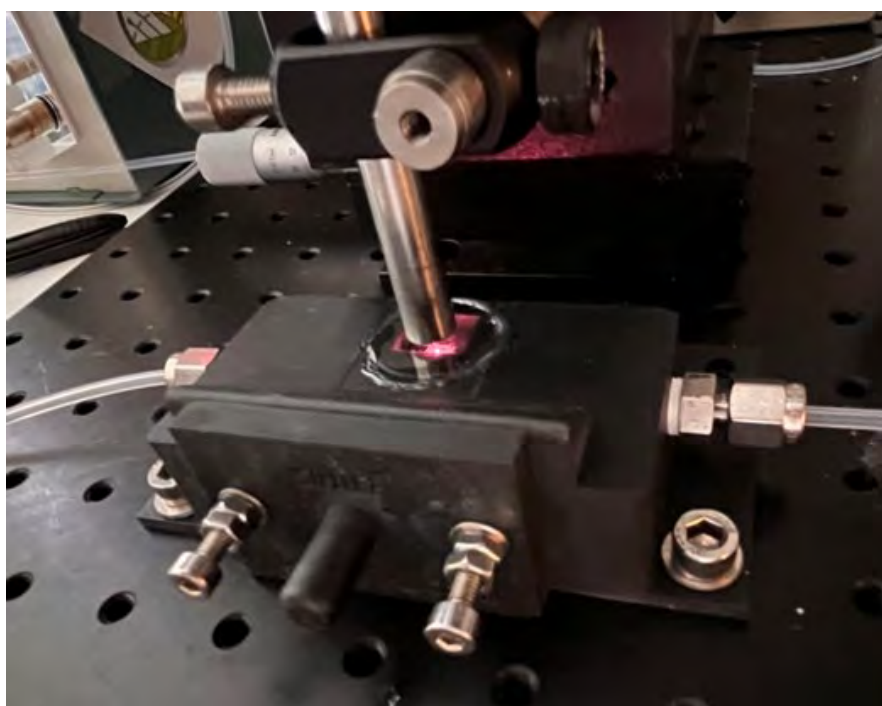
Figure 3-3: The new gas cell for Raman testing will be used from summer 2024.

The iRaman Plus is controlled by BWSpec software, which allows for both single measurements and timed sequential measurements. In the latter case the program saves the measurement automatically with a given file name and a numbered suffix. SINTEF made a script in the software Igor Pro (by Wavemetrics) to import and analyse the data.

The samples where first flushed with compressed air during which the dark- and the reference spectra were recorded. After this valve B6 was closed together with the air valve (not shown). After about 5-7 seconds the first recording was started. Alternatively, timed recordings were started during the clean air exposure to get multiple references, after which the sensor was exposed to VOCs.

3.1.2   Results SINTEF SERS

The first trials with SERS chips from SINTEF were done by measuring Raman signal of acetone. The acetone was in a permeation tube provided by AIRMOTEC and its concentration at various parameters were measured at Arimotec. As a starting point we used the settings to give the highest concentration, estimated at 0.5 ppm. In some cases, we wanted to have higher concentrations and therefore carried out "accumulation", where the outlet of the permeation oven was closed in order to slowly increase the concentration of acetone in the oven before the content was sent to the gas cell.

Figure 3-4 and **Figure 3-5** show Raman spectra of SERS dies with photoresist+Au and Si+Au, respectively. Ther was no clear indication of any acetone peaks, even when doing accumulation for the latter sample.
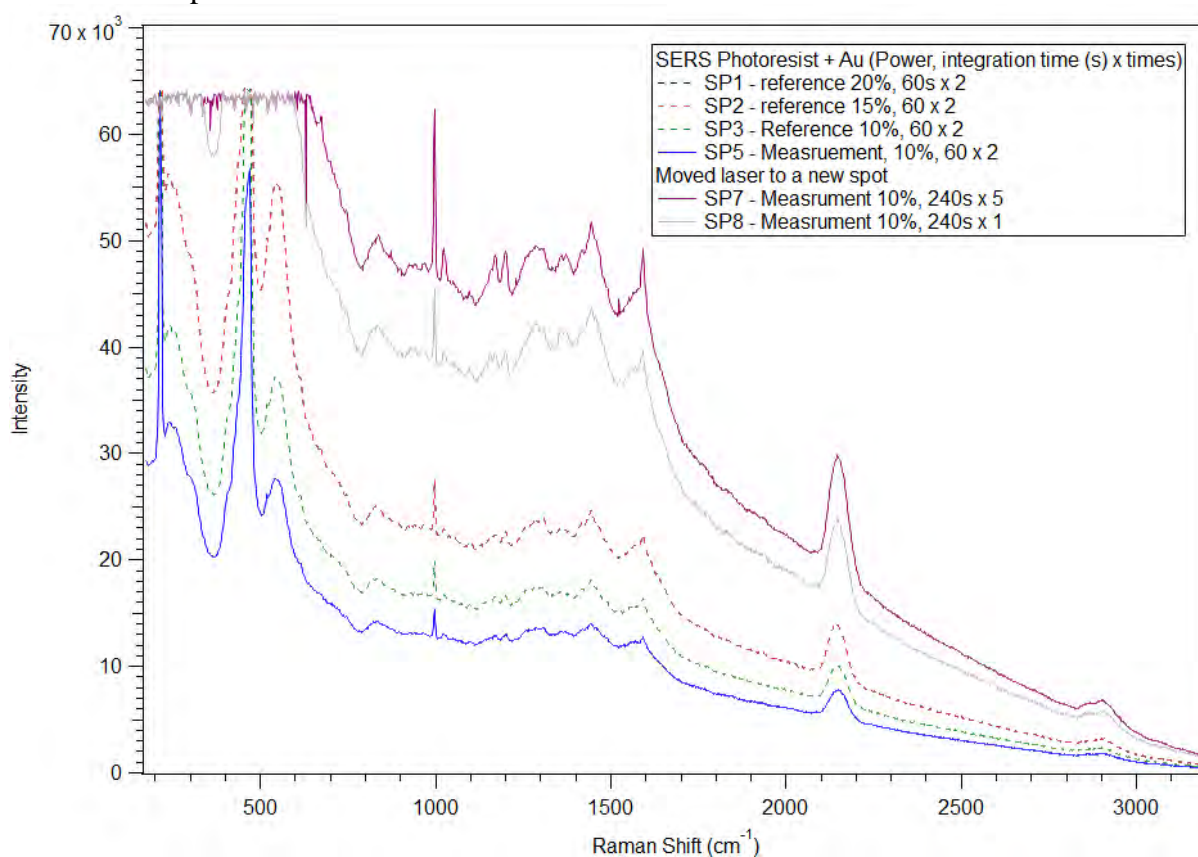
Figure 3-4: Raman spectra taken from SERS chip with patterned photoresist and Au. There was no indication of detection of acetone.
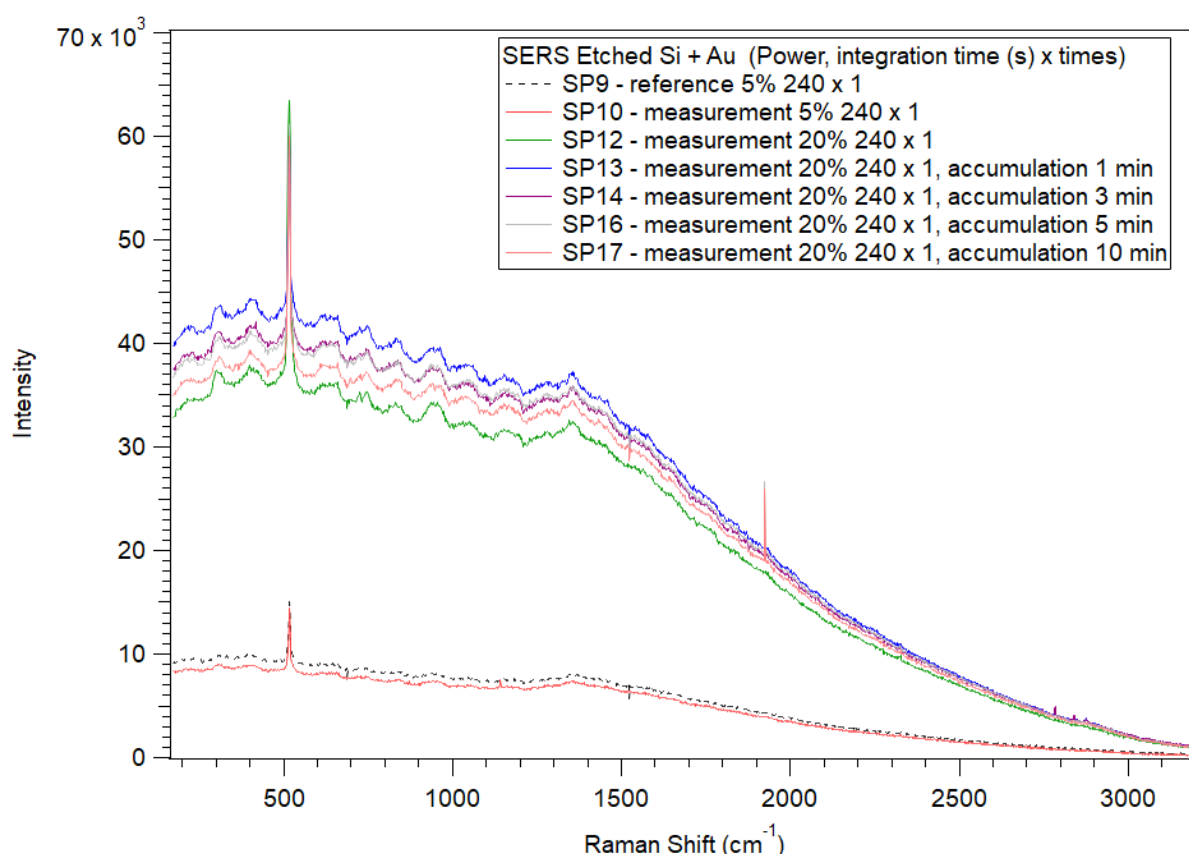
Figure 3-5: Raman spectra taken from SERS chip with etched Si and Au. There was no indication of detection of acetone, even when doing accumulation experiments which were expected to give higher concentrations.

3.1.3   Results SINTEF MOF on Au

It was decided to test if MOF powders could be used as SERS structures. The MOFs contain metal clusters and are able to concentrate a sample in testing. Moreover, the size of some of the MOF's crystals were observed to be in the same order of magnitude as the SERS designs promising enhancement for Raman signal.

The MOF samples were measured in air first to obtain the Raman spectra of the specific MOFs and establish the consistency of the measurements. These can be seen in **Figure 3-6**. For NU1000, the signal strength increases with the number of coats. The broader background also increases, indicating a fluorescent component in the MOFs. For the UiO-67, the samples with 2 coats have the strongest signal. This is probably due to the inhomogeneity of the deposition.
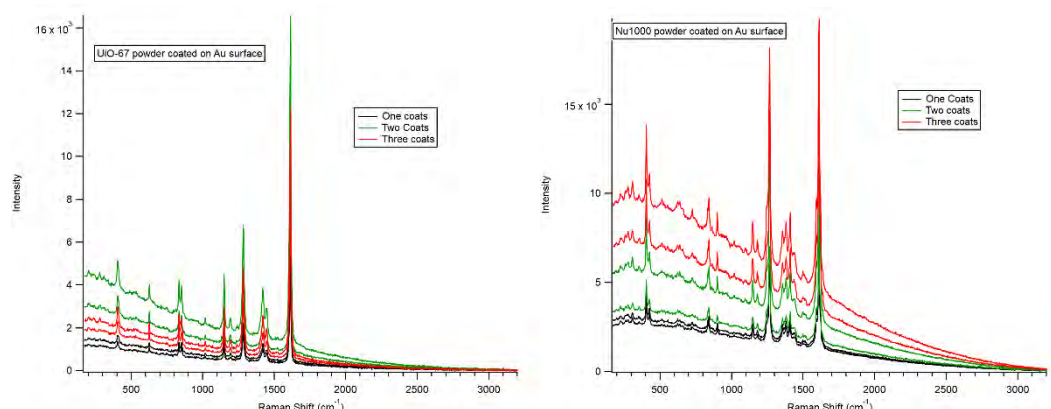
Figure 3-6: Measured Raman spectra of UiO-67 (left) and NU1000 (right) with three different coats.

The MOF UiO67 showed potential when exposed to high concentrations of d-limonene. For this experiment 2 ml of d-limonene was added to a glass wool in a small beaker and lowered into the permeation oven. The purpose of the glass wool was to increase the evaporation rate and thus increase the concentration of the VOC. We have not yet been able to estimate the concentration.

For the first ten measurements the MOF was flushed with compressed air after which the VOC valve was opened, and the MOF was exposed to d-limonene and Raman spectra were measured showing a formation of new peaks related to d-limonene (760, 1645, 1677 cm^{-1}), as well as a shift of multiple peaks (Figure 3-7).
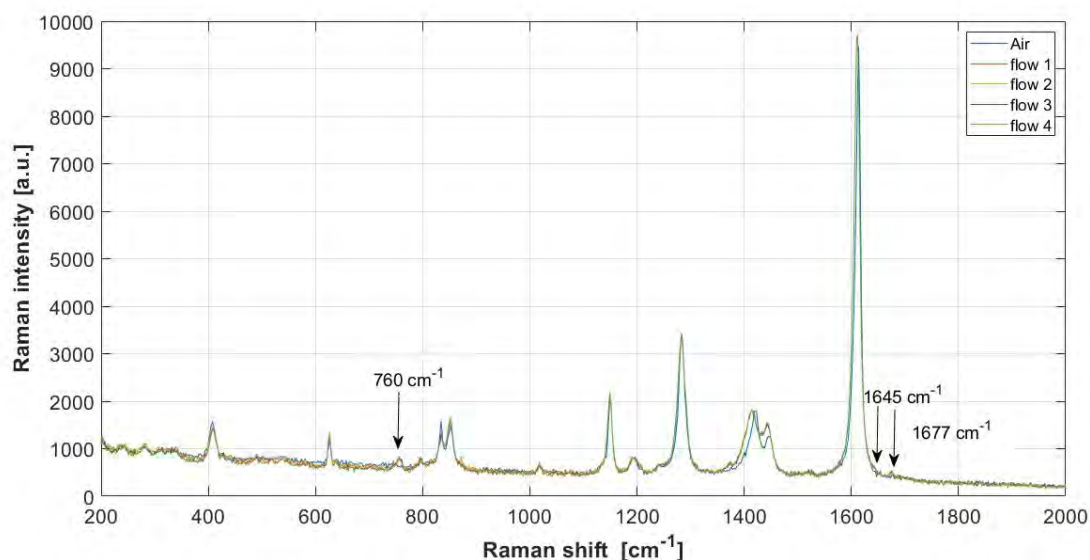
Figure 3-7 Measured Raman spectra of MOF UiO67 before and after exposing to d-limonene

The most significant difference, as seen from **Figure 3-**8 is a shift of the peak at 1421 cm^{-1} to 1412 cm^{-1} after the MOF has been exposed to the VOC. The peak is stable for about an hour or two (sequence 700) after which there is a clear decrease in the intensity. The latter is probably due to MOF burnout from the laser exposure.
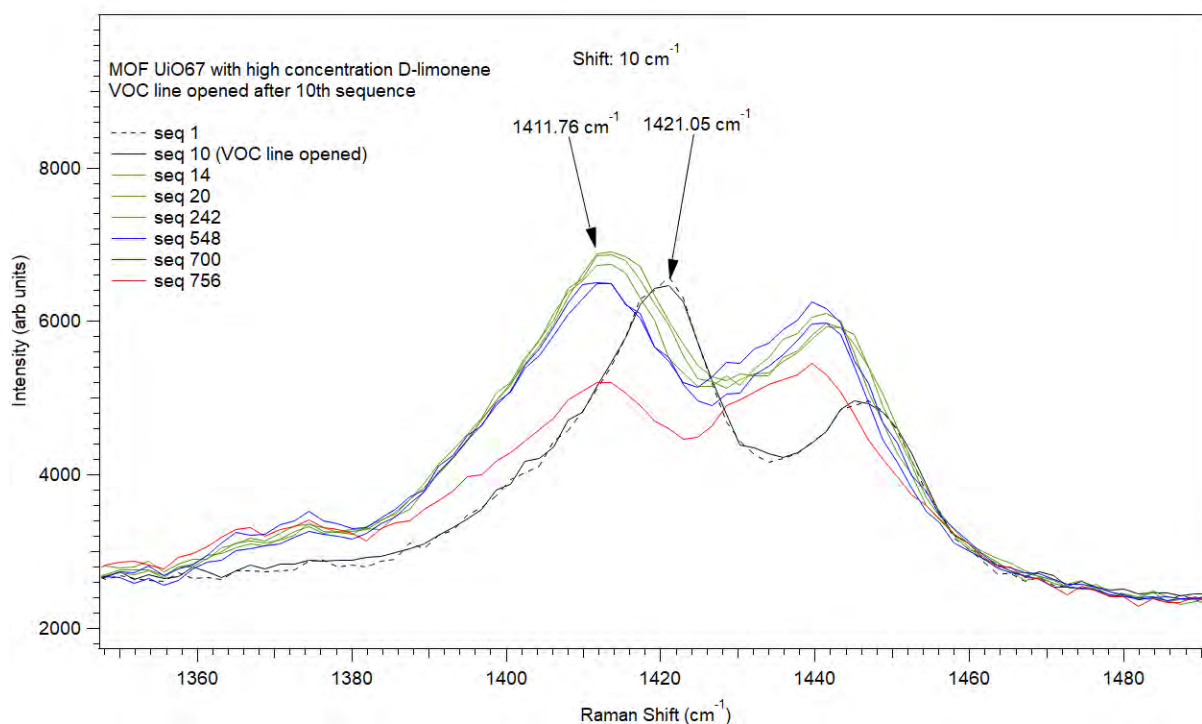
Figure 3-8: A Raman peak at 1421 cm^{-1} shifts to 1412 cm^{-1} after exposure to high concentrations of d-limonene.

This result is a very good indication that UiO67 can be used as a coating for SERS measurements to facilitate the detection of d-limonene by increasing the concentration of the VOC molecules close to the SERS surface and therefore enhancing the signal. Similar result was observed when measuring Raman signal with the NU1000 MOF exposed to d-limonene (Figure 3-9).
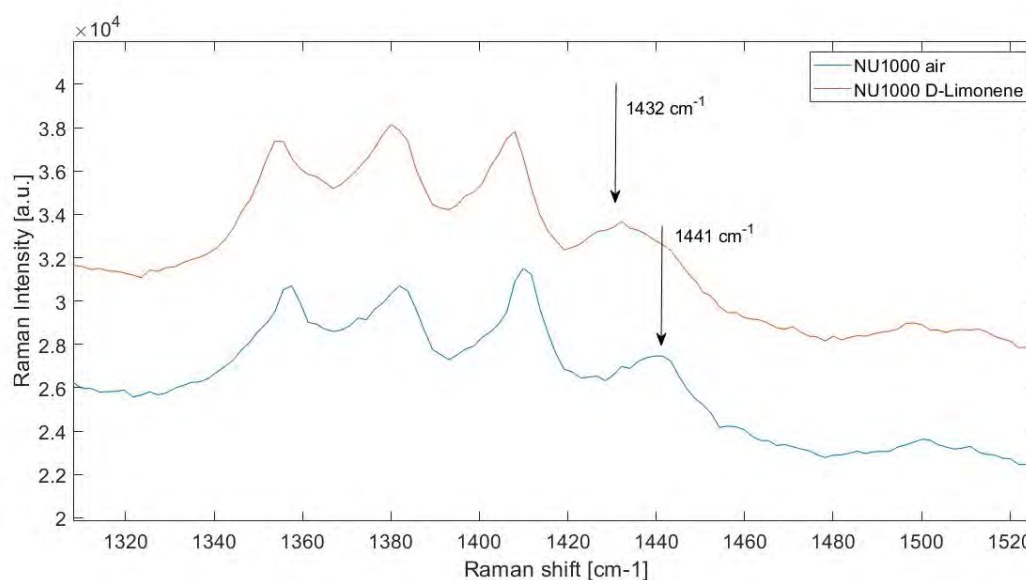
Figure 3-9 A Raman peak at 1441 cm^{-1} shifts to 1432 cm^{-1} after exposure to high concentrations of d-limonene.

3.1.4 Conclusions and further work for SINTEF SERS samples

The results obtained thus far from SINTEF SERS substrates, which include both Nanoimprint Lithography (NIL) resist and silicon (Si) etched substrates, have not demonstrated any significant sensitivity to exposure to volatile organic compounds (VOCs). Despite these findings, our measurements of the Raman signal using metal-organic frameworks (MOFs) exposed to d-limonene have indicated a promising response. Consequently, the focus of future research will shift towards integrating the tested MOFs onto the surface of Si etched SERS substrates to enhance their performance.

The further work will involve several steps. First, ten silicon wafers will be fabricated utilizing ultraviolet UV-NIL, RIE, and gold evaporation techniques. Next, a thin layer of the metal-organic framework UiO-67 will be grown on the surface of the prepared silicon substrates. The selection of UiO-67 is based on its favourable properties and previous success in detecting d-limonene. This growth process will be controlled to achieve uniform coverage and optimal thickness, which are crucial for enhancing the sensitivity of the SERS substrates.

Following the fabrication of the MOF-coated SERS substrates, they will undergo testing to evaluate their sensitivity and limit of detection (LOD) for a range of selected VOCs. These tests will include exposing the substrates to varying concentrations of the VOCs and measuring the resulting Raman signal intensities. The aim is to determine the lowest concentration of VOCs that can be reliably detected using the MOF-enhanced SERS substrates.

3.2 Previous results for e-nose tested at Warwick

3.2.1 Performance of individual SMR coated with CO_2 sensitive material.

The SMR device was coated with CO_2 sensitive polymer developed by Sorex Sensors Ltd., Cambridge, UK. The sensors and interface circuitry were placed in a commercial Memmert oven for testing. Figure 310 shows the response of the differential configuration to three consecutive exposures to 1%, 3%, and 5% CO_2 in dry air. The frequency shift for each gas concentration is found to be 7–8 kHz, 15–19 kHz, and 25–30 kHz, respectively. During these experiments the oven temperature was kept at 40 °C while the sensor micro-heater was set to 70 °C.
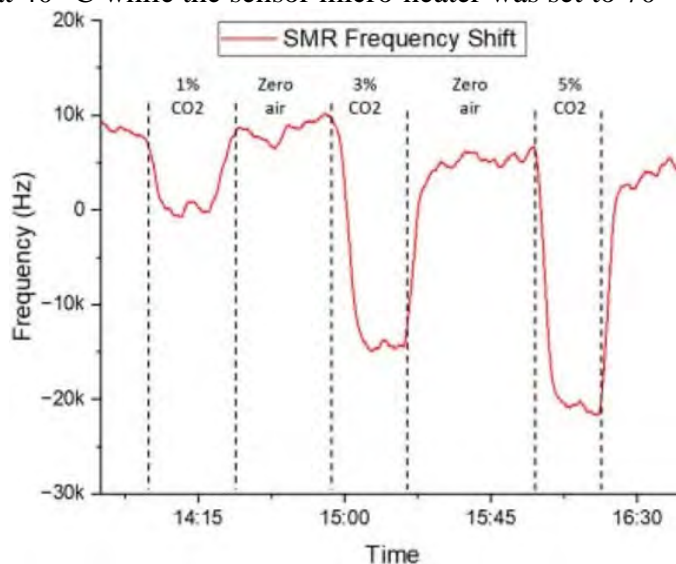
Figure 3-10: µ-GC testing setup results with PEG coated column to different compounds, (a) S1-S2 response to limonene and benzene as interest at different time intervals, (b), enlarged

view of the S2 response with limonene and benzene as interest, (c) S1-S2 response at higher concentration of 2-methyl butanol, and (d) S1-S2 response to higher concentration of limonene.

4 INTRODUCTION AND OBJECTIVE OF THE INTERCOMPARISON CAMPAIGN
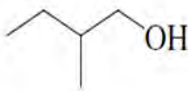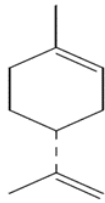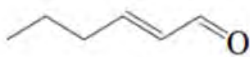
4.1 Context and Scope of the Intercomparison

As a first trial of detection of the Volatile Organic Compounds (VOCs) specific to the VOCs and VOC patterns that were observed from pests in pure culture (WP2), some of the newly developed sensors and analysers were ready to detect target VOCs that were chosen on the basis of permeation tube technology. The choice of these VOCs is considered important for the further optimization and improvement of the sensors and analyzers. In the scope PurPest project, 3 pests were highlighted as species that are targeted for their plant invasion in Europe:

- *Phytophthora ramorum*,
- Cotton bollworm (CBW, *Helicoverpa armigera*),
- Brown marmorated stink bug (BMSB, *Halyomorpha halys*).

Considering the first pest, **Phytophthora ramorum**, 2-methyl-1-butanol and ethanol were chosen as targeted VOC biomarkers, whereas for the **CBW**, d-limonene was selected and finally for the **BMSB**, (E)-2-hexenal or trans-2-hexenal was the target for detection as it is a major green leaf volatile (Arimura & Pearse, 2017). **Table 4-1** shows the targeted VOCs corresponding to each targeted pest is presented below along with the molecular weights and the CAS number of each compound.

Table 4-1: Targeted VOCs specific for 3 targeted pests for the intercomparison.

Targeted Pest	Targeted VOCs	Name	Molecular Weight (g/mol)	CAS number
Phytophthora ramorum		ethanol	46.07	64-17-5
		2-methyl-1-butanol	88.15	137-32-6
Cottom bollworm		d-limonene	136.24	5989-27-5
Brown marmorated stink bug		(E)-2-hexenal	98.14	6728-26-3

4.2 Objective of the Intercomparison

The objective of the intercomparison event held at AIRMOTEC in the second week of April 2024 was to test and compare the responses of the newly developed sensors and detection units from the PurPest project partners.

4.3 Attendees, systems and schedule of the intercomparison

In this chapter, attendees' names per institution along with their tested sensors are indicated in **Table 4-2**. The schedule of the experiments run during the intercomparison week is detailed in **Table 4-3**.

Table 4-2: Attendees per Institution and their Tested Systems in the Intercomparison.

Institution	Attendees per Institution	Tested Systems
AIRMOTEC	Ali Ghaddar Damien Bazin Stéphane Le Calvé Mathilde Mascles Audrey Grandjean	• Generation of VOCs System: airmoCAL-M • Reference System: GC-FID-MS • Portable System: microVOC
SINTEF	Daniel Nilsen Wright	• SERS Samples
SAFTRA	Pavol Miškovský	• Ramascope
VOLATILE AI	Adomas Malaiska Lucas Lopez	• Volatile Scout3 (GC-e-Nose)
UWAR	Usman Yaqoob Siavash Esfahani	• e-Nose System • Micro-GC Testing System
JKI	Ali Karimi	-

Table 4-3: The Targeted Concentrations in ppb for every Targeted PurPest VOCs throughout the intercomparison week.

Day	Hours	2-METHYL-1-BUTANOL	ETHANOL	LIMONENE	BENZENE	(E)-2-HEXENAL	HEXANAL
Monday 08/04/2024	10:36 - 12:06	700	0	0	0	0	0
	12:36-14:06	700	50	0	0	0	0
Tuesday 09/04/2024	08:41-12:43	0	0	620	0	0	0
	14:24-16:54	0	0	620	1100	0	0
	17:24-19:54	0	0	0	0	910	0
	20:24-21:54	0	0	0	0	910	30
Wednesday 10/04/2024	07:24-12:54	0	0	0	0	910	0
	14:54-16:24	0	0	0	0	910	0
	20:50-23:50	550	8	157	410	965	23
Thursday 11/04/2024	00:20-00:50	550	8	157	410	965	23
	03:50-07:20	1060	15	293	710	1700	43
	11:50-15:20	600	11	200	484	1200	32
	15:50-20:17	1090	49	1018	1013	1700	37
	22:47-23:47	700	36	706	697	1200	28
Friday 12/04/2024	00:17-01:17	700	36	706	697	1200	28
	03:47-06:17	480	26	550	531	965	20
	08:47-09:17	1090	49	1018	1013	1770	37
	12:53-14:23	300	6	157	180	965	23

4.4 STANDARD GENERATION SYSTEM

4.4.1 Permeation Tubes Technology

Repeatable generation of gaseous compounds, whether separately or within a mixture of other compounds, can be quite challenging. Using standardized mixtures of gases, enclosed in a pressurized cylinder, for example, is not as practical as using permeation as an alternative. For a representative quantitation, a dilution factor by air or usage of a multi-pressurizing system is necessarily required. If this is not the case, the purchase of several cylinders will be costly, and the analysis won't be as accurate as it should be when covering a wide range of different concentrations for calibration. Permeation comes into play when the targeted compounds for generation are unstable or highly reactive even at low concentrations when blended with other gaseous mixtures in a cylinder. In-house preparation of these compounds, using permeation technology, becomes critical and at point-of-use in the scope of the PurPest project.

Gas standards generation using permeation turns out to be easy and simple for production of parts per billion (ppb) to parts per million (ppm) concentrations. By adjusting the length, diameter and wall thickness of an inert metallic or polymeric tube, the VOCs can permeate with a constant rate through the walls of the tubes at a constant temperature whenever the tubes are continuously flushed by a controlled flow of pure air or nitrogen (that can be rather diluted). In fact, these permeation tubes are capable of delivering the concentrations of the compounds provided that the liquid product in the tube is still present, the gaseous product in the tube remains entrapped and that the flow of the matrix gas and the temperature of the housing flushed container are constant throughout the whole analysis. To cover the wide range of the concentrations, the diluent flow rate is easily varied along with the setpoint temperature.

In a permeation chamber, a single permeation tube or more (of several compounds) can be added to the permeation chamber to generate a mixture of the standards in question. Several methods for the determination of the concentration of the compound being emitted can be employed. Gravimetry, being one of these methods, is focused on the measurement of the mass of the permeation device. It involves weighing it then sealing it in an enclosure at one specific temperature, then having several weight measurements periodically after several days to determine the exact weight loss of the permeate in microgram or milligram order of magnitude. The concentration will be calculated by calculating the ratio of the permeation rate of the compound in mass per time over the total flow of the matrix gas flushing the chamber in unit of volume per time period. The permeation rate of the compound will change with the temperature, and thus repeating the weight measurement after changing the temperature is a must. Through these repeatable measurements, a plot to monitor the change of the permeation rate with the temperature is constructed. It is reported that stabilizing the permeation rate using the gravimetric method (microbalance weight measurement) for certification can extend to 4 days long for a high permeation rate of 2000 ng/min, 40 days long for a medium permeation rate of 200 ng/min, and up to 400 days for a low permeation rate of 20 ng/min (all values reported with a 2% precision)(Dietz et al. 1974). This suggests that the stabilization is somehow extremely time consuming if the targeted concentrations are of sub-ppb or ppb levels and sometimes non-efficient industrially.

Luckily, with the help of AIRMOTEC gas chromatographic analysers, the stabilization of the permeation rate of the PurPest VOCs can be studied when compared with an already stabilized permeation rate of reference compounds, such as benzene, as those are capable of establishing the two-phase equilibrium (liquid-gas phases) inside the device's walls (Schmidt et al. 1983). For

routine lab analysis, it is essentially important to determine the emitted concentration from the permeation tube and its emission durability. By varying the dynamic diluent flow of the matrix gas, the concentration of the permeated compound will change accordingly. It is rather more practical to adjust the diluent flow rate than to adjust the initial permeating gas flow rate, since in some cases, reaching an equilibrium state can extend over a long time. As the flow of the permeating gas remains unchanged, the permeation rate can be calculated by diluting an added diluent gas flow that can be set using a calibrated mass flow controller (MFCs).

The concentration of the targeted VOC then can be calculated using Equation (1):

$$C_1 (VOC) = \frac{PR}{F} \qquad\qquad\qquad Equation\ (1)$$

where C_1 is the concentration of the targeted VOC in $\frac{\mu g}{m^3}$, PR is the permeation rate in $\frac{ng}{min}$, and F is the total flow rate (permeating gas flow rate and the diluent flow rate) in $\frac{L}{min}$.

The concentration can also be expressed in ppb using Equation (2):

$$C_2 (VOC) = \frac{(C_1 (VOC) \times V_m)}{MW} \qquad\qquad Equation\ (2)$$

where C_2 is the concentration of the targeted VOC in ppb , V_m is the molar volume at room temperature in $\frac{L}{mol}$ (which is equal to 24.04 $\frac{L}{mol}$ at 20°C) and MW is the molecular weight of the targeted VOC in $\frac{g}{mol}$.

The permeation rate depends on the temperature, and thus the permeation source must be calibrated against one reference temperature of a temperature-controlled permeation chamber. Depending on the various characteristics of the permeation tube regarding its type, configuration, shape, thickness of any used membrane and many other factors, the permeation rate can be estimated for a different temperature.

It is noteworthy, in the end, to point out that the permeation technology can exhaustively be more advanced than using cylinders for VOCs generation, especially when targeting low range concentration (between sub-ppb and high ppm levels) and when exploited in the field as portable units or just for typical routine lab standardization.

4.4.2   Setup of Generation of Targeted PurPest VOCs

The general setup for the generation of the targeted PurPest VOCs was based practically on the simple placement/ displacement of the permeation devices from a permeation chamber/oven that was temperature controlled automatically. To generate a single VOC for the intercomparison, we placed a permeation tube filled with the targeted VOC alone in the permeation oven with a constant permeating gas flow rate, while adjusting the diluent zero-air flows and the temperature of the oven to reach the targeted concentrations. Whereas when a mixture of several PurPest VOCs was to be generated, several permeation devices were placed in the same permeation oven, or in a different oven at a lower/higher temperature. Zero-air was allowed to pass over the permeation ovens, and the VOCs were then generated and diluted with an additional higher flow rate of zero-air.

In the case of the interferent VOCs, the permeation devices were placed in a separate permeation oven at a manually controlled temperature. The full scheme of the generation of the VOCs (sent to all the sensors and the analysers used in the intercomparison through the sampling

line) is represented in the figure below (**Figure 4-1**). Each unit placed in a dotted box in the figure will be separately explained along with an explanatory schematic diagram. First, zero-air - generated from AIRMOTEC's zero-air generator - passed through a dryer to be completely dried and then catalysed to prevent oxidation and to purify it from any hydrocarbons. The flow of zero-air was regulated using a pressure regulator and a flow regulation. The flow of the generated interferent VOCs was transferred to the sampling line when the electrovalve was switched to position 2, and to the exhaust when switched to position 3 to prevent the addition of the interferent to the sampling line. Each electrovalve connected to any sensor represents manual switch between sampling either from the sampling line or the zero-air.

In the airmoCAL-M (**Figure 4-2**), a calibration unit that housed 2 in-series permeation ovens containing the main VOCs of interest for the intercomparison, 2 MFCs were utilized, one for flushing continuously the ovens with a flow of 62 ml/min, and one for diluting this continuous permeating flow. This MFC's flow was adjustable to target the required concentrations. Afterwards, these two flows were combined and allowed to mix in a dilution chamber. An electrovalve was also set in the setup to turn on/off the flow for dilution.

For some of the PurPest sensors, usage of a 1L heated glass bulb (**Figure 4-3**) was necessary to obtain the ppm levels needed for detection. First, the bulb is heated and evacuated using a pump. Then, injection of specific volumes of pure liquid compound into the bulb was done to reach the targeted concentrations. The bulb is opened to atmospheric pressure and then air is allowed to flush the gaseous compounds into the desiring sensor.
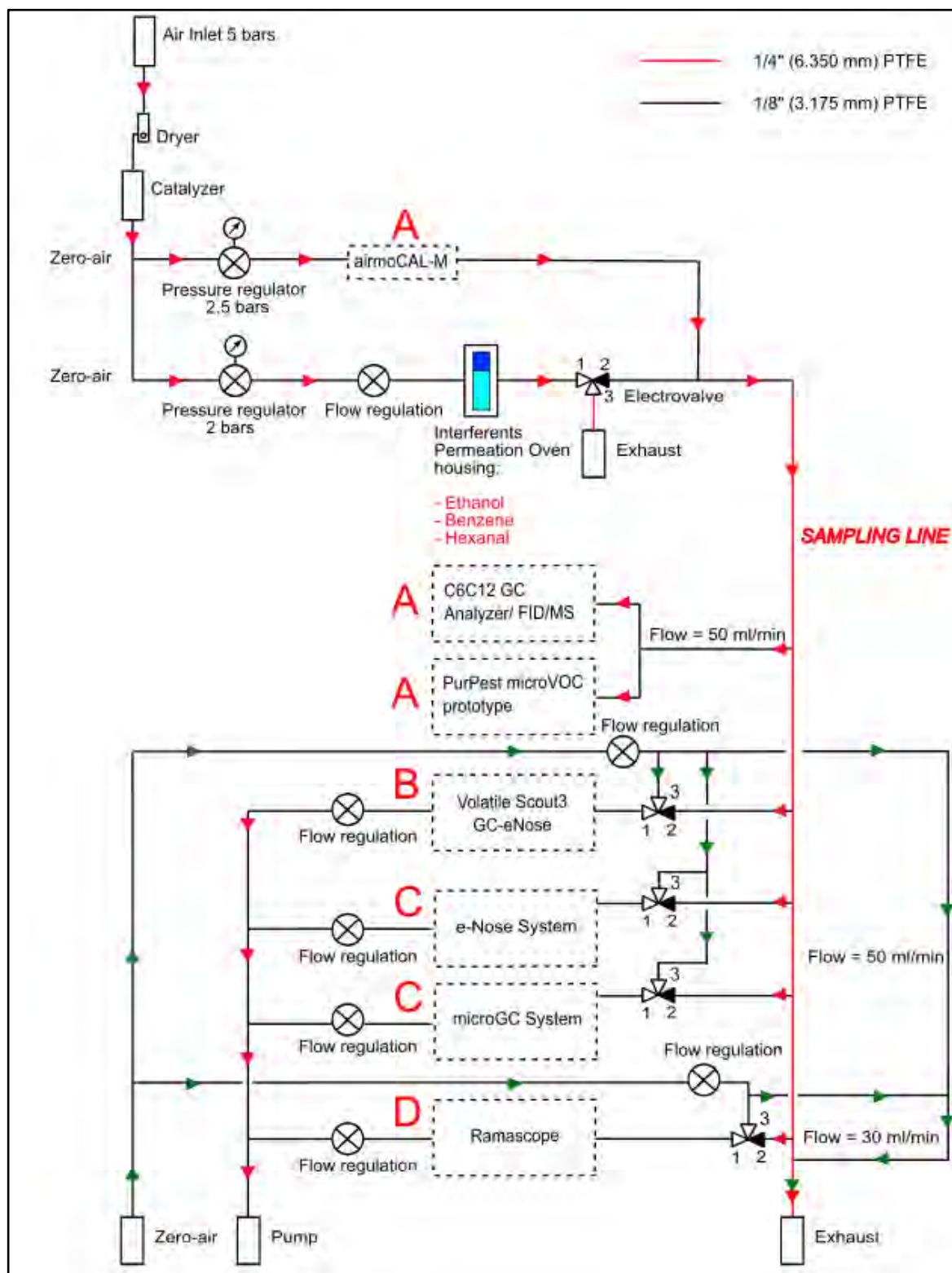
Figure 4-1: Pneumatic Scheme of the VOCs Generation Setup for all the PurPest Partners' sensors and analysers. AIRMOTEC sensors in dotted boxes are illustrated schematically in the next sections (A = AIRMOTEC, B = Volatile AI, C = UWAR, D = SINTEF/ SAFTRA).
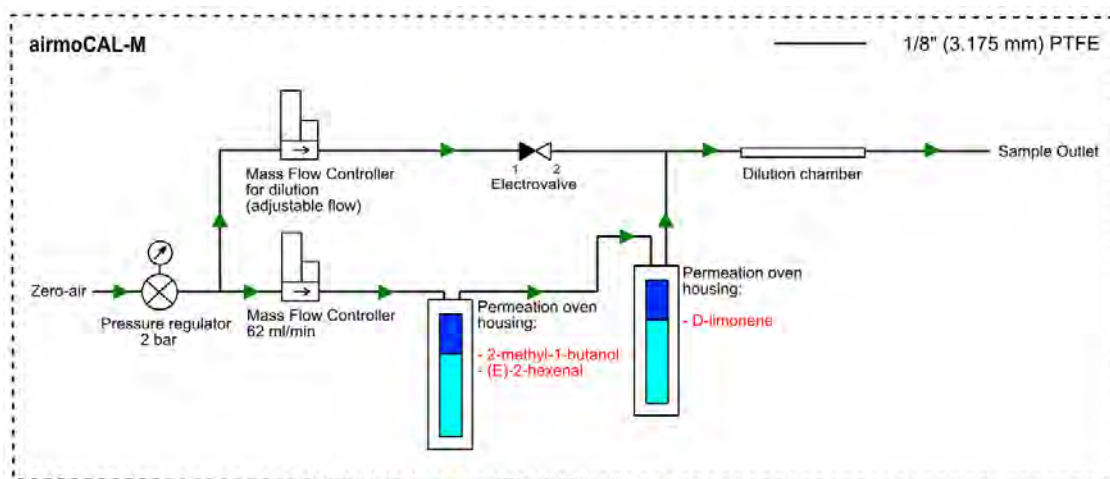
Figure 4-2: Pneumatic Scheme of airmoCAL-M for the Generation of the Targeted VOCs.
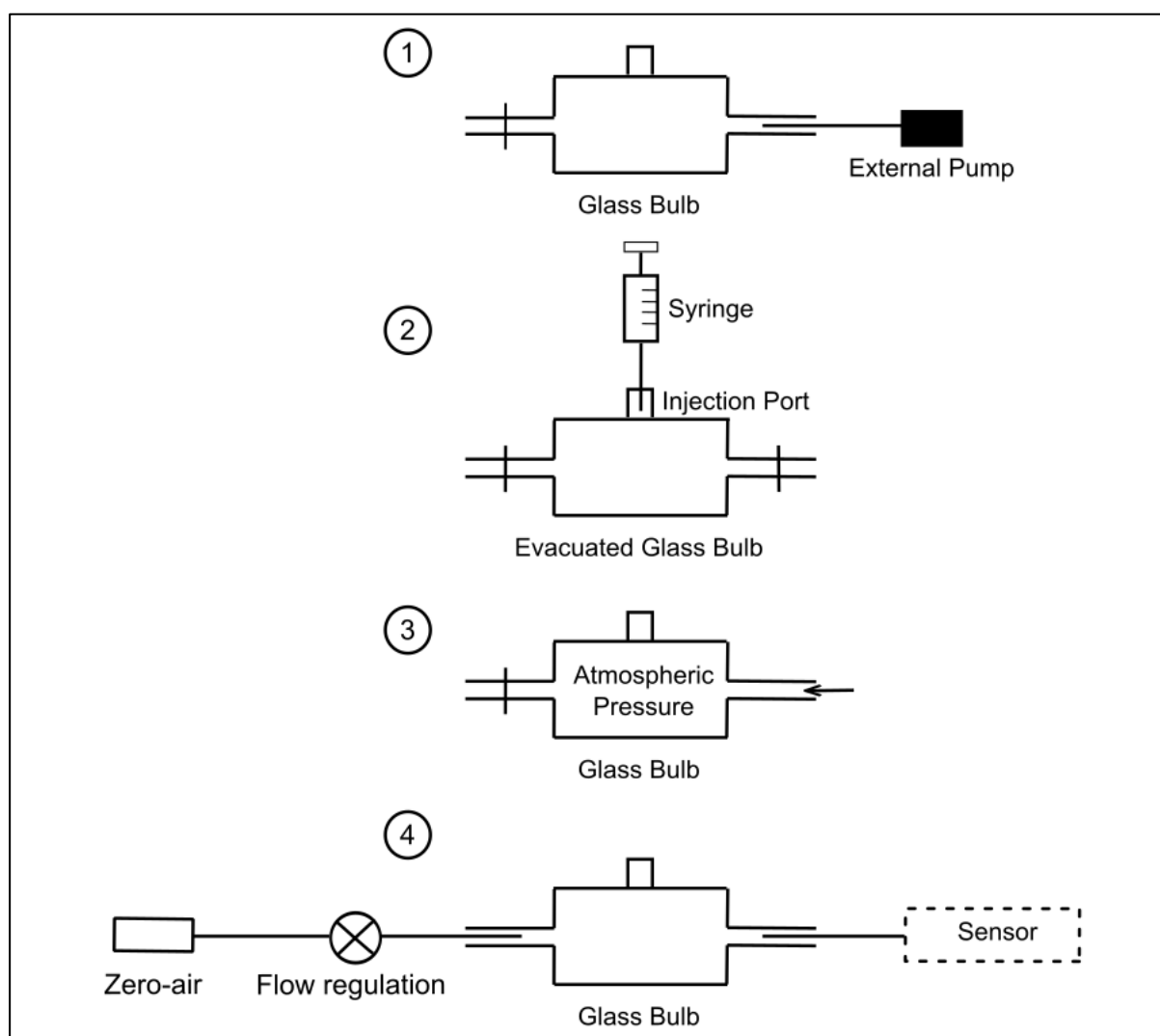
Figure 4-3: Scheme of a glass bulb injection.

5 RESULTS OF THE INTERCOMPARISON

5.1 AIRMOTEC Tested Technologies

5.1.1 GC-FID-MS

An autonomous AIRMOTEC gas chromatograph (airmoVOC C6-C12, Chromatotec, France) equipped with a Flame Ionization Detector (FID) and coupled to a Mass Spectrometer (DET QMS, Chromatotec, France) was used as a reference system during the intercomparison (**Figure 5-1Error! Reference source not found.**). This online gas chromatograph is able to separate VOCs that contain at least 6 carbons up to 12 carbon atoms. The gas chromatograph and the mass spectrometer are both housed in a cabinet along with a hydrogen gas generator (Hydroxychrom, Chromatotec, France) for generation of the ultra-pure carrier gas (99.9999%), a calibration system (airmoCAL, Chromatotec, France) and another chromatograph (airmoVOC C2-C6). For the intercomparison purposes, and since the targeted VOCs are better separated using a non-polar column, only the airmoVOC C6-C12 was operating as the reference system. To ignite the flame of the FID, zero-air flow was supplied by an AIRMOTEC zero-air generator (airmoPURE, Chromatotec, France). To sample from the sampling line, a total flow of 30 mL/min is allowed to pass to the whole system. 600 mL will be sucked separately to airmoVOC C6-C12 using an external diaphragm pump and a flow regulator for 4 minutes every 30 minutes with a 20 mL/min flow rate. The sample was then pre-concentrated at room temperature on a pre-concentrator composed of Carbopack trapping adsorbents. Then the sample was desorbed from the pre-concentrator at 380°C for 4 minutes and then injected to the non-polar analytical column (an MXT30CE column, 30m x 0.28 mm x 1.0 µm) situated in a temperature programmed oven. Within the first minute of injection, the temperature of the oven increased from 36 to 38°C, and then up to 50°C for 6 minutes. Afterwards, the oven temperature increased up to 80°C with a rate of 10°C/min for 3 minutes followed by a heating rate of 12°C/min for 8 minutes until it reached 200°C. Then, the temperature was held at 200 °C for 4-5 minutes before cooling. Finally, the sample eluted from the column and passed onto the FID at 200 °C. The temperature of the FID itself was held at 170°C and the signal amplification was set at middle amplification (Level 2).

A single quadruple mass spectrometer coupled to the chromatograph through a heated transfer line at 200 °C has an ion source operating by 70 eV electron impact at 150 °C. A full-scan mode allowed for the acquisition of spectra with a mass-to-charge ratios between 35 and 155 amu.
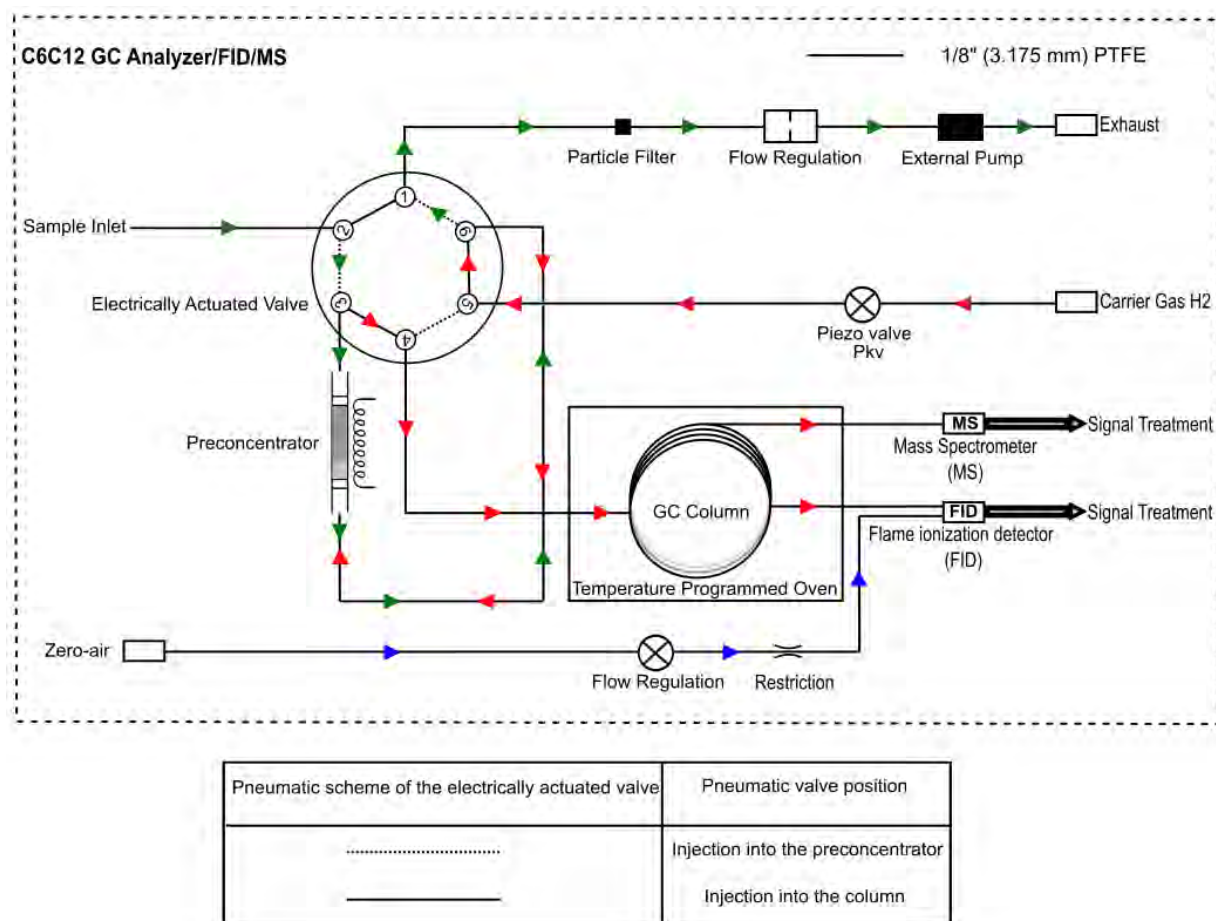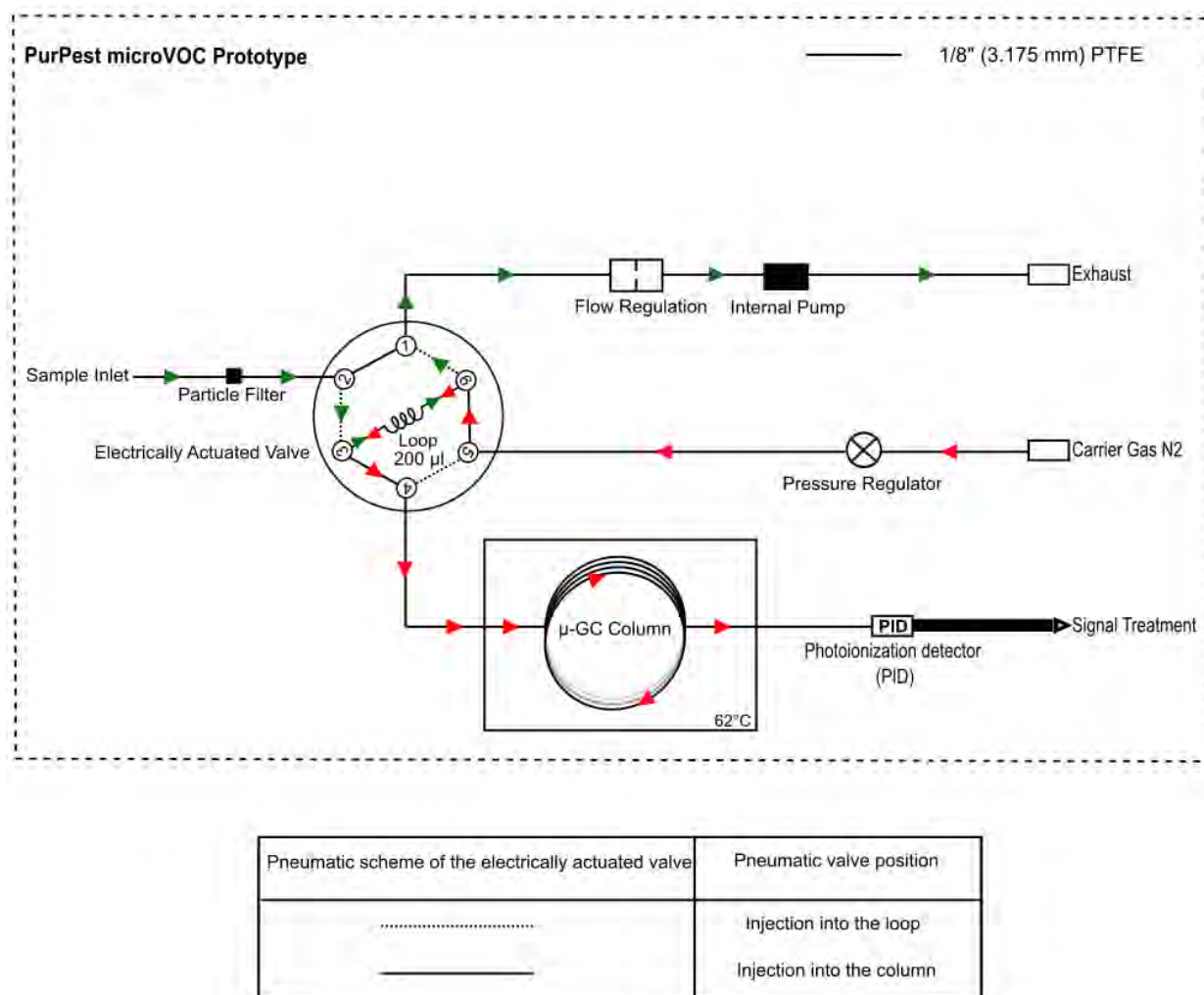
Figure 5-1: Pneumatic Scheme of AIRMOTEC's C6C12 GC Analyzer/FID/MS.

5.1.2 GC-PID

A portable, compact and online AIRMOTEC µ-GC chromatograph (microVOC, Chromatotec, France) equipped with a Photo Ionization Detector (PID) was also used as a newly-developed unit during the intercomparison (**Figure 5-2**). Each filtered sample was sampled for 2 minutes with a regulated flow. With a flow of 20 mL/min, 40 mL sample was sucked using an internally integrated compact pump at room temperature each 30 minutes. The sample was loaded into a 200 µL loop using an electrically actuated valve that actuates at time of injection. When the valve actuated, an MFC-controlled flow of carrier gas (about 2.5 mL/min nitrogen (N_2), supplied from a nitrogen cylinder, flushed the already-loaded sample into a µ-GC column (RXI 624, 20m x 0.18 mm x 1.0 µm) that was set at an isothermal temperature of 62°C. Then, the sample eluted and was detected using the PID. Data was then visualized using the visualization feature offered by the touch-screen for manual fast peak integration for the calculation of the concentration. The portable analyser is designed to detect benzene, toluene, ethylbenzene and derivatives of xylene, or as commonly known BTEX compounds, along with other compounds like methanol, phenol, acrolein, 1,3-butadiene, naphthalene and many other compounds.

**Figure 5-2**: Pneumatic Scheme of AIRMOTEC's PurPest microVOC Prototype.

5.1.3 AIRMOTEC's Reference System and microVOC Responses

#### 5.1.3.1 Day 1: Monday 08/04/2024 – Generation of 2-methyl-1-butanol and ethanol

On the first day of the intercomparison, the 2-methyl-1-butanol permeation tube was put inside the permeation oven at 35°C. After running measurements of zero-air for the system during the first hours, the generation of the targeted concentration of 700 ppb or 0.7 ppm started. Within 2 hours of running analyses of this targeted concentration, 8 chromatograms were acquired on the reference system, with the peak of 2-methyl-1-butanol detected at a retention time of 360 seconds (**Figure 5-3**). With each chromatogram, 1 detected concentration of the compound was recorded, summing up in total 8 concentrations. With respect to the microVOC, with also an acquisition time of 3 hours, 8 chromatograms were also acquired. However, the detection was based on areas rather than concentrations because it is the tested portable model. The 2-methyl-1-butanol peaks were manually integrated, and the areas were thus estimated manually. **Figure 5-4** shows the 2-methyl-1-butanol peak centred at a retention time of 200 seconds. At the end of this day, an additional line of generation of 50 ppb (0.05 ppm) ethanol was added for another 2 hours to study the effect of the interferent. Ethanol was detected at a retention time of 8 seconds at the start of the chromatogram on the reference system (**Figure 5-5**), whereas on the microVOC, no peaks were detected for ethanol, considering ethanol has much lower boiling point than 2-methyl-1-

butanol, its retention time would be remarkably before the targeted compound. Thus, the chromatograms were compared with the chromatograms with no addition of any interferent, and they were similar, as shown in **Figure 5-6**.

Figure 5-7 shows the temporal generation of the concentrations of 2-methyl-1-butanol and ethanol on the reference system along with the areas recorded on microVOC for 2-methyl-1-butanol. More exhaustive details about this temporal variation are presented in **Table 8-1**: Response of the reference system and the microVOC during Monday for 2-methyl-1-butanol and ethanolin Section 8.
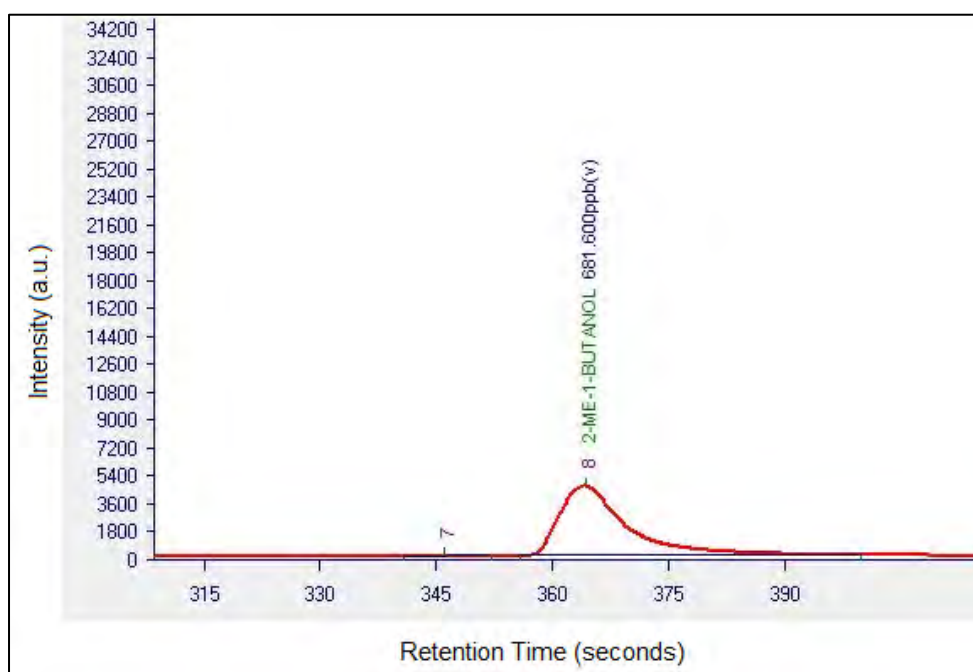
Figure 5-3: Zoomed-in 2-methyl-1-butanol peak [retention time = 360 seconds, concentration = 681.600 ppb(v)] after acquisition of the reference system chromatograms.
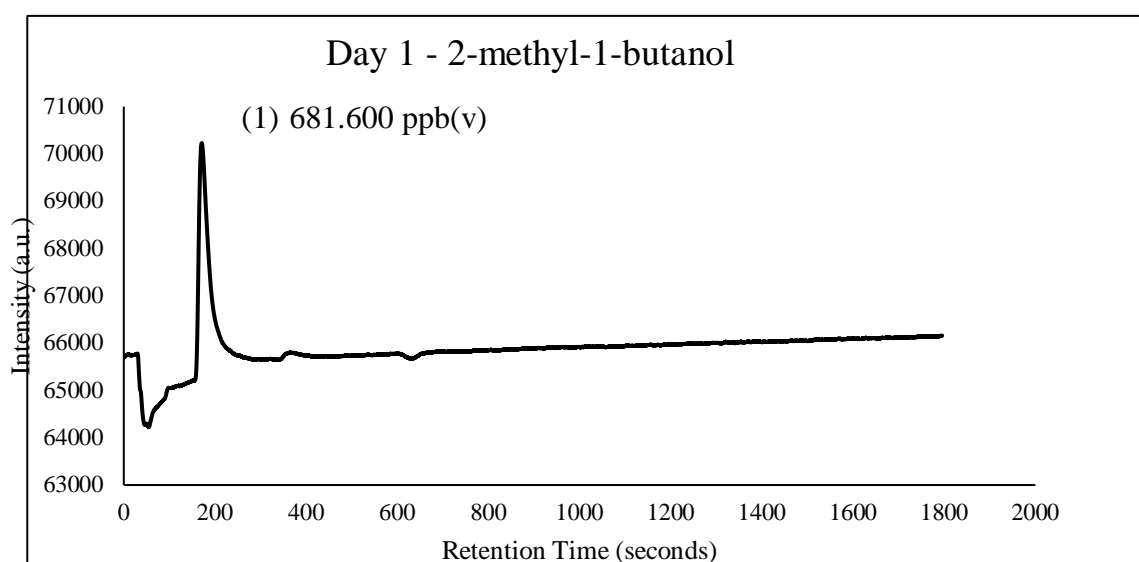
Figure 5-4: *(1)* 2-methyl-1-butanol peak [retention time = 200 seconds, concentration = 681.600 ppb(v)] after acquisition of the microVOC chromatograms.

Figure 5-5: Zoomed-in ethanol peak [retention time = 8 seconds, concentration = 47.200 ppb(v)] after acquisition of the reference system chromatograms.

Figure 5-6: Ethanol (not identified), *(1)* 2-methyl-1-butanol peak [retention time = 360 seconds, concentration = 726.200 ppb(v)] after acquisition of the microVOC chromatograms.
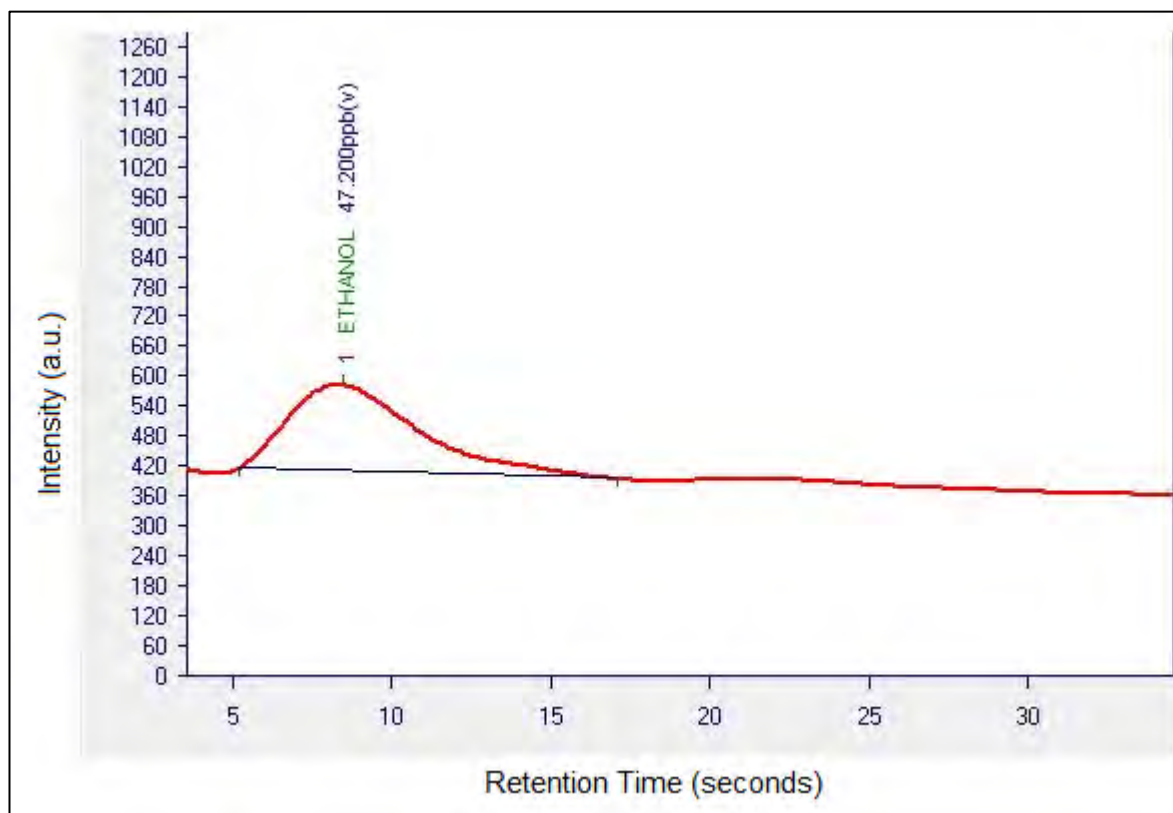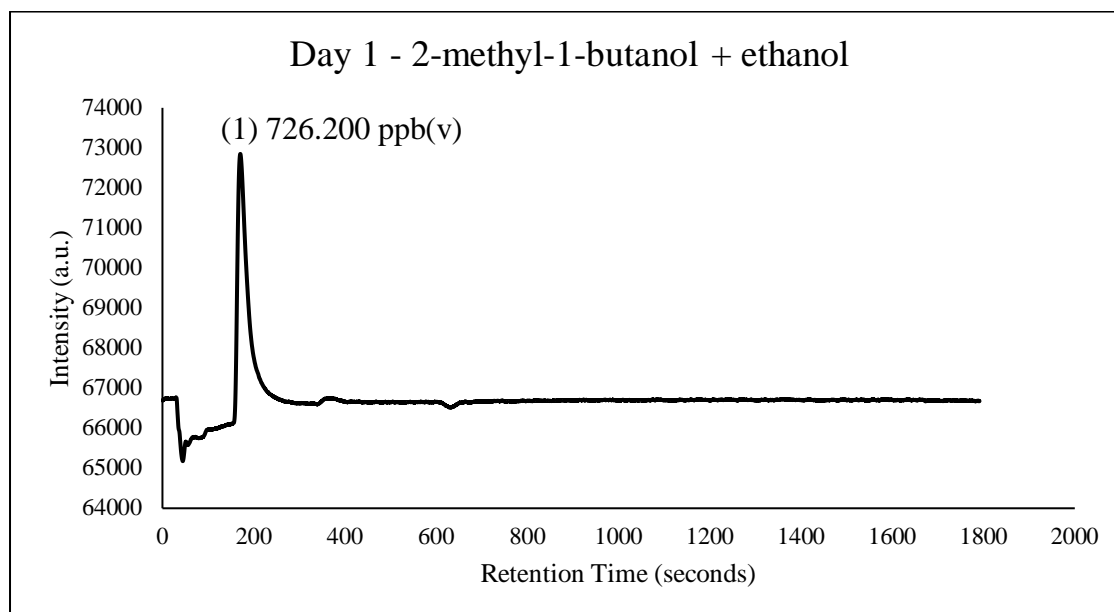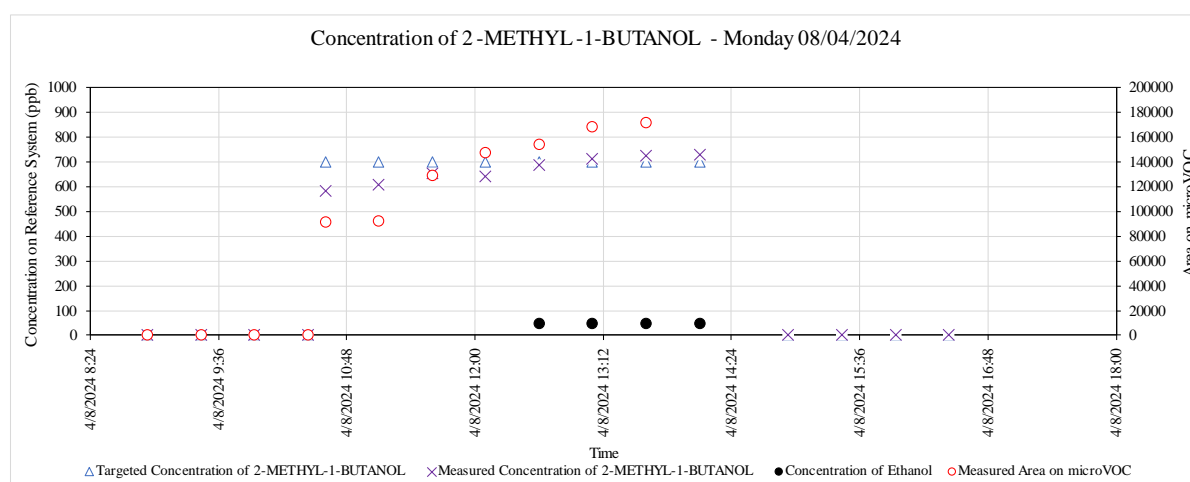

Figure 5-7: Temporal generation of the concentrations of 2-methyl-1-butanol and ethanol on the reference system along with the areas recorded on microVOC for 2-methyl-1-butanol.

5.1.3.2 *Day 2: Tuesday 09/04/2024 – Generation of d-limonene and benzene*

At the end of Monday, the 2-methyl-1-butanol permeation tube was removed from the permeation oven that was set at 35°C, and a d-limonene permeation tube was put instead at another oven set at 80°C. The same procedure as Monday was followed. Zero-air measurements were done at first followed by generation of 620 ppb or 0.62 ppm of d-limonene, and ending up with adding benzene as an interferent in a separate oven at 35°C. 5 chromatograms were recorded for the generation of d-limonene alone, and 6 chromatograms were recorded for the generation of both

benzene and d-limonene together on the reference system, with retention times of 180 seconds and 965 seconds respectively. The peaks of benzene and d-limonene are shown in **Figure 5-8** respectively. On the microVOC, d-limonene peak was sharp as the compound eluted from the column alone (not separated) at a retention time of 900 seconds, with an intensity of a peak close to 71000 a.u (**Figure 5-9**). However, adding benzene as an interferent (retention time of 100 seconds) drastically changed the peak shape as the intensity of the benzene peak was significantly larger compared to the intensity of the d-limonene peak (**Figure 5-10**). **Figure 5-11** shows the temporal generation of the concentrations of d-limonene and benzene on the reference system along with the areas recorded on microVOC for d-limonene. More details about exact generated concentration of these compounds can be found in **Table 8-2** in Section 8.

Figure 5-8: Benzene peak [retention time = 180 seconds, concentration = 1192.000 ppb(v)] and d-limonene [retention time = 965 seconds, concentration = 620.400 ppb(v)] after acquisition of the reference system chromatograms.
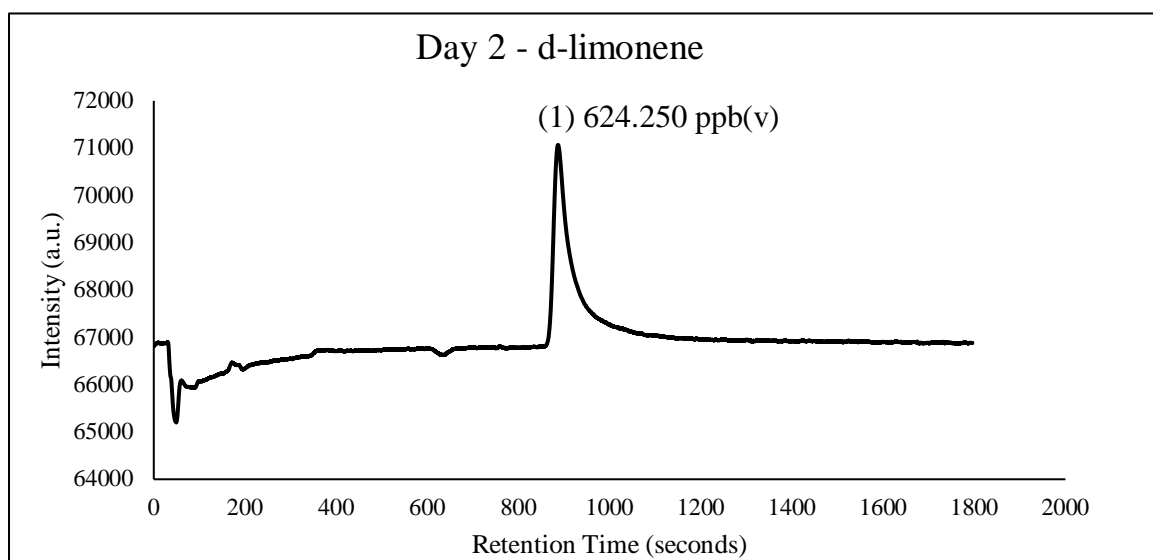
**Figure 5-9:** *(1)* Zoomed-in d-limonene peak [retention time = 900 seconds, concentration = 624.250 ppb(v)] after acquisition of the microVOC chromatograms.

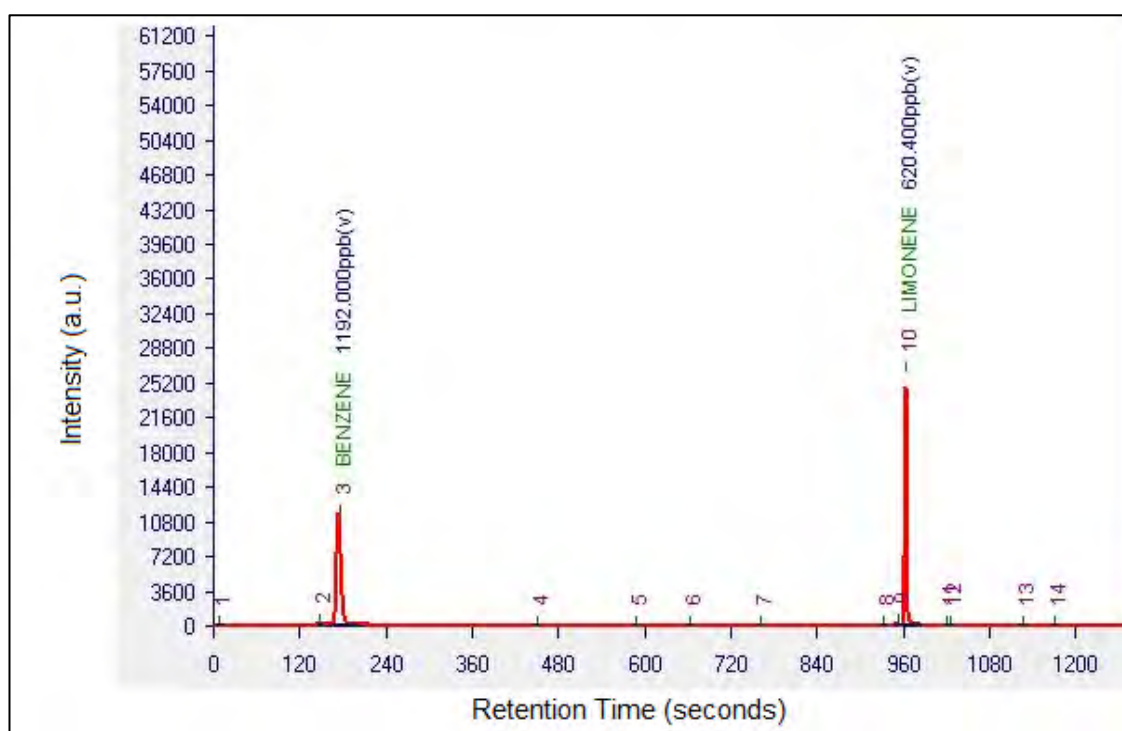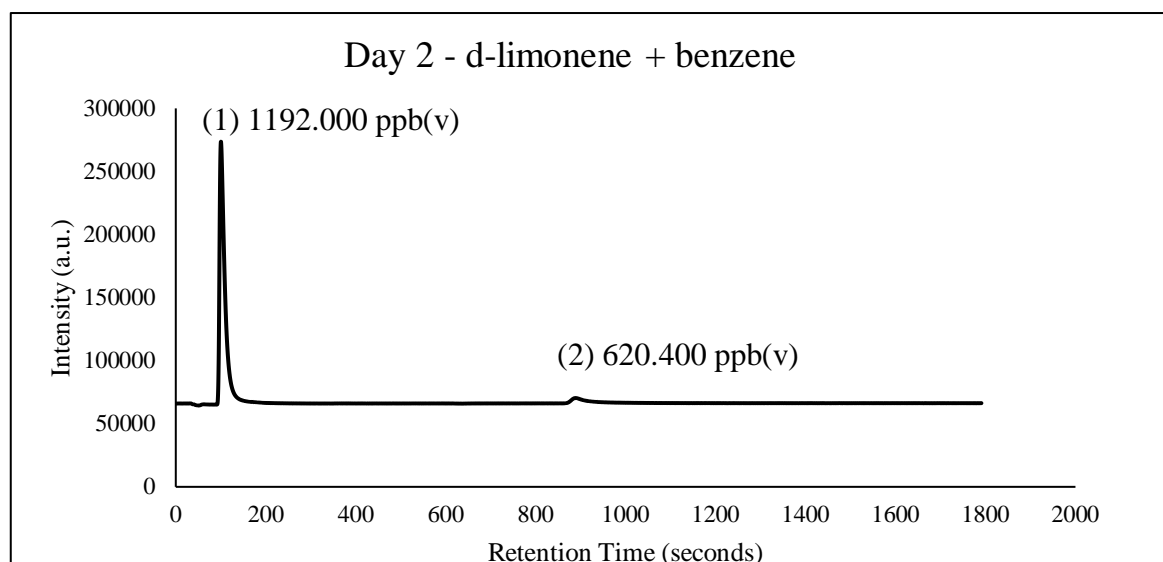**Figure 5-10:** *(1)* Benzene peak [retention time = 100 seconds, concentration = 1192.000 ppb(v)] and *(2)* d-limonene peak [retention time = 900 seconds, concentration = 620.400 ppb(v)] after acquisition of the microVOC chromatograms.
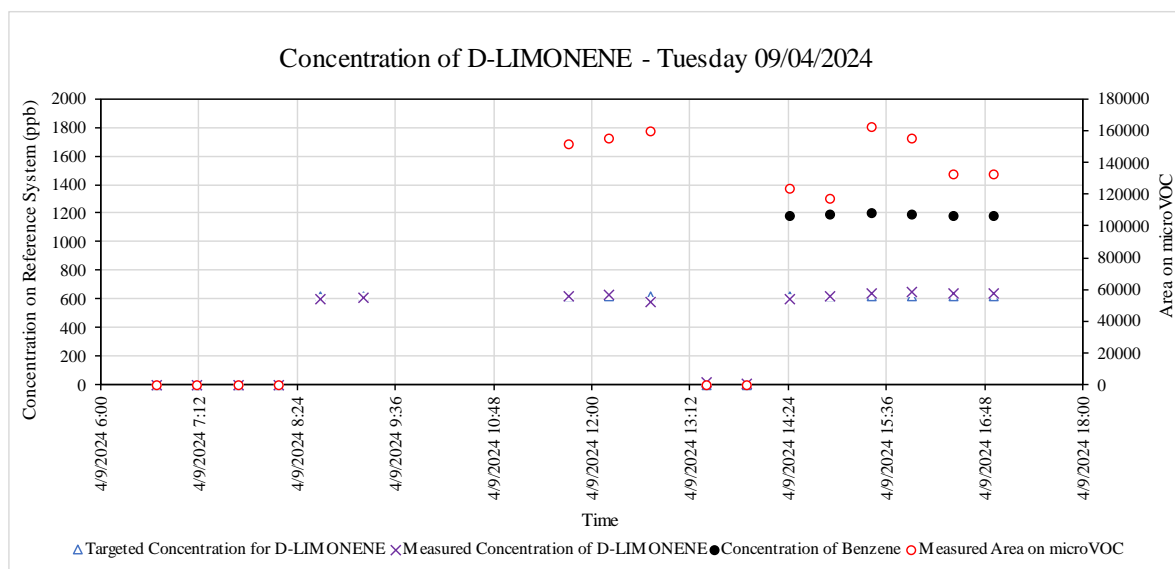
Figure 5-11: Temporal generation of the concentrations of d-limonene and benzene on the reference system along with the areas recorded on microVOC for d-limonene.

5.1.3.3 Day 3: Wednesday 10/04/2024 – Generation of (E)-2-hexenal and hexanal

On Tuesday's afternoon, the two permeation tubes, d-limonene and benzene, were both removed from the permeation oven. (E)-2-hexenal permeation tube was put inside the permeation oven at 35°C, and the same procedure as the days before was followed. The targeted concentration of this compound was 910 ppb pr 0.91 ppm. After running several measurements, the interferent hexanal was added to the separate permeation oven set at 50°C (4 chromatograms – 2 hours). Several chromatograms were acquired, with the peak of the targeted compound retaining at 660 seconds on the reference system (**Figure 5-12**) and at 400 seconds on the microVOC (**Figure 5-13**). As shown in **Figure 5-14**, hexanal eluted at an earlier retention time (525 seconds) and the two peaks were as a result clearly separated. Hexanal was also well-separated on the microVOC, as it is expected for the hexanal to have a retention time of 170 seconds. **Figure 5-15** shows the full chromatogram of both (E)-2-hexenal and hexanal. **Figure 5-16** shows the temporal generation of the concentrations of (E)-2-hexenal and hexanal on the reference system along with the areas recorded on microVOC. More details about exact generated concentration of these compounds can be found in **Table 8-3** in Section 8.

Figure 5-12: Zoomed-in (E)-2-hexenal peak [retention time = 660 seconds, concentration = 907.500 ppb(v)] after acquisition of the reference system chromatograms.

Figure 5-13: *(1)* (E)-2-hexenal peak [retention time = 400 seconds, concentration = 928.240 ppb(v)] after acquisition of the microVOC chromatograms.
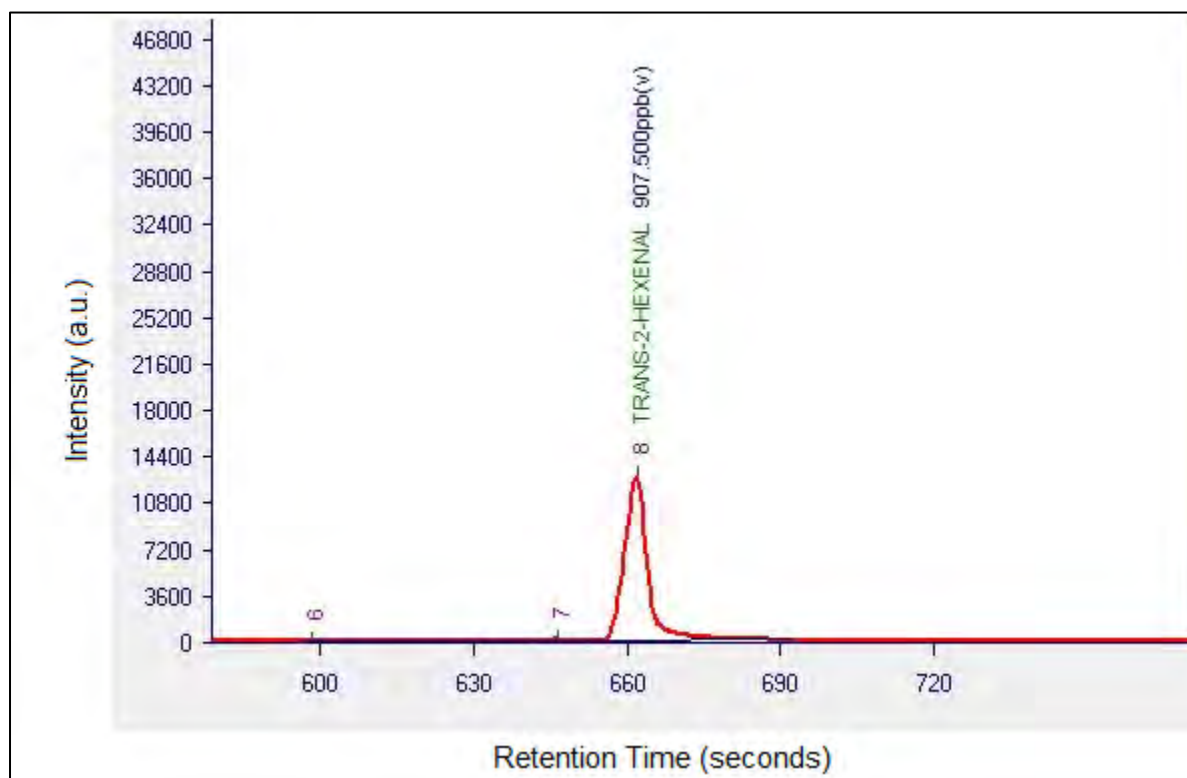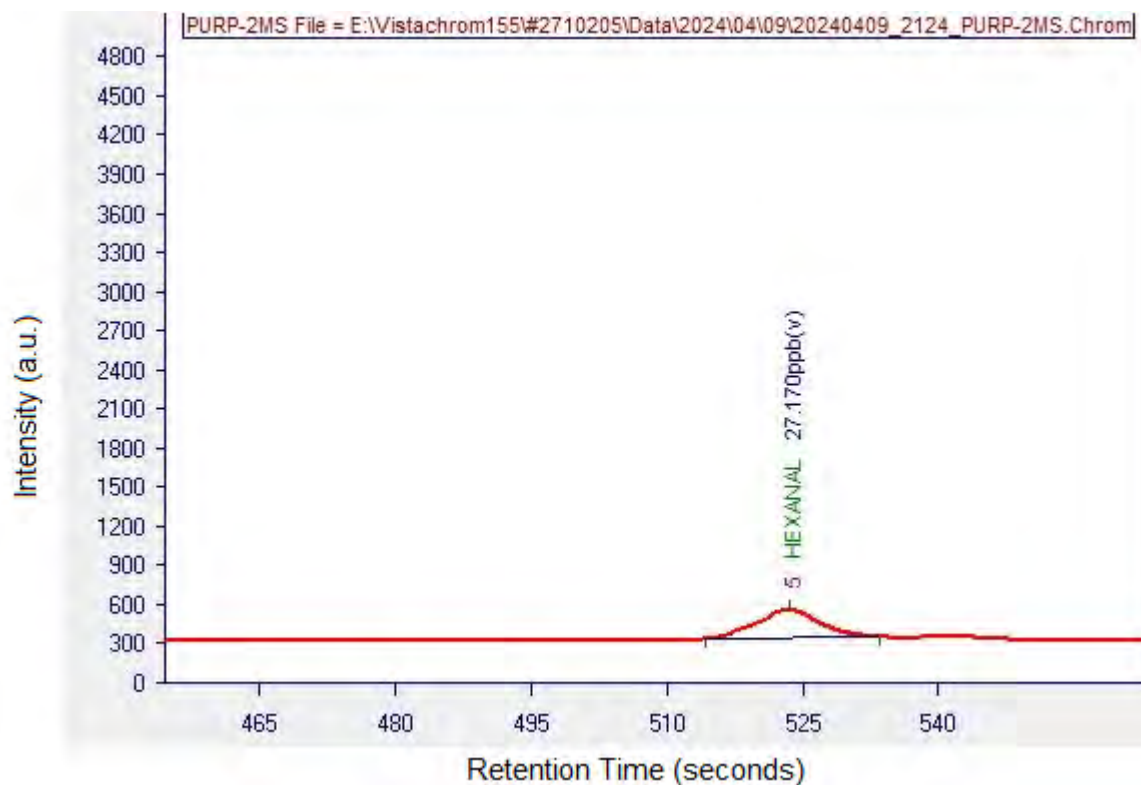
Figure 5-14: Zoomed-in hexanal peak [retention time = 525 seconds, concentration = 27.170 ppb(v)] after acquisition of the reference system chromatograms.

Figure 5-15: *(1)* Hexanal peak [retention time = 170 seconds, concentration = 28.680 ppb(v)] and *(2)* (E)-2-hexenal peak [retention time = 400 seconds, concentration = 904.460)] after acquisition of the microVOC chromatograms.
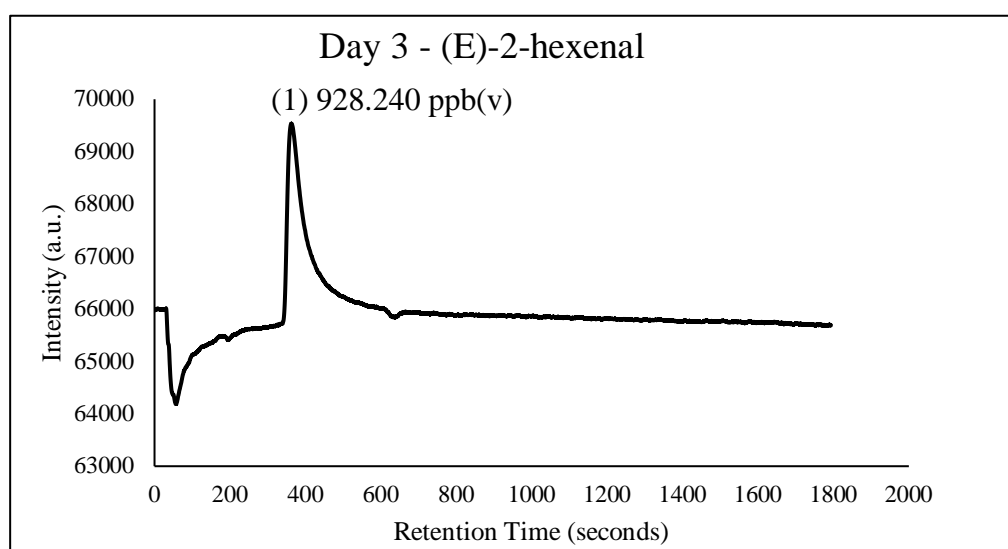
Figure 5-16: Temporal generation of the concentrations of (E)-2-hexenal and hexanal on the reference system along with the areas recorded on microVOC for (E)-2-hexenal.

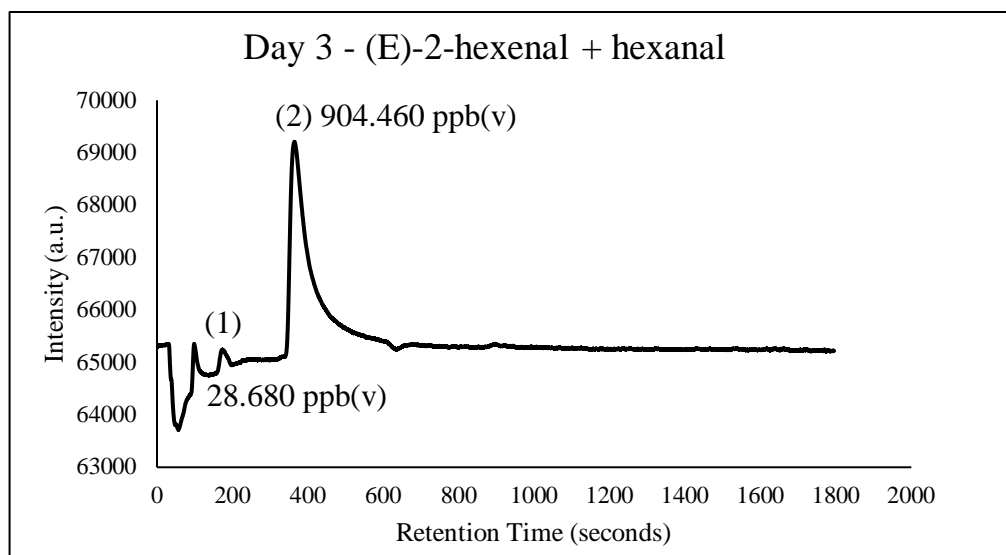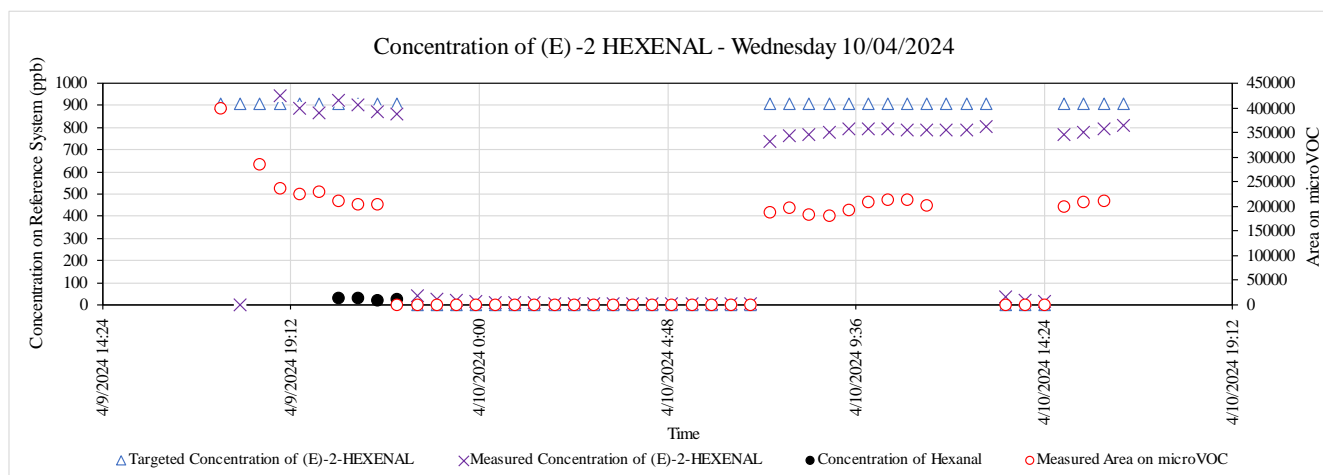#### 5.1.3.4 *Day 4 & 5: Thursday 11/04/2024 & Friday 12/04/2024 – Generation of a mixture of all VOCs*

On the fourth day of the intercomparison, all the compounds were placed in their appropriate permeation ovens at specific temperatures. Several concentrations were targeted for each compound. On the reference system, all the compounds were detected with an order of elution of ethanol, benzene, 2-methyl-1-butanol, hexanal, (E)-2-hexenal, and d-limonene as shown in **Figure 5-17**. The same procedure was followed on Friday but with different targeted concentrations for each compound. The significance of running these analyses is to check if the systems are able to detect all the VOCs at once and how good the separation of these VOCs is. Regarding the microVOC, the PID1 detector was changed to PID2 on Wednseday's afternoon. This affected significantly the response of the microVOC to the compounds, which were in turn better improved in terms of areas and thus response factors (**Figure 5-18**). The concentrations and areas detected by the reference system and the microVOC for 2-methyl-1-butanol, d-limonene and (E)-2-hexenal are all represented in **Figure 5-19**, **Figure 5-20** and **Figure 5-21** respectively. To better depict the improvement analytically, the response factor for the three major targeted compounds for the PurPest project along with benzene on the microVOC was calculated according to the following equation:

$$Response\ Factor = \frac{Area\ on\ PurPest\ microVOC\ (a.u.)}{Concentration\ on\ Reference\ System\ (ppb)}$$

This equation was used for the signals to study the effect of using PID2 instead of PID1. Using these calculated response factors, the concentrations for each measurement (averaged after stabilization) were derived and compared with the targeted concentrations. Those concentrations were closer in value to the targeted value as the response factor improved by a factor of 2 or more for the four compounds. The difference between the derived and the targeted concentrations is denoted by $\Delta_{concentration}$ in absolute value (ppb) (See **Table 5-1**, **Table 5-2**, **Table 5-3** and **Table 5-4**):

$$|\Delta_{concentration}|\ (ppb) = |Derived\ Concentration\ (ppb) - Targeted\ Concentration\ (ppb)|$$

Figure 5-22 is a bar graph showing the ratio of the responses on both PIDs along with the ratio of these responses of PID1 relative to PID2. One can conclude from this bar graph that the response factor change for benzene is not as much pronounced as that of the other 3 compounds. Hence, this allows for a selectivity study of the PID for those biogenic VOCs. **Table 8-4**, **Table 8-5** and **Table 8-6** in Section 8 show the average measured values of the reference system concentrations and the microVOC areas for 2-methyl-1-butanol, d-limonene and (E)-2-hexenal respectively.
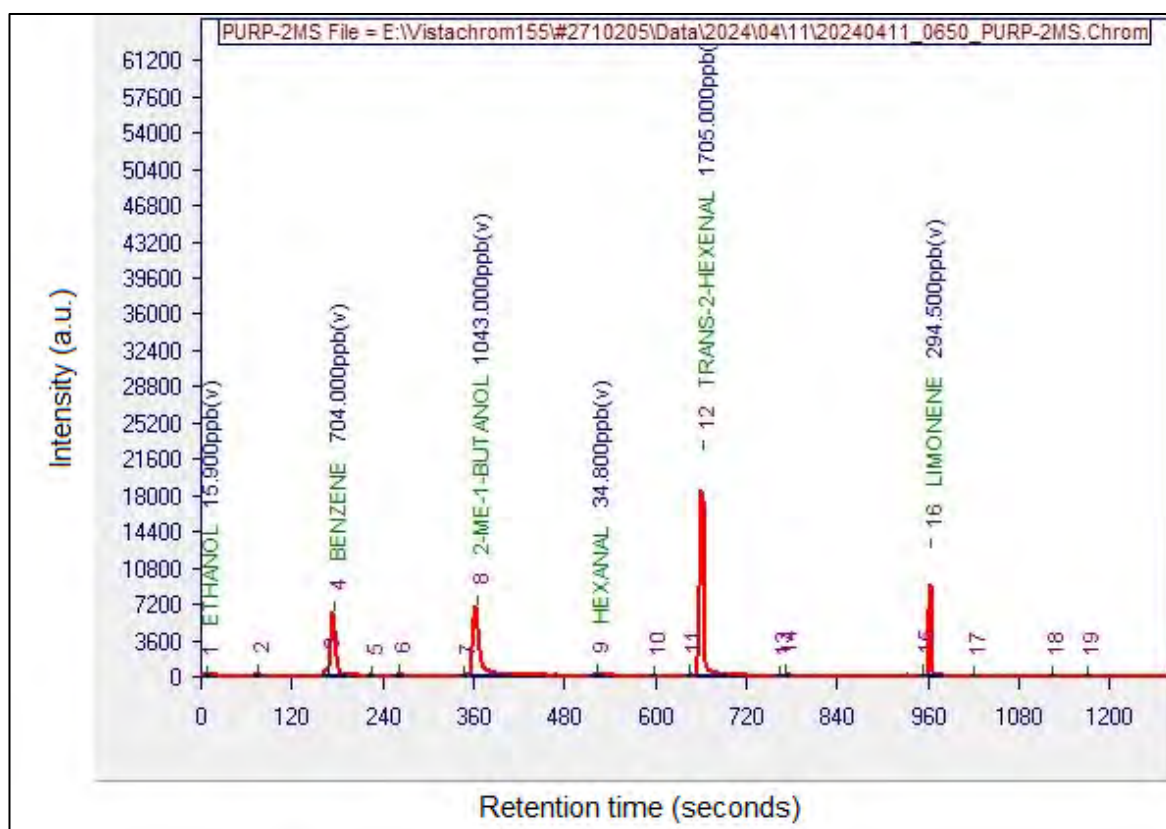
Figure 5-17: Acquisition of reference system chromatogram of the mixture of the targeted VOCs in the intercomparison

Compounds are listed from left to right in order of elution from the chromatographic column

ethanol [retention time = 8 seconds, concentration = 12.900 ppb(v)],
benzene [retention time = 180 seconds, concentration = 704.000 ppb(v)],
2-methyl-1-butanol [retention time = 360 seconds, concentration = 1043.000 ppb(v)],
hexanal [retention time = 525 seconds, concentration = 34.800 ppb(v)],
(E)-2-hexenal [retention time = 660 seconds, concentration = 1705.000 ppb(v)],
& d-limonene [retention time = 965 seconds, concentration = 294.500 ppb(v)].
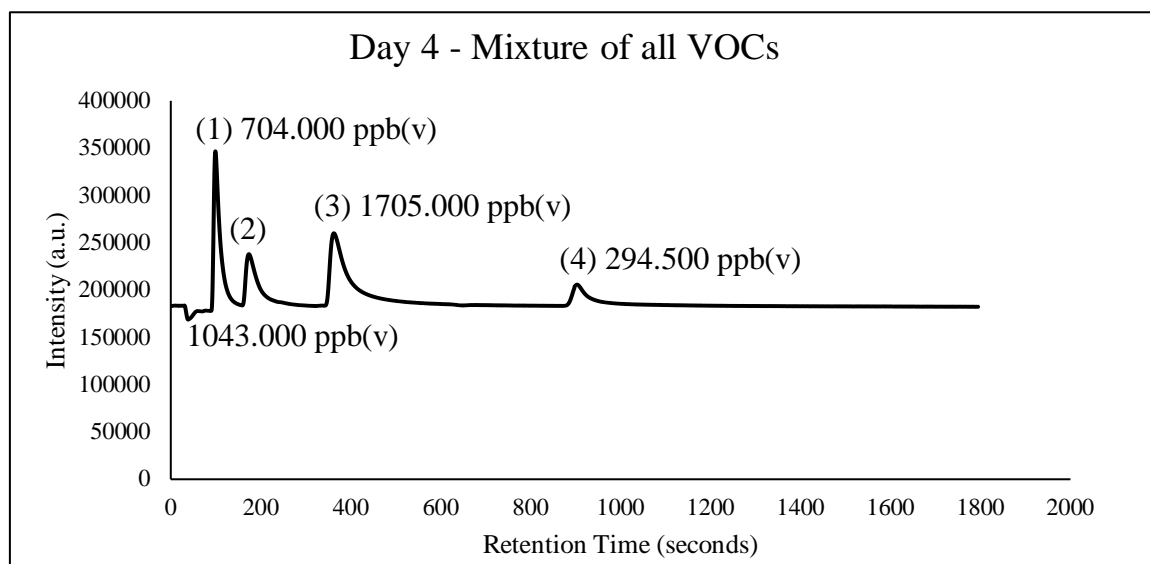
Figure 5-18: Zoomed-out microVOC chromatogram of the mixture of the targeted VOCs in the intercomparison, *apparent* compounds listed in order of elution

(1) benzene [retention time = 180 seconds, concentration = 704.000 ppb(v)], *(2)* 2-methyl-1-butanol [retention time = 360 seconds, concentration = 1043.000 ppb(v)], *(3)* (E)-2-hexenal [retention time = 660 seconds, concentration = 1705.000 ppb(v)], *(4)* d-limonene [retention time = 965 seconds, concentration = 294.500 ppb(v)].
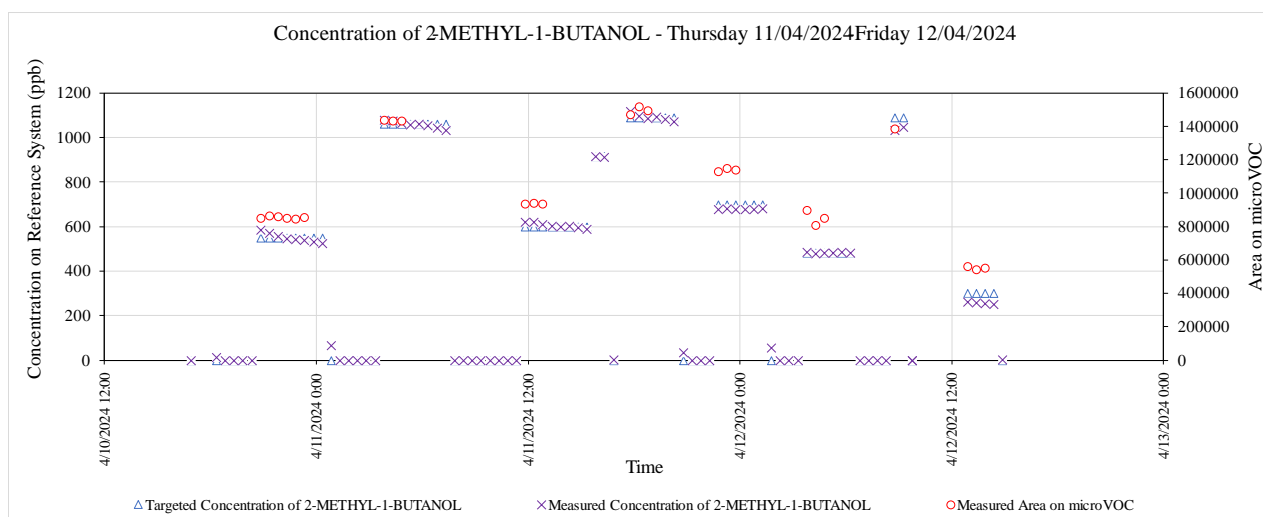
Figure 5-19: Temporal generation of the concentrations of 2-methyl-1-butanol on the reference system along with the areas recorded on microVOC for the last two days of the intercomparison.
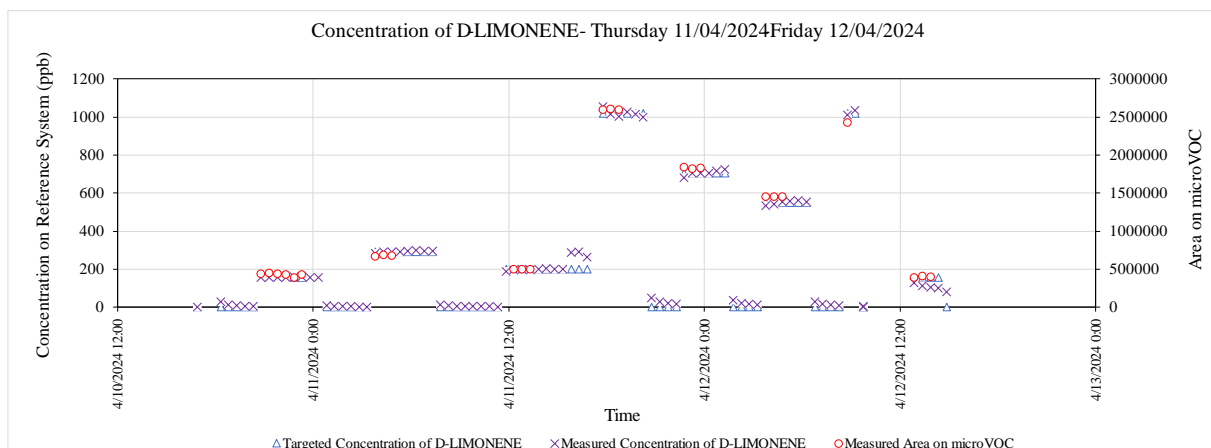
Figure 5-20: Temporal generation of the concentrations of d-limonene on the reference system along with the areas recorded on microVOC for the last two days of the intercomparison.
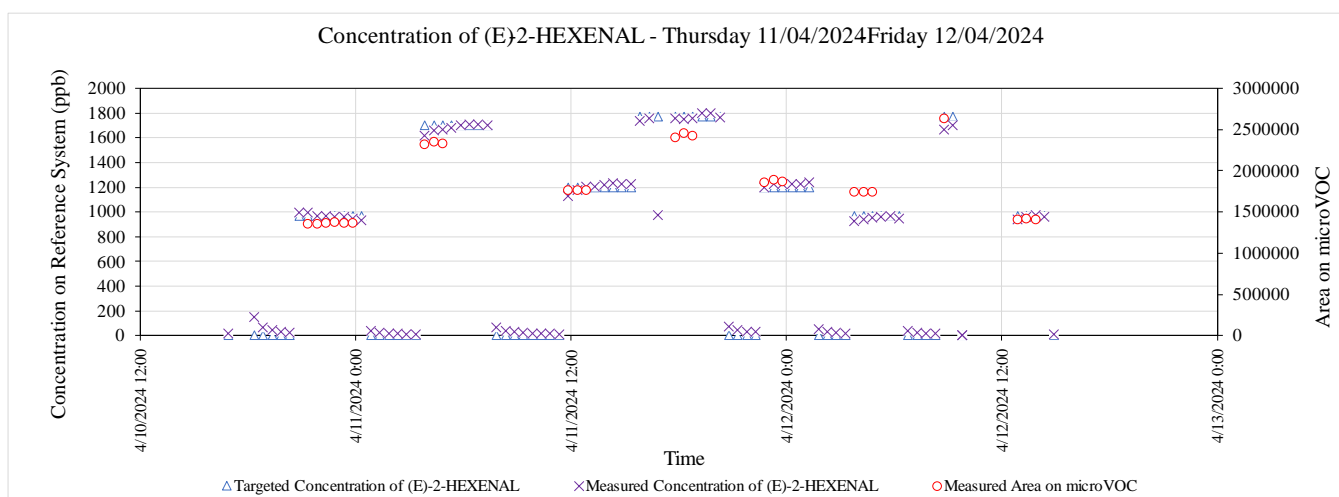
Figure 5-21: Temporal generation of the concentrations of (E)-2-hexenal on the reference system along with the areas recorded on microVOC for the last two days of the intercomparison.
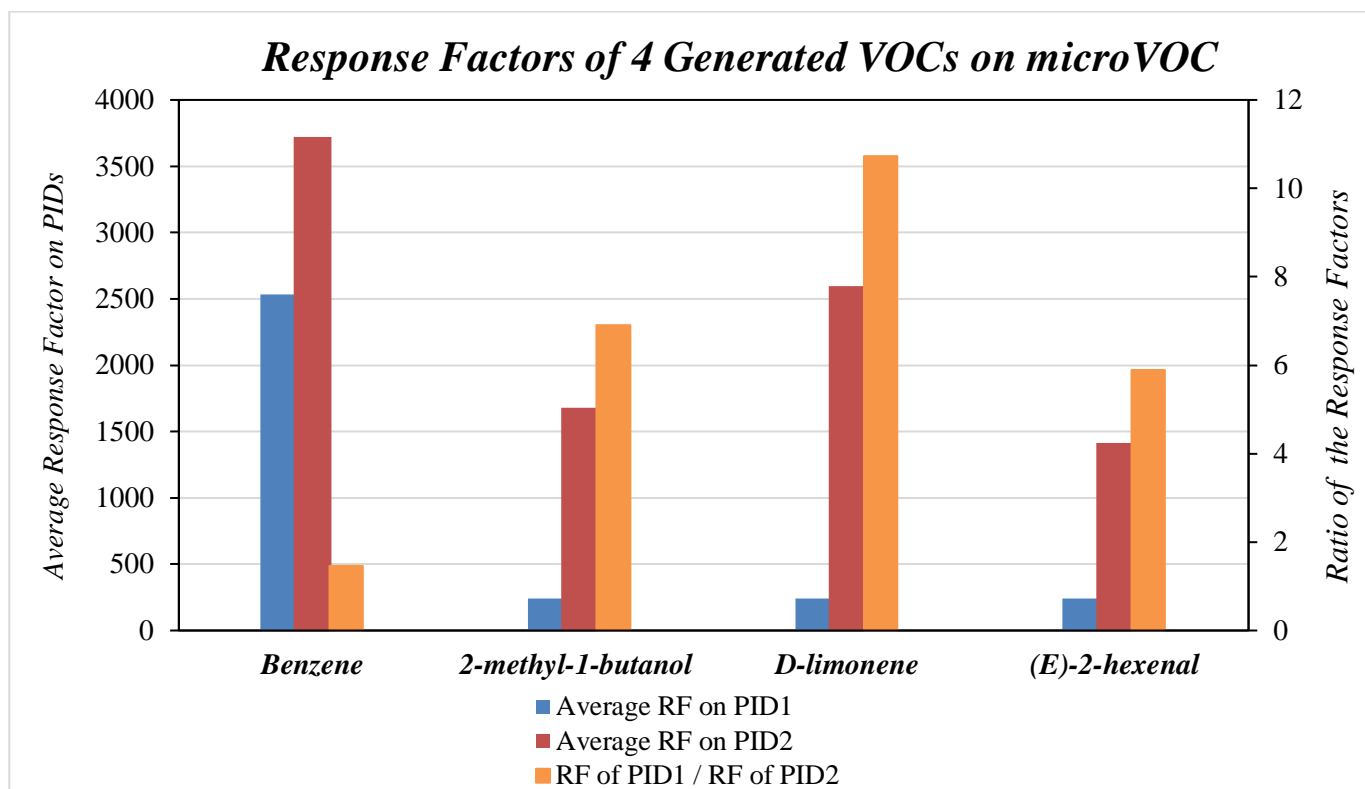
Figure 5-22: Response Factors of 4 Generated VOCs on microVOC using PID1 & PID2 (RF = Response Factor).

Table 5-1: Derived concentrations for benzene from the average calculated response factors in ppb with their uncertainties when using PID1 & PID 2

	Targeted Concentration of benzene (ppb)	Average Measured Concentration on Reference System (ppb)	Average Area on PurPest microVOC (a.u.)	Average Response Factor	Concentrations Derived from Average Response Factor (ppb)	$|\Delta_{concentration}|$ (ppb)
PID 1	1,100	1,191.80	2,806,200.00	2,533.65	1,074.81	25.19
					1,123.95	23.95
					1,123.95	23.95
PID 2	1,013	1,013.30	3,769,480.00	3,721.10	1,026.19	13.19
					999.81	13.19

Table 5-2: Derived concentrations for 2-methyl-1-butanol from the average calculated response factors in ppb with their uncertainties when using PID1 & PID2

	Targeted Concentration of 2-methyl-1-butanol (ppb)	Average Measured Concentration on Reference System (ppb)	Average Area on PurPest microVOC (a.u.)	Average Response Factor	Concentrations Derived from Average Response Factor (ppb)	$|\Delta_{concentration}|$ (ppb)
PID1	700	668.33	170,280.50	243.26	635.31	33.02
					693.64	25.31
					706.36	38.04
PID2	700	678.15	1,139,465.00	1,678.10	673.46	4.69
					684.58	6.43

Table 5-3: Derived concentrations for d-limonene from the average calculated response factors in ppb with their uncertainties when using PID1 & PID2

	Targeted Concentration of d-limonene (ppb)	Average Measured Concentration on Reference System (ppb)	Average Area on PurPest microVOC (a.u.)	Average Response Factor	Concentrations Derived from Average Response Factor (ppb)	$\|\Delta_{concentration}\|$ (ppb)
PID 1	620	612.61	150,027.67	241.98	670.10	57.49
					642.88	30.27
					547.01	65.60
PID 2	706	706.15	1,833,545.00	2,597.09	709.53	3.37
					702.47	3.68

Table 5-4: Derived concentrations for (E)-2-hexenal from the average calculated response factors in ppb with their uncertainties when using PID1 & PID2

	Targeted Concentration of (E)-2-hexenal (ppb)	Average Measured Concentration on Reference System (ppb)	Average Area on PurPest microVOC (a.u.)	Average Response Factor	Concentrations Derived from Average Response Factor (ppb)	$\|\Delta_{concentration}\|$ (ppb)
PID1	910	893.49	218,229.20	239.80	989.50	96.01
					938.75	45.25
					954.10	60.60
					876.74	16.76
					854.06	39.44
					846.85	46.64
PID2	965	964.43	1,363,228.00	1,412.70	958.39	6.04
					962.28	2.15
					963.79	0.64
					974.84	10.41
					965.70	1.27

5.1.4   CONCLUSION

During the second week of April, AIRMOTEC hosted PurPest partners from SINTEF, SAFTRA, Volatile AI, UWAR and JKI where an intercomparison was held. The aim of this intercomparison was to validate the response of the generated VOCs from the AIRMOTEC's

generation system on the newly developed sensors and analysers of the partners. During the first day, concentrations of 2-methyl-1-butanol and ethanol were generated. During the second day, concentrations of d-limonene and benzene were generated. During the third day, concentrations of hexanal and (E)-2-hexenal were generated. While during the fourth and fifth day, a mixture of all beforementioned VOCs were generated. On the reference system of AIRMOTEC, C6-C12/FID/MS, AIRMOTEC was able to detect all the compounds accordingly whether generated alone or along with other compounds. However, on the PurPest microVOC, all the compounds: 2-methyl-1-butanol, benzene, d-limonene, hexanal and (E)-2-hexenal were detected - except ethanol, which due to its early elution and nature of the column used for the microVOC and the low targeted concentration, it was not obviously detected. At the end of the third day of the intercomparison, PID1 was changed to PID2 and the responses for the targeted VOCs were improved for terpenes (D-limonene) and for the OVOCs (2-methyl-1-butanol and (E)-2-hexenal). The next step would be to target much lower concentrations that would more resemble the concentrations emitted by the plants along with a wider range of compounds to standardize the analysers accordingly before sampling in the real environment of pest invasion by the help of AIRMOTEC's designed permeation tubes. It is noteworthy to point out that all of the mixtures were analyzed under isothermal conditions of the microVOC column, the condition that usually applies when the detector is rather specific to the detection of compounds of certain chemical classes, which is not the case in this intercomparison. It then necessitates the usage of a temperature gradient for the oven to be able to target the elution of different compounds knowing that the microVOC was capable of separating several compounds.

5.2 Volatile AI portable sensor platform testing during the Intercomparison campaign

Volatile AI brought the Scout3 instrument for parallel testing against other sensor technologies. The Scout3 device is built to be easy to integrate with different sensor technologies and during the test contained 4 different gas sensors: PID 10.0 eV, PID 10.6 eV and PID 11.7 eV and BME680. In addition, it has many different sensors to control the sampling conditions such as pressure, humidity and flow and a number of mass flow controllers.

The instrument was used as another measurement device next to different sensor technologies.

Figure 5-23 Volatile AI Scout3 setup (left hand side)

Out of the sensors tested in Scout3 instrument, the following conclusions were drawn:
1. 10.0 PID reacted to most of the compounds of interest and provides an additional level of triangulation. However, 10.6 PID was slightly more sensitive to the compounds measured.
2. 10.6 PID was considered the optimal sensor for the matrix measured, and the below results are based on it.
3. 11.7 PID generated little meaningful signal. The sensor typically only reacts to much higher concentrations of compounds than measured during the campaign.
4. BME680 MOX sensor did not respond in line with the measured peaks and was considered insufficient for the measurement task.

5.2.1 Data collected with Scout3: PID2

Below is a snapshot of the chromatograms collected during Thursday
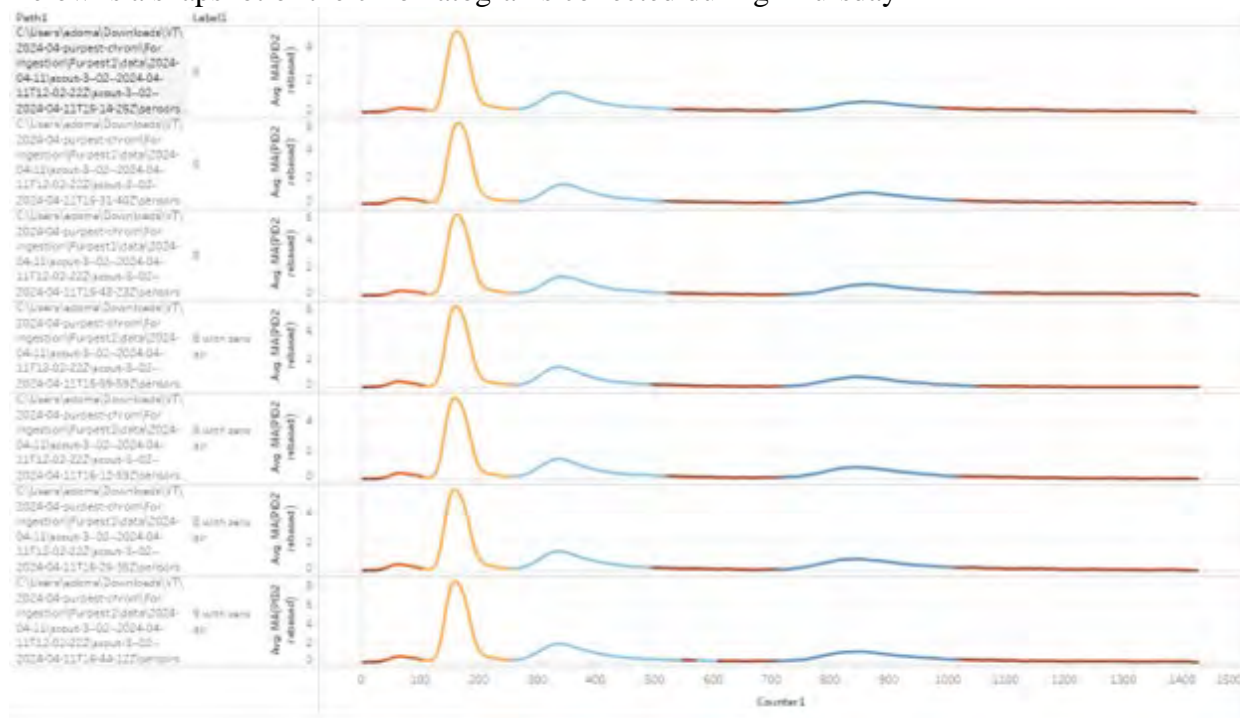
Figure 5-24: The different colours represent different peaks / compounds. The very first peak is considered unknown. Peak 2 corresponds to benzene, peak 3 to 2-ME-1-BUTANOL and peak 4 to 2-HEXENAL

In summary the collected chromatograms for peaks of significance can be found below:
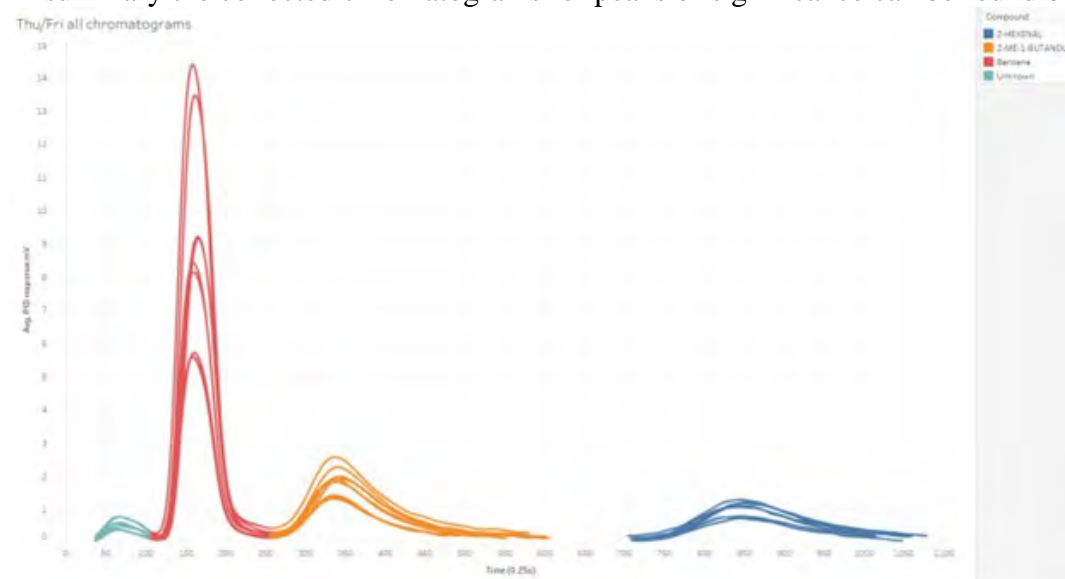
Figure 5-25: The different peak areas correspond to different concentrations of the VOCs measured.

5.2.2 Scout3 compound detection conclusions

The expected detection limits of Scout3 for the compounds measured were sufficient to detect concentrations above 180 PPB, but not enough to detect concentrations equal to and below 50 PPB. The setup from the compounds of interest could detect the following VOCs: 2-ME-1-BUTANOL, 2-HEXENAL. Limonene was not detected; however, its lower volatility likely requires a column heating regime to be able to see it, which was not applied due to lack of time.

5.3 UWAR's SMR testing during the Intercomparison campaign

UWAR brought and installed their μ-GC testing setup and SMR e-nose system to the Intercomparison campaign at AIRMO for testing with target compounds. Both the setups installed at AIRMO are shown in **Figure 5-26**.
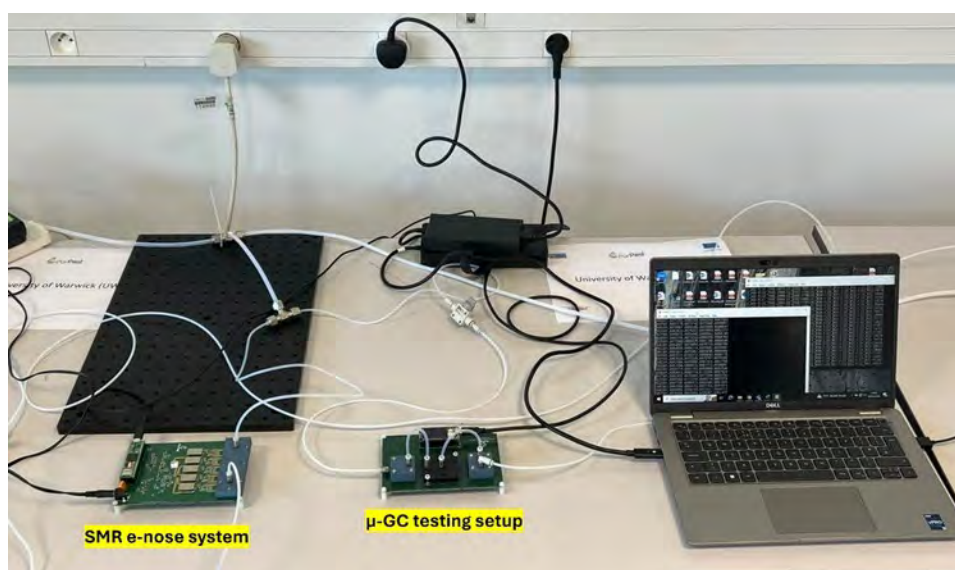
Figure 5-26: Both the setups installed at AIRMO.

5.3.1 μ-GC testing setup

UWAR developed a μ-GC testing setup comprises commercial metal oxide sensors positioned before and after the μ-GC columns, with a microcontroller connected to facilitate data collection (see **Figure 5-27**). This configuration enables the monitoring of gas samples before (S1) and after (S2) they pass through the μ-GC columns. In this arrangement, the target VOCs pass first through the S1 chamber, then the μ-GC column, and finally the S2 chamber, while the microcontroller continuously monitors the resistance change of both sensors over time. In this way, the species separation ability of the column can be read out by the S2 sensor, allowing for real-time assessment of the efficiency of the separation process.
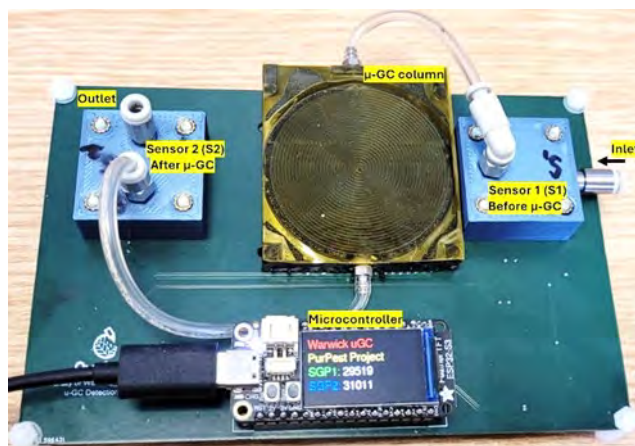
Figure 5-27: UWAR Micro-GC testing setup.

5.3.2   μ-GC testing setup

The study involved testing two 1.2-meter-long micro gas chromatography (μ-GC) columns, each coated with a different stationary phase: OV-1 and PEG. These columns were evaluated for their performance during the intercomparison campaign at AIRMO. The results are depicted in **Figure 5-28** and **Figure 5-29**, with **Figure 5-28** illustrating the performance of the OV-1 coated μ-GC column. In the experiment, the OV-1 coated μ-GC column was tested with various compounds and their interferents, specifically methyl butanol, limonene, and trans-2-hexenal. The results showed that the relatively short length of 1.2 meters made it challenging to effectively separate the interferents from the target compounds. Despite this, a notable delay and degradation in the S2 response were observed for all the tested compounds. Similarly, the PEG coated μ-GC column also showed a delay and degradation in the S2 response for different tested compounds, as shown in **Figure 5-26**. These results suggest that the 3D printed μ-GC columns, while economical, exhibit potential for separating compound mixtures if their design and testing parameters are optimized. Therefore, a sequential research plan has been developed to optimize the μ-GC performance by studying different column dimensions and operating parameters. The flow chart diagram of the research plan is shown in **Figure 5-30**. The research plan involves:

Assessment of Current Design: Analysing the performance data from the initial tests to identify specific areas for improvement.

Variation of Column Dimensions: Testing columns of different lengths and diameters to find optimal dimensions for better separation efficiency.

Optimization of coating thickness: Testing different stationary phase coating thickness to optimize the column performance.

Optimization of Operating Parameters: Adjusting parameters such as carrier gas flow rate, temperature gradient, and injected pulse width.

Iteration and Testing: Repeatedly testing and refining the columns based on performance data.

Final Evaluation for calibration: Conducting a comprehensive evaluation of the optimized columns under various conditions to validate improvements and calibrate the column.
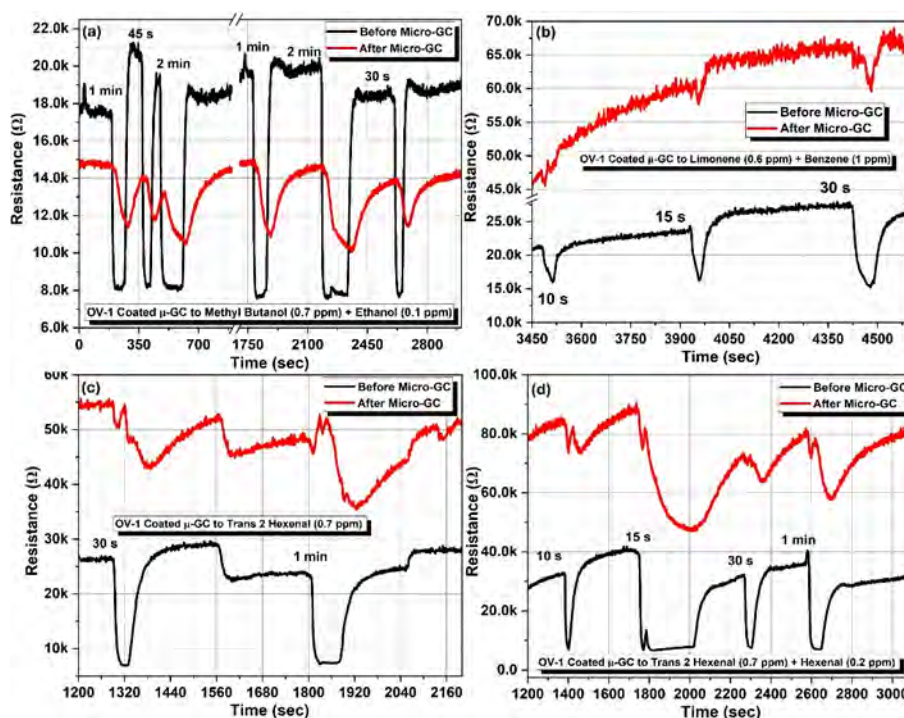
Figure 5-28: μ-GC testing setup results with OV-1 coated column to different compounds, (a) S1-S2 response to 2-methyl-1-butanol and ethanol as interest at different time intervals, (b) S1-S2 response to limonene and benzene as interest at different time intervals, (c) S1-S2 response to trans-2-Hexenal at different time intervals, and (d) S1-S2 response to trans-2-hexenal and hexenal as interest at different time intervals.
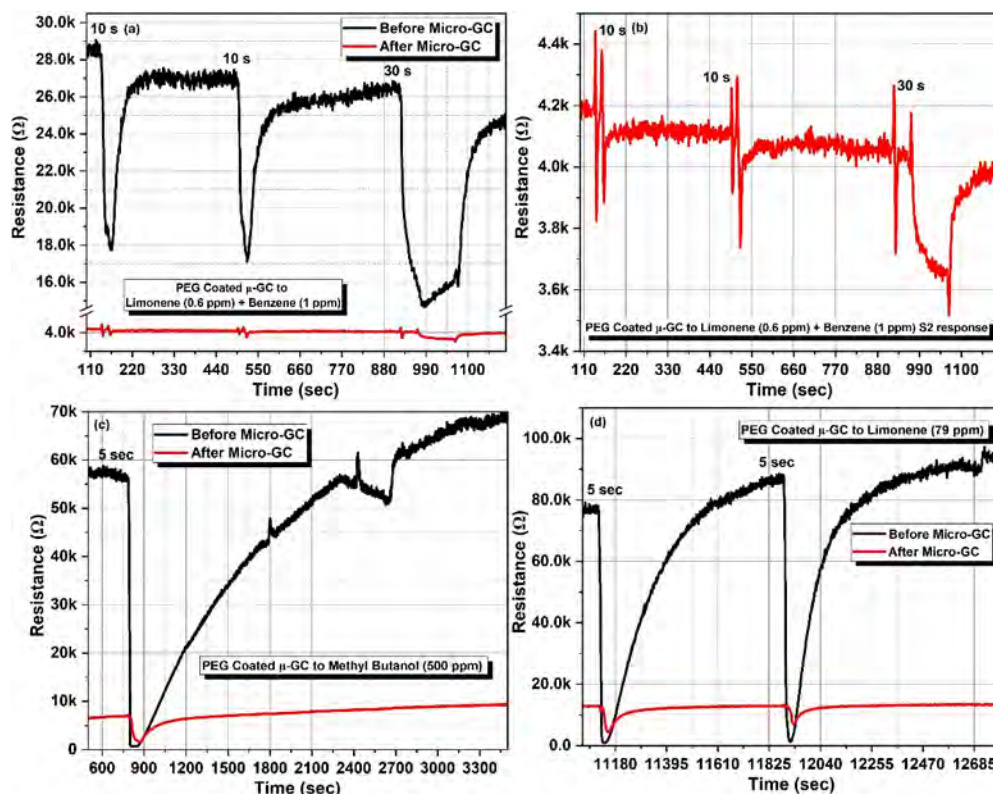
Figure 5-29: µ-GC testing setup results with PEG coated column to different compounds, (a) S1-S2 response to limonene and benzene as interest at different time intervals, (b), enlarged view of the S2 response with limonene and benzene as interest, (c) S1-S2 response at higher concentration of 2-methyl butanol, and (d) S1-S2 response to higher concentration of limonene.
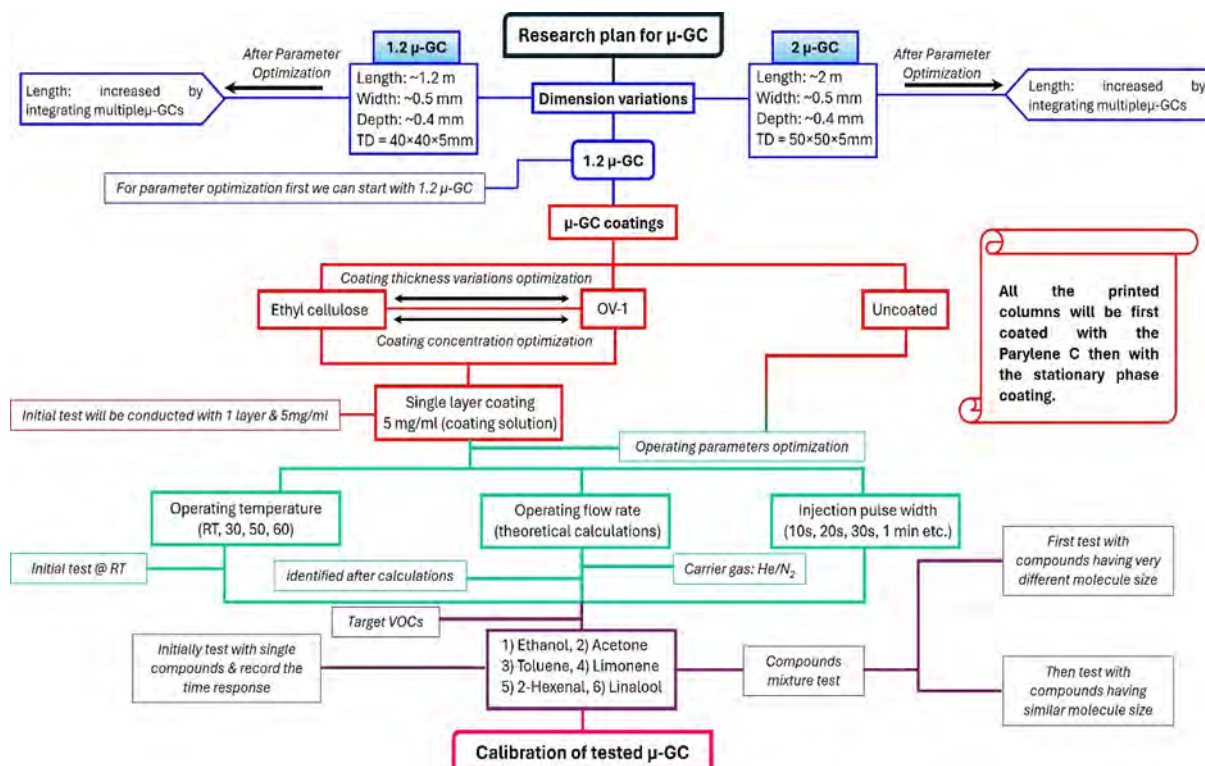
Figure 5-30: Research plan flow chart for the optimization of the fabricated µ-GC Columns.

5.3.3 Development of SMR e-nose system

The system operates in a dual mode configuration to suppress common environmental effects, with SMR as a reference channel and the second as a sensing channel. SMR driving circuitry contains an oscillator circuit and a mixer circuit. The output signal of the mixer board, which is the differential frequency of sensing SMR and reference SMR, goes to the microcontroller. The microcontroller reads the frequency value. The output frequency data is stored in a PC via USB serial communication data. **Figure 5-31** shows the block diagram of the interface electronics circuitry for SMR devices.
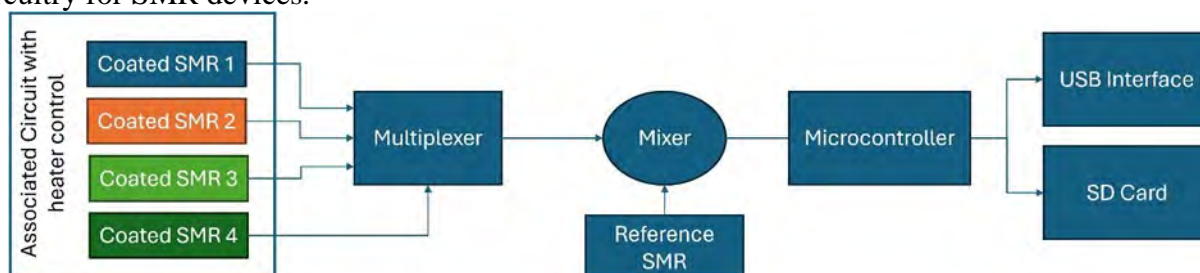
Figure 5-31: Block diagram of the interface electronics circuitry for e-nose system.

Based on the above-mentioned electronic readout circuitry, we have built an e-nose PCB comprised of arrays of sensors (4-SMRs, 1 reference) with commercial BME 688 sensor (for temperature, humidity), oscillators and band pass filter at 1 GHz, multiplexers, mixer, and a band pass filter at lower frequencies. After coating the SMRs with PEG, PDMS, and EC the e-nose system was tested during the intercomparison campaign at AIRMO and the results are displayed in the next section. **Figure 5-32** displays the developed e-nose board.
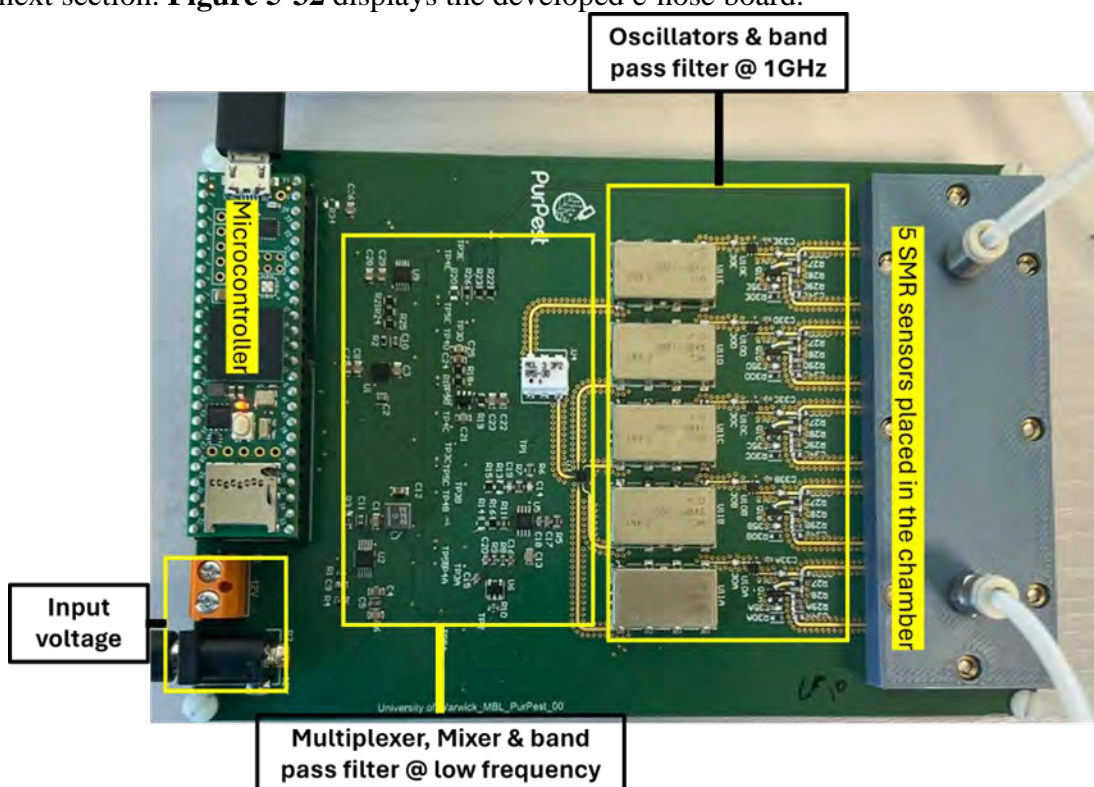
Figure 5-32: E-nose board based on SMR sensors. (Figure 16)

5.3.4   Performance of SMR e-nose system.

To test the performance of the fabricated e-nose system, the array of SMRs devices was coated with polyethylene glycol, ethyl cellulose, and PDMS targeting the polar and non-polar compounds. The e-nose system was exposed to the target compounds at AIRMO during the Intercomparison campaign. The system was also tested at higher concentration of 2-methyl butanol, limonene and trans-2-hexenal. Unexpectedly, the results show identical variations in the response of all the SMRs for all tested compounds. This might be happening due to the phase locking phenomenon; we are currently working to solve this problem. We are considering multiple options such as adding packaging for each SMR and placing them further apart from each other. **Figure 5-31** shows an example of e-nose system output response variations for each SMR.
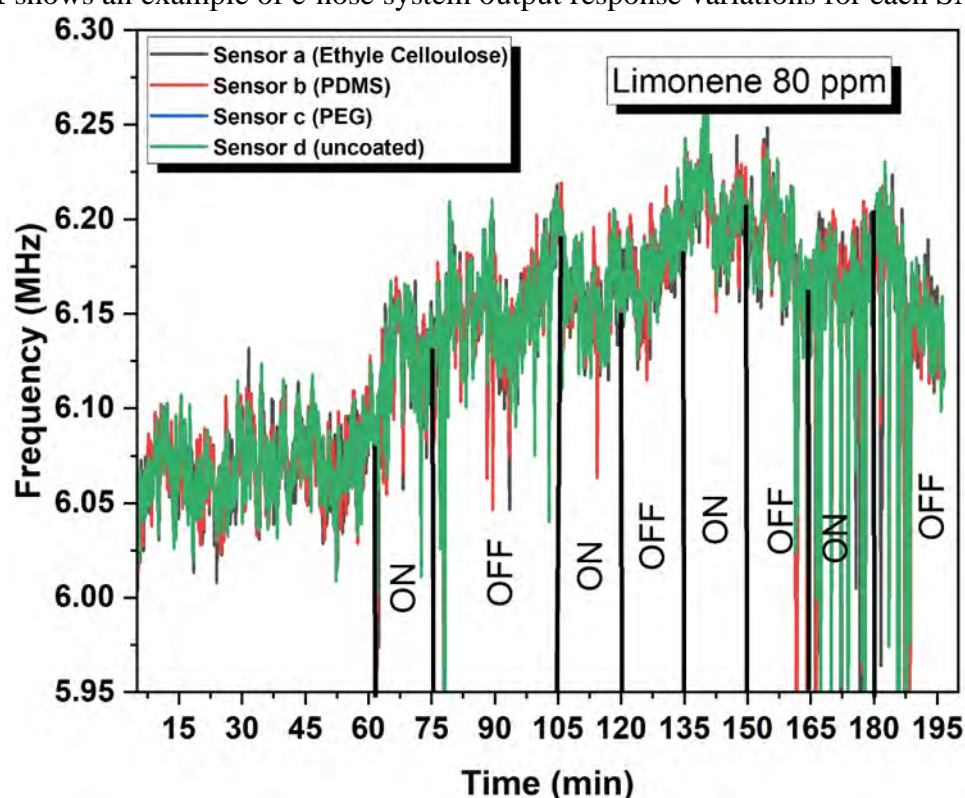
Figure 5-33: E-nose system output response variations of all SMRs to higher concentration of limonene.

5.3.5   Conclusions for the Warwick's µ-GC and e-nose

The results suggest that the 3D printed µ-GC columns, while economical, exhibit potential for separating compound mixtures if their design and testing parameters are optimized. Therefore, a sequential research plan has been developed to optimize the µ-GC performance by studying different column dimensions and operating parameters.

The results for the array of SMRs forming the e-nose showed that it was plagued with a phase locking phenomenon. It might also be due to the low performance of the LiteVNA used to take the resonance spectra.

5.4   Saftra Pickmol SERS chips

5.4.1   Tests at Intercomparison campaign

Due to the shortness of time, specialized chips for the detection of proposed VOCs could not be prepared for the experiments in Bordeaux. Therefore, we prepared only basic chips and chips with simple functionalization for the tests, which gave a certain, but small chance of detecting the proposed VOCs. The results confirmed it. Only small, insignificant changes in the detection spectra were presented for VOCs – limonene and 2M1B. Considering the above facts, it was not a surprising result.

On the other hand, a low sensitivity of the detection of DMS by the PickMol technology was surprising, as the same molecule has been detected without any problems in laboratories of SAFTRA photonics.
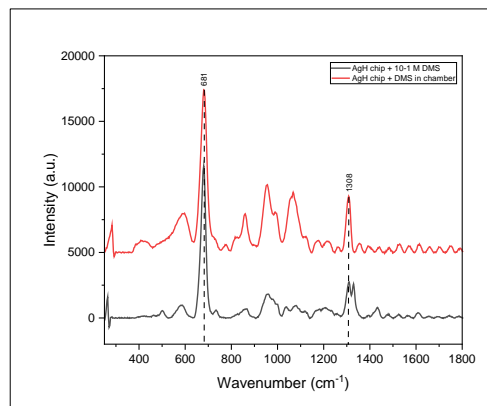
Figure 5-34: Dimethyl sulfide (DMS) – spectrum on PickMol nano-chip

5.4.2   Conclusions from Intercomparison campaign for Saftra's SERS chips

The tests in Bordeaux have shown:
1.   RAMASCOPE: optical arrangement of the detection system tailored for VOCs detection works properly (optical as well as mechanical part including scanning system)
2.   Flow cell: construction of the flow cell optimized for VOCs detection seems to work properly. To confirm or deny this statement it will be necessary to accurately measure the gas flow through the cuvette where nanostructured chip is placed (tests with DSM have created doubts about appropriate air flow in cell).
3.   Detection nanostructured chips: no optimally constructed chips(tailoring) were used, which caused a very low sensitivity of selected VOCs detection. Low sensitivity of DMS detection remains unclear and must be verified by new experiments.

5.4.3   Recommendations

Successful detection of VOCs depends on two factors:
1.   **Optimalization of the detection system for sensitive identification of selected VOC**s. Performed modification of hardware and software of the RAMASCOPE detection systems has been evaluated as suitable for VOCs detection in different approaches including a continuous repetitive measurement. Some minor modification of hardware mainly related to the construction of a complex SSP system are envisaged. Software modifications will respect specific needs related to a rapid, sensitive, and selective detection of VOCs as well as specific needs related to an incorporation of RAMASCOPE into the SSP.
2.   **Development/tailoring of specific nanostructured chips for a detection of selected VOCs**. Development tailored chips for the detection of specific VOCs represents the main bottleneck at this period of the project implementation for the SAFTRA photonics. What we propose is to define three (maximum five) VOCs of interest for which SAFTRA will work on preparing specific nanostructured chips for their selective and sensitive detection.

Development of one such nanostructure needs necessary time and related budget (see related budget modification proposed by SAFTRA).

5.5 SINTEF SERS and MOF chips

The SINTEF SERS and MOF chips were used for Raman measurements in Saftra's Ramascope flow cell. The first experiments were conducted using the samples from the common line. In some instances, the bulb injection method shown in **Figure 4-3** was used.

Table 5-5: approximate concentrations of VOC using the bulb injection method.

VOC	Conc (ppm)
Trans-2-Hexanal	2698
Limonene	1903
2-methyl-1-butanol	3118
Di-Methyl Sulphide	1030

5.5.1 SERS chips

SINTEF had prepared chips with two different nanolithography imprints (IMP467). The "-4" is a C-pattern while "-6" is a star-pattern. The following sections show different Raman spectra with different VOCs and DMS (di methyl sulphide).

None of the recorded Raman spectra indicate any detection of any of the VOCs but are shown here for reference.

5.5.1.1 IMP467-6
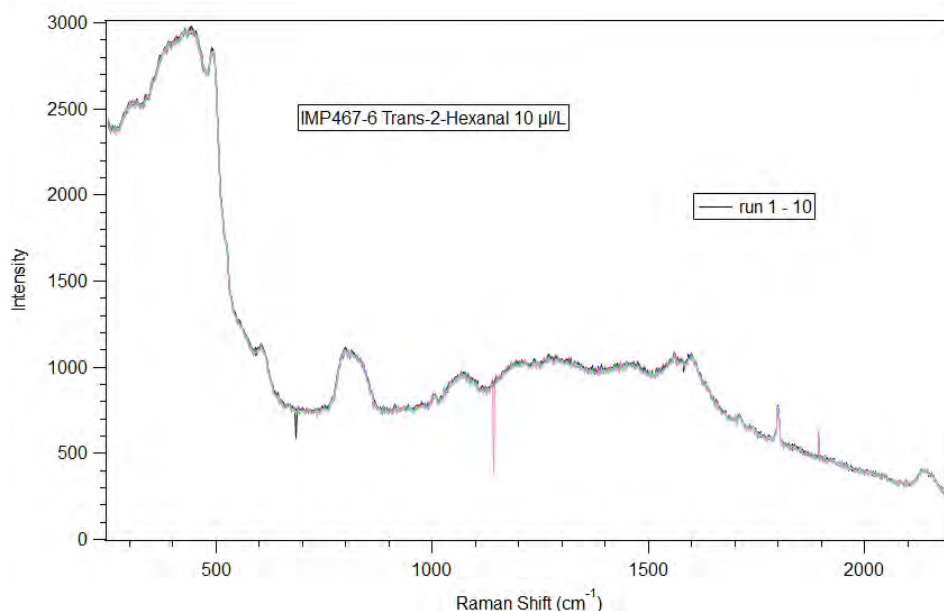
Figure 5-35: IMP467-6 Trans-2-Hexanal, 10 µl/L
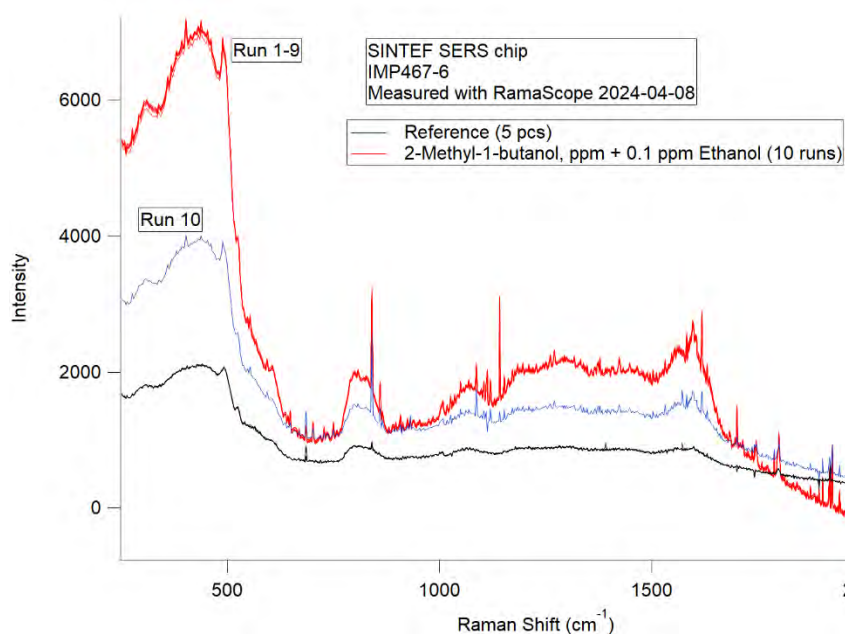
Figure 5-36: IMP467-6 with 2-methyl-1-butanol & 0.1 ppm ethanol
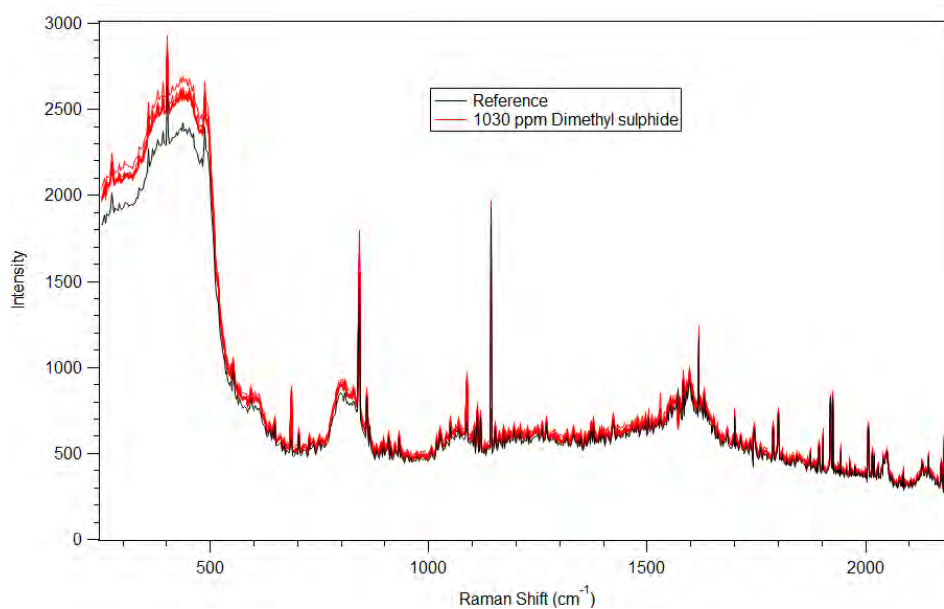
Figure 5-37: IMP467-6 with 1030 ppm DMS
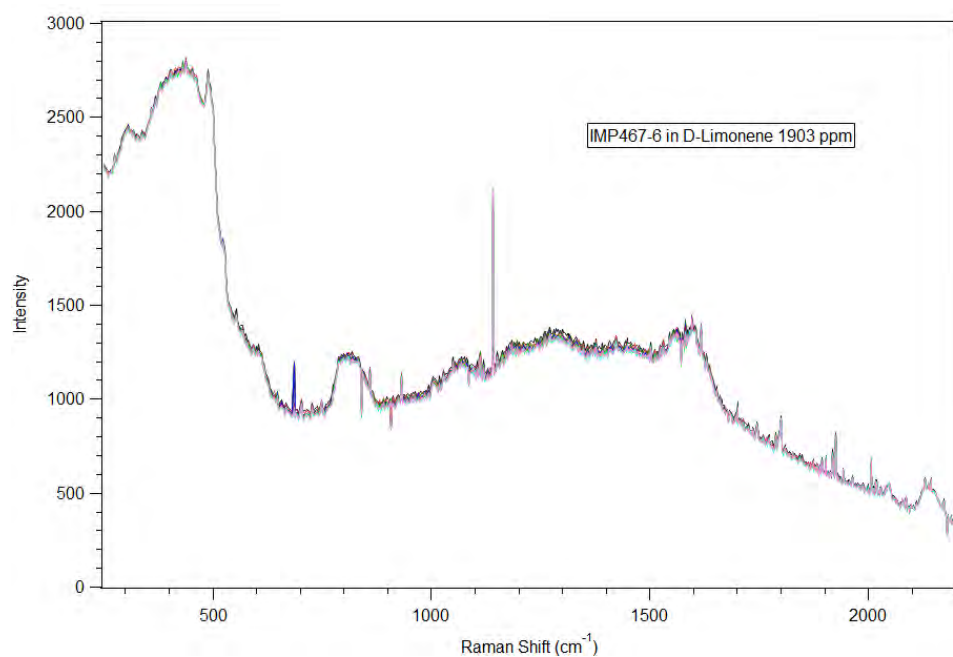
Figure 5-38: IMP467-6 with 1903 ppm d-limonene

5.5.1.2 IMP467-4
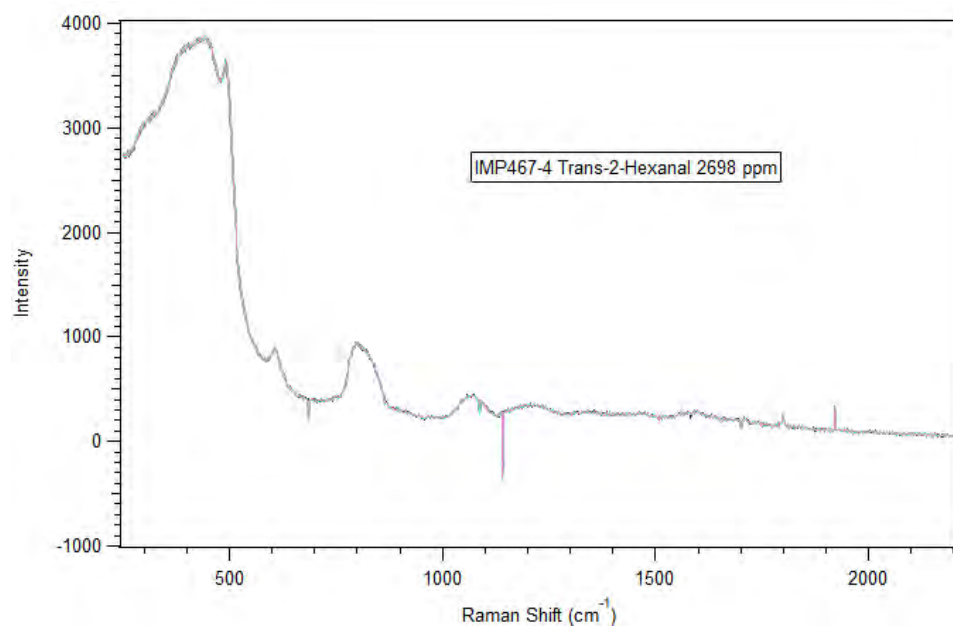
Figure 5-39: IMP467-4 in trans-2-hexanal 2698 ppm
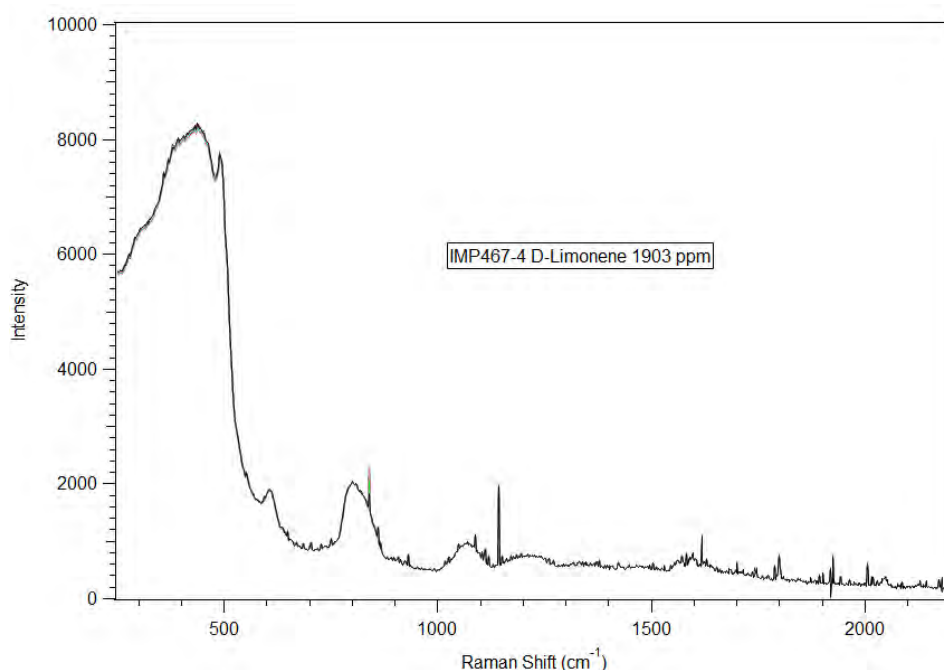
Figure 5-40: IMP467-4 in d-limonene 1903 ppm

5.5.2 MOF powders on Au surface

MOFs NU1000 and UiO67 were tested as SERS substrates. Both showed a certain level of fluorescence, which lead to changing background intensities. In some cases, an effort was made to remove the background with polynomial fitting.

5.5.2.1 MOF UiO67
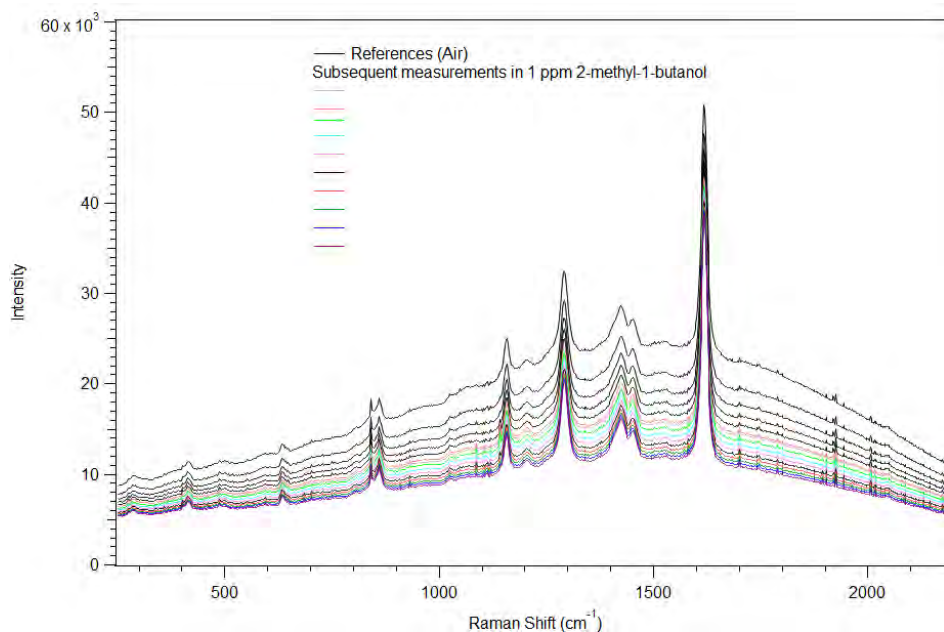
Figure 5-41: Raman spectroscopy of MOF UiO67 when exposed to 1 ppm of 2-methyl-1-butanol. Without background removal.
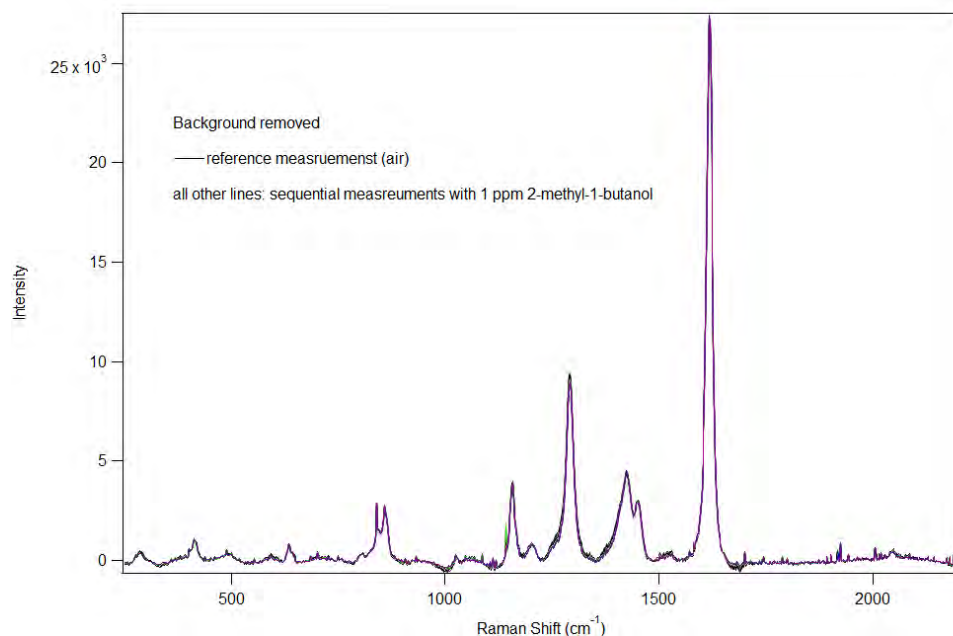
Figure 5-42 Raman spectroscopy of MOF UiO67 when exposed to 1 ppm of 2-methyl-1-butanol. With background removal.

The background removed spectra for UiO67 exposed to 1030 ppm of DMS is shown in**Figure 5-43**. Although there is no large signal change, when zooming in on some peaks, there is a clear difference between the reference measurements and the subsequent measurements. This increase in signal only happens at peaks, and not in the surrounding noise.
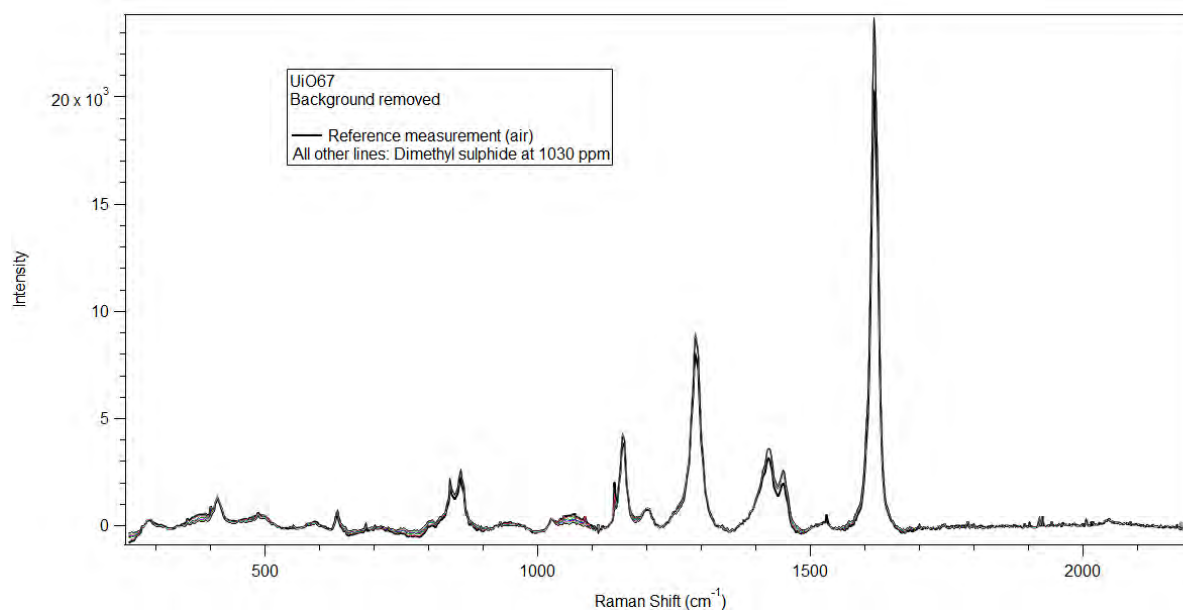
Figure 5-43: Spectra of UiO67 exposed to 1030 ppm DMS. Background has been removed.
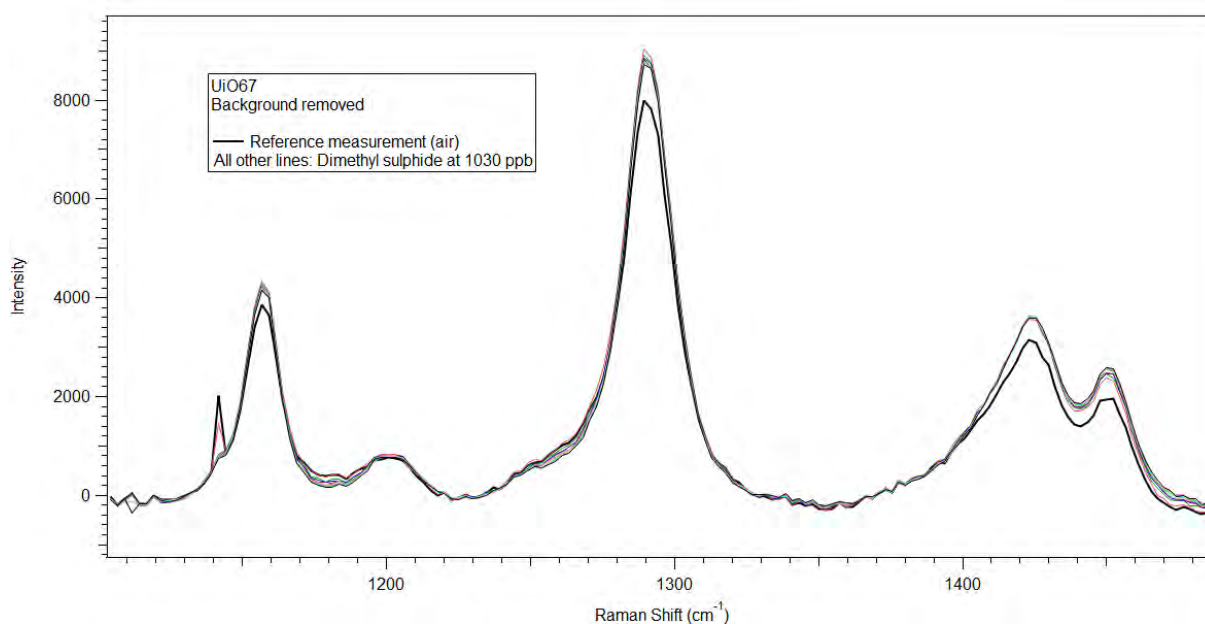
Figure 5-44: Close up of peaks for UiO67 exposed to 1030 ppb DMS show that there is some increase in signal.

The same increase in signal can be seen when UiO67 is exposed to Trans-2-Hexanal at 2689 ppm, as seen in **Error! Reference source not found.**.
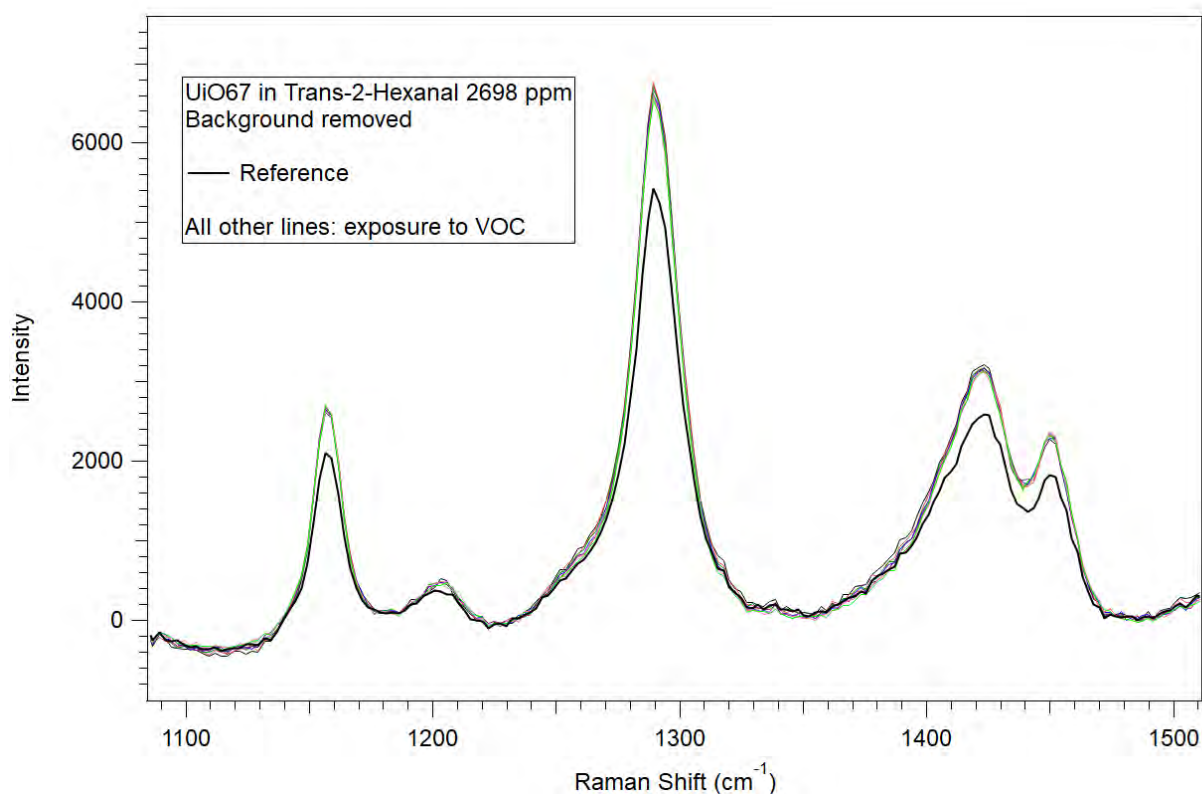
Figure 5-45: UiO67 exposed to trans-2-hexanal at 2689 ppm. There is a clear change in intensity at the peaks.

5.5.2.2 NU1000
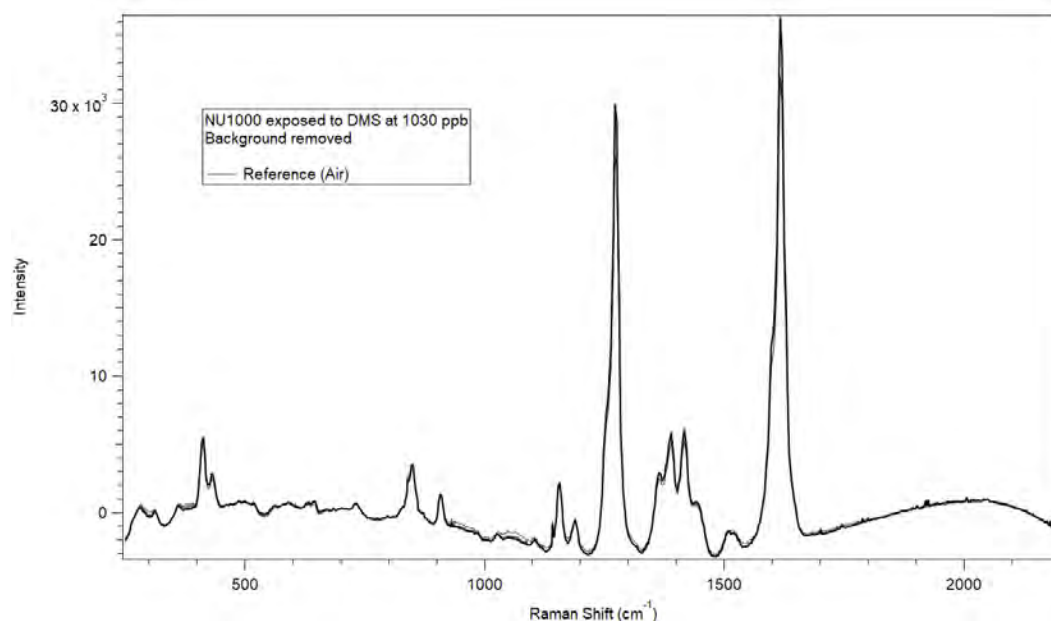
Figure 5-46: NU1000 exposed to DMS at 1030 ppb showed no signal change.
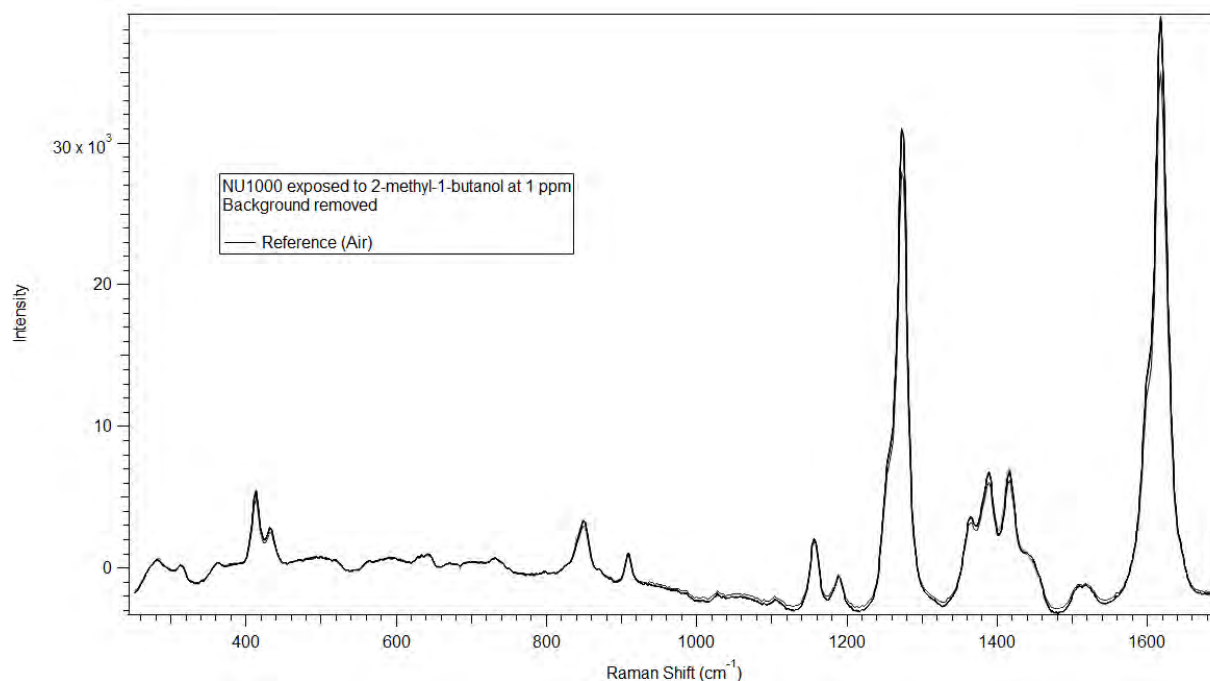
Figure 5-47: NU1000 exposed to 2-methyl-1-butanol at 1 ppm showed no indication of spectrum change.
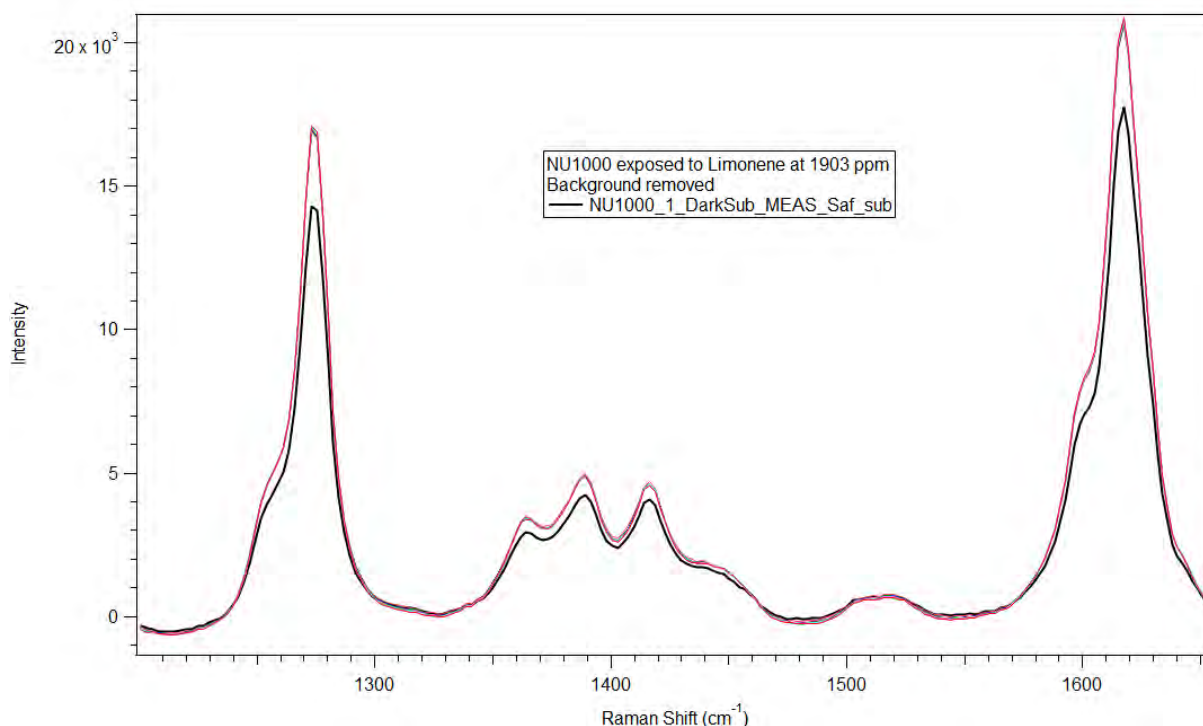
Figure 5-48: NU1000 exposed to Limonene a 1903 ppm. There is a slight indication of a change in intensity at the peaks.

5.5.3 Conclusion on SINTEF's SERS chips and MOFs

Regrettably, none of the SERS chips gave any indication of enhancing the Raman spectrum of any of the VOCs. One reason may be that for the SERS maximum enhancement factor, the molecules in testing must be located very close to the SERS surface (few to tens of nm). The obtained results suggest that tested VOCs have low affinity to gold surface.

The MOF UiO67 showed a slight change in peak intensity for some of the VOCs. This might indicate that the VOCs attach to the MOF.

To address the issue of poor VOC adherence to SERS surfaces, SINTEF plans to investigate the deposition of MOFs onto the SERS chips. By combining the MOF's ability to capture VOCs with the SERS chip's potential for enhancing the Raman signal, we aim to develop a more effective detection system. The MOF will serve as a medium to attach the VOCs to the SERS surface, while the SERS substrate will enhance the Raman spectrum, potentially leading to improved detection sensitivity and specificity.

6   SUMMARY AND CONCLUSION

6.1   Summary

This deliverable has reported the performance of systems and the potential components to be fitted in the SSP. Two systems were tested
1. MicroVOC – AIRMO's miniature GC system
2. Scout 3 – VOL's portable GC system

In addition, the following components were tested
1. Warwick's 3D printed µ-GC
2. Warwick's 4-array SMR e-nose
3. Saftra Photonics' RAMASCOPE
4. Saftra Photonics' Colloidal SERS chips
5. SINTEF's SERS chips
6. SINTEF's MOF powder on Au surface.

6.2   Conclusion

Warwick's µ-GC showed potential for separating VOCs in the time domain but needs optimisation to enhance the separation.

The sensors being developed by SINTEF, Warwick and Saftra need further development to enable detection of VOCs.

The two systems, microVOC and Scout 3, performed well and managed to detect and identify VOCs.

The components in AIRMO's microVOC are the first compatible sensor system components to be integrated in WP3 (D2.3). These components are
1. Pneumatic Valve: allows the operation in 'sampling' position or in 'injection' position. In 'sampling' position, the gas sample is drawn by a pump into a preconcentrator (trapping unit = a fine tube that contains porous substances). In 'injection' position, the valve is actuated. The trap starts to heat up to desorb the sample components. The components are then flushed into the analytical column by the carrier gas flow.
2. Preconcentrator: a trapping unit that adsorbs the gaseous components being sampled. The components are then desorbed after flushing with a carrier gas (nitrogen).
3. Analytical Column: is situated in an isothermal oven operating at a constant temperature. The components elute from the column at a characteristic rate depending on the interaction with the stationary phase situated on the column. The retention time gives the characteristic peak for every component.
4. Detector: a mini photoionization detector (PID) equipped with an ultra-violet lamp. An electrical signal is generated and digitized to be processed for automatic integration and peak identification.

7 REFERENCES

Arimura, G. et Pearse, I., «From the Lab Bench to the Forest: Ecology and Defence Mechanisms of Volatile-Mediated 'Talking Trees',» *How Plants Communicate with their Biotic Environment ,* pp. 3-17, 2017.

Che Harun, F.K., 2009. *Mimicking the human olfactory system: a portable e-mucosa* (Doctoral dissertation, University of Warwick).

Dietz, R. N., Cote, E. A. et Smith, J. D., «New method for calibration of permeation wafer and diffusion devices,» *Analytical Chemistry,* vol. 46, n° %12, pp. 315-318, 1974.

Esfahani, S., Dawson, D., Wojcik, B. Cole, M. and Gardner, J.W., accepted 2023, June. Indoor Air Quality CO2 Thermally Modulated SMR Sensor†. In XXXV International Eurosensor conference.10-13 September. Lecce, Italy.

Harun, F.C., Covington, J.A. and Gardner, J.W., 2009. Portable e-Mucosa System: Mimicking the biological olfactory. *Procedia Chemistry*, 1(1), pp.991-994.

Harun, F.C., Taylor, J.E., Covington, J.A. and Gardner, J.W., 2009. An electronic nose employing dual-channel odour separation columns with large chemosensor arrays for advanced odour discrimination. *Sensors and Actuators B: Chemical*, 141(1), pp.134-140.

Schmidt, W. P. et Rook, H. L., «Preparation of gas cylinder standards for the measurement of trace levels of benzene and tetrachloroethylene,» *Analytical Chemistry,* vol. 55, n° %12, pp. 290-294, 1983.

Specht, J.P., 2022. *Thermally modulated solidly mounted resonators for air quality monitoring* (Doctoral dissertation, University of Warwick).

Specht, J.P., Esfahani, S., Cole, M. and Gardner, J.W., 2021, June. CMOS compatible aluminium nitride solidly mounted resonator with an integrated microheater for temperature modulation. In *2021 21st International Conference on Solid-State Sensors, Actuators and Microsystems (Transducers)* (pp. 1396-1399). IEEE.

Specht, J.P., Esfahani, S., Xing, Y., Köck, A., Cole, M. and Gardner, J.W., 2022. Thermally Modulated CMOS-Compatible Particle Sensor for Air Quality Monitoring. *IEEE Transactions on Instrumentation and Measurement*, 71, pp.1-13.

8 SUPPLEMENTARY INFORMATION FOR INTERCOMPARISON CAMPAIGN

Table 8-1: Response of the reference system and the microVOC during Monday for 2-methyl-1-butanol and ethanol

Time	VOC	Targeted Concentration (ppb)	Reference System Result (ppb)	Areas of the MicroVOC (a.u.)	Interferent	Interferent on Reference System	Interferent on MicroVOC
4/8/2024 8:56	2M1B*	0	0	0	NONE	NO	NO
4/8/2024 9:26	2M1B	0	0	0	NONE	NO	NO
4/8/2024 9:56	2M1B	0	0	0	NONE	NO	NO
4/8/2024 10:26	2M1B	0	0	0	NONE	NO	NO
4/8/2024 10:36	2M1B	700	583.326	91962.6	NONE	NO	NO
4/8/2024 11:06	2M1B	700	609.781	92738.2	NONE	NO	NO
4/8/2024 11:36	2M1B	700	653.513	129197	NONE	NO	NO
4/8/2024 12:06	2M1B	700	643.476	147561	NONE	NO	NO
4/8/2024 12:36	2M1B	700	687.797	154544	ETHANOL	47.1687	N.I.
4/8/2024 13:06	2M1B	700	712.126	168733	ETHANOL	48.0491	N.I.
4/8/2024 13:36	2M1B	700	726.232	171828	ETHANOL	48.836	N.I.
4/8/2024 14:06	2M1B	700	730.352	-	ETHANOL	49.359	N.I.
4/8/2024 14:56	2M1B	0	0	0	NONE	NO	NO
4/8/2024 15:26	2M1B	0	0	0	NONE	NO	NO
4/8/2024 15:56	2M1B	0	0	0	NONE	NO	NO
4/8/2024 16:26	2M1B	0	0	0	NONE	NO	NO

*2M1B = 2-methyl-1-butanol, N.I. = not identified

Table 8-2: Response of the reference system and the microVOC during Tuesday for d-limonene and benzene

Time	VOC	Targeted Concentration (ppb)	Reference System Result (ppb)	Areas of the MicroVOC (a.u.)	Interferent	Interferent on Reference System	Interferent on MicroVOC
4/9/2024 6:41	d-lIM*	0	0	0	NONE	NO	NO
4/9/2024 7:11	d-lIM	0	0	0	NONE	NO	NO
4/9/2024 7:41	d-lIM	0	0	0	NONE	NO	NO
4/9/2024 8:11	d-lIM	0	0	0	NONE	NO	NO
4/9/2024 8:41	d-lIM	620	607.9	-	NONE	NO	NO
4/9/2024 9:13	d-lIM	620	612.19	-	NONE	NO	NO
4/9/2024 11:43	d-lIM	620	624.25	151398	NONE	NO	NO
4/9/2024 12:13	d-lIM	620	634.94	155272	NONE	NO	NO
4/9/2024 12:43	d-lIM	620	583.79	159525	NONE	NO	NO
4/9/2024 13:24	d-lIM	0	26.88	0	NONE	NO	NO
4/9/2024 13:54	d-lIM	0	12.5	0	NONE	NO	NO
4/9/2024 14:24	d-lIM	620	600.37	124051	BENZENE	1185.9	2.62E+06
4/9/2024 14:54	d-lIM	620	620.36	117307	BENZENE	1192.1	2.66E+06
4/9/2024 15:24	d-lIM	620	646.73	162152	BENZENE	1200.3	2.73E+06
4/9/2024 15:54	d-lIM	620	649.56	155565	BENZENE	1199.6	2.72E+06
4/9/2024 16:24	d-lIM	620	640.89	132366	BENZENE	1186.9	2.85E+06
4/9/2024 16:54	d-lIM	620	639.82	132366	BENZENE	1186.5	2.85E+06

*d-lIM = d-limonene

Table 8-3: Response of the reference system and the microVOC during Tuesday for (E)-2-hexenal and hexanal

Time	VOC	Targeted Concentration (ppb)	Reference System Result (ppb)	Areas of the MicroVOC (a.u.)	Interferent	Interferent on Reference System	Interferent on MicroVOC
4/9/2024 18:24	(E)-2-HEX*	910	1131.4	286361	NONE	NO	NO
4/9/2024 18:54	(E)-2-HEX	910	941.5	237295	NONE	NO	NO
4/9/2024 19:24	(E)-2-HEX	910	885.13	225123	NONE	NO	NO
4/9/2024 19:54	(E)-2-HEX	910	864.05	228805	NONE	NO	NO
4/9/2024 20:24	(E)-2-HEX	910	924.06	210252	HEXANAL	31.49	-
4/9/2024 20:54	(E)-2-HEX	910	904.46	204814	HEXANAL	28.68	-
4/9/2024 21:24	(E)-2-HEX	910	873.63	203086	HEXANAL	21.17	7513.5
4/9/2024 21:54	(E)-2-HEX	910	861.65	-	HEXANAL	26.19	7142.1
4/9/2024 22:24	(E)-2-HEX	0	42.18	0	NONE	NO	-
4/9/2024 22:54	(E)-2-HEX	0	25.7	0	NONE	NO	-
4/9/2024 23:24	(E)-2-HEX	0	18.51	0	NONE	NO	NO
4/9/2024 23:54	(E)-2-HEX	0	14.45	0	NONE	NO	NO
4/10/2024 0:24	(E)-2-HEX	0	11.84	0	NONE	NO	NO
4/10/2024 0:54	(E)-2-HEX	0	10.22	0	NONE	NO	NO
4/10/2024 1:24	(E)-2-HEX	0	8.62	0	NONE	NO	NO
4/10/2024 1:54	(E)-2-HEX	0	7.53	0	NONE	NO	NO
4/10/2024 2:24	(E)-2-HEX	0	6.6	0	NONE	NO	NO
4/10/2024 2:54	(E)-2-HEX	0	5.83	0	NONE	NO	NO
4/10/2024 3:24	(E)-2-HEX	0	5.36	0	NONE	NO	NO
4/10/2024 3:54	(E)-2-HEX	0	4.69	0	NONE	NO	NO

Time	VOC	Targeted Concentration (ppb)	Reference System Result (ppb)	Areas of the MicroVOC (a.u.)	Interferent	Interferent on Reference System	Interferent on MicroVOC
4/10/2024 4:24	(E)-2-HEX	0	4.36	0	NONE	NO	NO
4/10/2024 4:54	(E)-2-HEX	0	3.89	0	NONE	NO	NO
4/10/2024 5:24	(E)-2-HEX	0	3.65	0	NONE	NO	NO
4/10/2024 5:54	(E)-2-HEX	0	3.25	0	NONE	NO	NO
4/10/2024 6:24	(E)-2-HEX	0	3.02	0	NONE	NO	NO
4/10/2024 6:54	(E)-2-HEX	0	2.68	0	NONE	NO	NO
4/10/2024 7:24	(E)-2-HEX	910	739.94	187580	NONE	NO	NO
4/10/2024 7:54	(E)-2-HEX	910	761.7	196709	NONE	NO	NO
4/10/2024 8:24	(E)-2-HEX	910	770.93	182835	NONE	NO	NO
4/10/2024 8:54	(E)-2-HEX	910	780.28	179897	NONE	NO	NO
4/10/2024 9:24	(E)-2-HEX	910	793.78	191652	NONE	NO	NO
4/10/2024 9:54	(E)-2-HEX	910	796.26	209496	NONE	NO	NO
4/10/2024 10:24	(E)-2-HEX	910	793.09	213536	NONE	NO	NO
4/10/2024 10:54	(E)-2-HEX	910	789.98	212769	NONE	NO	NO
4/10/2024 11:24	(E)-2-HEX	910	786.54	201387	NONE	NO	NO
4/10/2024 11:54	(E)-2-HEX	910	788.99	-	NONE	NO	NO
4/10/2024 12:24	(E)-2-HEX	910	789.55	-	NONE	NO	NO
4/10/2024 12:54	(E)-2-HEX	910	802.8	-	NONE	NO	NO
4/10/2024 13:24	(E)-2-HEX	0	34.84	0	NONE	NO	NO
4/10/2024 13:54	(E)-2-HEX	0	20.94	0	NONE	NO	NO
4/10/2024 14:24	(E)-2-HEX	0	14.93	0	NONE	NO	NO
4/10/2024 14:54	(E)-2-HEX	910	765.96	200087	NONE	NO	NO

Time	VOC				Interferent	Interferent on Reference System	Interferent on MicroVOC
4/10/2024 15:24	**(E)-2-HEX**	**910**	**778.57**	**208276**	NONE	NO	NO
4/10/2024 15:54	**(E)-2-HEX**	**910**	**794.48**	**212038**	NONE	NO	NO
4/10/2024 16:24	**(E)-2-HEX**	**910**	**809.01**	-	NONE	NO	NO
4/10/2024 16:54	(E)-2-HEX	0	18.95	0	NONE	NO	NO
Time	**VOC**	**Targeted Concentration (ppb)**	**Reference System Result (ppb)**	**Areas of the MicroVOC (a.u.)**	**Interferent**	**Interferent on Reference System**	**Interferent on MicroVOC**
4/10/2024 18:20	(E)-2-HEX	0	145.79	0	NONE	NO	NO
4/10/2024 18:50	(E)-2-HEX	0	63.51	0	NONE	NO	NO
4/10/2024 19:20	(E)-2-HEX	0	40.93	0	NONE	NO	NO
4/10/2024 19:50	(E)-2-HEX	0	28	0	NONE	NO	NO
4/10/2024 20:20	(E)-2-HEX	0	20.64	0	NONE	NO	NO

*(E)-2-HEX = (E)-2-hexenal

Table 8-4: Average measured concentration on the reference system in ppb and average area on microVOC of 2-methyl-1-butanol in a.u. during Thursday and Friday

Date	2-methyl-1-butanol		
	Targeted Concentration (ppb)	Average Measured Concentration on Reference System (ppb)	Average Area on PurPest microVOC (a.u.)
Thursday 11/04/2024	550	549.07	855,156.80
	1,060	1,058.05	1,435,140.00
	600	604.54	937,762.50
	1,090	1,091.35	1,495,915.00
	700	678.15	1,139,465.00
Friday 12/04/2024	700	678.15	1,139,465.00
	480	482.62	852,465.50
	1,090	1,038.75	1,387,690.00
	300	255.92	551,556.50

Table 8-5: Average measured concentration on the reference system in ppb and average area on microVOC in a.u. of d-limonene during Thursday and Friday

Date	d-limonene		
	Targeted Concentration (ppb)	Average Measured Concentration on Reference System (ppb)	Average Area on PurPest microVOC (a.u.)
Thursday 11/04/2024	157	156.86	431,720.60
	293	292.64	677,908.50
	200	221.36	501,828.50
	1,018	1,018.14	2,599,245.00
	706	706.15	1,833,545.00
Friday 12/04/2024	706	706.15	1,833,545.00
	550	550.18	1,453,455.00
	1,018	1,021.95	2,427,280.00
	157	105.11	400,652.00

Table 8-6: Average measured concentration on the reference system in ppb and average area on microVOC in a.u. of (E)-2-hexenal during Thursday and Friday

Date	Targeted Concentration (ppb)	Average Measured Concentration on Reference System (ppb)	Average Area on PurPest microVOC (a.u.)
		(E)-2-hexenal	
Thursday 11/04/2024	965	964.42	1,363,228.00
	1,700	1,679.30	2,334,095.00
	1,200	1,200.41	1,760,910.00
	1,770	1,6749.91	2,427,980.00
	1,200	1,221.58	1,871,705.00
Friday 12/04/2024	1,200	1,221.58	1,871,705.00
	965	946.59	1,741,790.00
	1,770	1,685.15	2,633,500.00
	965	958.55	1,411,730.00